
Chemical and Biological Evaluation of *Palythoa*

***tuberculosa* Collected from the Red Sea**

by

Abdulrahman Mohammed Elbagory

**A thesis submitted in partial fulfilment of the requirement for the
award of the degree of Master of Science in the Faculty of Natural
Sciences University of the Western Cape**



**Department of Chemistry
Faculty of Natural Sciences
University of the Western Cape**

Supervisor: Dr. Ahmed Mohammed

Co-supervisor: Dr. Mervin Meyer

March 2015

ABSTRACT

A chemical study on the total extract of the zoanthid *Palythoa tuberculosa*, collected from the Red Sea, resulted in the isolation of seven polyhydroxylated sterols *viz*: palysterols A-G, six of which are new. Their chemical structures were elucidated on the basis of their 1D and 2D NMR and MS spectroscopic data. Palysterols B and G demonstrated cytotoxic activity on three human cancer cell lines (MCF-7, HeLa, and HT-29). Palysterol G, in particular, was able to induce apoptosis in breast adenocarcinoma (MCF-7) cells.



Keywords: Marine natural product, Red Sea, *Palythoa tuberculosa*, Polyhydroxylated sterols, Cytotoxicity, Apoptosis.

DECLARATION

I, Abdulrahman Mohammed Mohammed Nagy Elbagory hereby declare that this work is my original dissertation and to my knowledge, it has not been submitted anywhere else for the award of a degree at any other University.

Date Signed

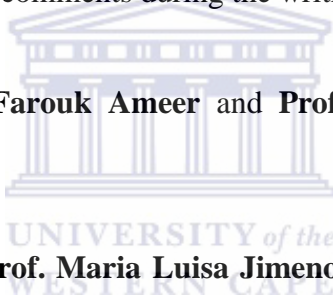


ACKNOWLEDGMENTS

First and foremost, I want to thank my mentor **Dr. Ahmed Mohammed**. I will be forever grateful to him for providing me with the opportunity to rejuvenate my research career. It is an honour to be his first post-graduate student at UWC with him as the main supervisor. I am extremely grateful for the patient guidance, continuous motivation and brotherly support he has always offered.

I feel very fortunate also to have learnt so much from my co-supervisor **Dr. Mervin Meyer**. I will always appreciate him for expanding my mind and allowing me to experience the different field of Biotechnology. Again, I am very thankful for his tireless efforts and constructive critical comments during the writing process of this thesis.

I would like to thank **Prof. Farouk Ameer** and **Prof. Wilfred Mabusela** for their academic support.



My sincere gratitude goes to **Prof. Maria Luisa Jimeno** (Spain) for the assistance with spectroscopic analysis. In addition, I wish to thank **Dr. Abdel-hamid Ali** (Egypt) and **Dr. Shirley Parker-Nance** (South Africa) for their assistance in collection and identification of the marine specimen I have used in this research. I would like also to express my appreciation to **Mustafa Drah** for guiding me through Cell Culture techniques.

I extend thanks to the **National Research Foundation** for the financial support.

Special thanks to, **Olubenga Popoola** for being a patient roommate and cooperative colleague. **Henry Muwangi** for the amazing support he has given me both inside and outside the department.

I thank all the wonderful people I met in the Chemistry and Biotechnology Departments and in the ISC 153 module from whom I have learnt so much.

DEDICATION

To my family.

*To my friends in the Pink Room,
for the unequalled company.*

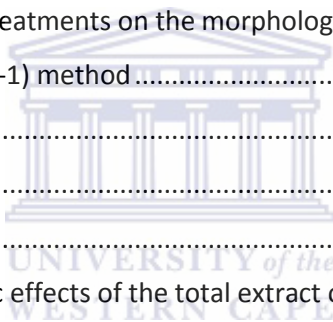


TABLE OF CONTENTS

ABSTRACT	ii
DECLARATION.....	iii
ACKNOWLEDGMENTS	iv
DEDICATION	v
TABLE OF CONTENTS	vi
LIST OF ABBREVIATIONS.....	ix
LIST OF FIGURES	xii
LIST OF TABLES	xvii
LIST OF SCHEMES.....	xviii
CHAPTER ONE: INTRODUCTION AND LITERATURE REVIEW.....	2
1.1 Introduction	2
1.1.2 Background on marine natural products	3
1.1.3 Background on cancer	7
1.1.3.1 Definition of cancer	7
1.1.3.2 Cancer statistics.....	7
1.1.3.3 Progression of cancer.....	9
1.1.3.4 Metastasis of cancer.....	10
1.1.3.5 Aetiology of cancer.....	11
1.1.3.6 Marine natural products in cancer treatment	12
1.1.3.6.1 Ecteinascidin-743 (ET-743, Yondelis™).....	14
1.1.3.6.2 Eribulin mesylate	15
1.1.3.6.3 Kahalalide F (KF)	17
1.1.3.6.4 Didemnin B	18
1.1.3.7 Cell death mechanisms.....	19
1.1.3.7.1 Apoptosis.....	20
1.2 Literature review on <i>Palythoa tuberculosa</i>	23
1.2.1 Taxonomy	23
1.2.2 Ecological background.....	23
1.2.3 Chemical studies on the species <i>P. tuberculosa</i>	26
1.2.4 Chemical studies on the genus <i>Palythoa</i>	33
1.3 Statement of research problem.....	36

1.4 Problem identification	37
1.5 Research aim.....	37
CHAPTER TWO: CHEMICAL STUDY OF <i>Palythoa tuberculosa</i>	39
2.1 Abstract.....	39
2.2 Methodology of chemical isolation	40
2.2.1 Reagents and solvents.....	40
2.2.2 Solvent evaporation	40
2.2.3 Chromatography.....	40
2.2.3.1 Thin layer chromatography (TLC)	40
2.2.3.2 Column chromatography.....	41
2.2.3.3 High Pressure Liquid Chromatography (HPLC)	41
2.2.4 Spectroscopy	41
2.2.4.1 Nuclear magnetic resonance (NMR) spectroscopy	41
2.2.4.2 Mass spectroscopy (MS).....	41
2.2.4.3 Infrared (IR) spectroscopy	42
2.2.4.4 Optical rotation measurements	42
2.3 Sample collection and identification	42
2.4 Extraction of the marine sample	42
2.5 Fractionation of the total extract	43
2.6 Isolation of the pure compounds	46
2.6.1 Isolation of palysterols C, E and G	46
2.6.2 Isolation of palysterol F	49
2.6.3 Isolation of palysterol B.....	50
2.6.4 Isolation of palysterol A and D	52
2.7 Spectroscopic data of the isolated compounds.....	54
2.8 Results and discussion	55
2.8.1 Analysis of Palysterol A.....	55
2.8.2 Analysis of palysterol B.....	59
2.8.3 Analysis of palysterol C.....	64
2.8.4 Analysis of palysterol D	68
2.8.5 Analysis of palysterol E	72
2.8.6 Analysis of palysterol F	76

2.8.7 Analysis of palysterol G	79
CHAPTER THREE: ANTICANCER EVALUATION OF <i>Palythoa tuberculosa</i>	86
3.1 Introduction	86
3.2 Materials	87
3.2.1 General reagents	87
3.2.2 Commercial kits	87
3.2.3 Instruments	87
3.3 Cell culture	88
3.3.1 Trypsinization of cells	89
3.3.2 Storage of cells	89
3.3.3 Counting of cells	89
3.4 Preparation of stock solutions of the compounds.....	89
3.5 Evaluation of the effects of treatments on the morphology of cells	90
3.6 Cell proliferation assay (WST-1) method	90
3.7 Annexin V apoptosis assay.....	92
3.8 Statistical analysis	92
3.9 Results.....	93
3.9.1 Evaluating the cytotoxic effects of the total extract of <i>P. tuberculosa</i>	93
3.9.2 Evaluating the cytotoxic effects of the isolated compounds	94
3.9.3 Evaluating the apoptotic activity of the isolated compounds.....	95
3.10 Discussion	98
REFERENCES	101



LIST OF ABBREVIATIONS

^{13}C -NMR	Carbon-13 nuclear magnetic resonance
1D-NMR	One-dimensional nuclear magnetic resonance
^1H -NMR	Proton nuclear magnetic resonance
2D-NMR	Two-dimensional nuclear magnetic resonance
ABB	Annexin binding buffer
APL	Aplidine [®]
BC	Before Christ
d	Doublet
DCM	Dichloromethane
DIW	De-ionized water
DMEM	Dulbecco's modified Eagle's medium
DMSO	Dimethyl sulfoxide
DNA	Deoxyribonucleic acid
ED ₅₀	Median effective dose
ESI	Electrospray ionization
ET-743	Ecteinascidin-743
EtOAc	Ethyl acetate
FBS	Foetal bovine serum
gCOSY	Gradient-enhanced correlation spectroscopy
gHMBC	Gradient-enhanced heteronuclear multiple bond coherence
gHSQC	Gradient-enhanced heteronuclear single quantum coherence
HPLC	High pressure liquid chromatography

HRMS	High resolution mass spectroscopy
IARC	International Agency for Research on Cancer
IC ₅₀	Half maximal inhibitory concentration
IPP	Initiation, promotion, and progression model
IR	Infrared
<i>J</i>	Coupling constant in Hz
KH	Kahalalide
MAA	Mycosporine like amino acids
MeOH	Methanol
min	Minute
MNP	Marine natural product
MS	Mass spectroscopy
NADPH	Nicotinamide adenine dinucleotide phosphate (reduced form)
NCI	National cancer institute
NMR	Nuclear magnetic resonance
NP	Natural product
PBS	Phosphate buffered saline
PI	Propidium iodide
PLTX	Palytoxin
PS	Phosphatidylserine
q	Quartet
ROESY	Rotating-frame overhauser enhancement spectroscopy
ROS	Reactive oxygen species

s	Singlet
SD	Standard deviation
SI	Selectivity index
sp.	Species
td	Triplet of doublets
TLC	Thin layer chromatography
TNF	Tumour necrosis factor
USA	United States of America
UV	Ultra violet
WHO	World health organization
WST-1	Sodium 5-(2,4-disulfophenyl)-2-(4-iodophenyl)-3-(4-nitrophenyl)- <i>2H</i> -tetrazolium inner salt
XTT	Sodium 2,3-bis(2-methoxy-4-nitro-5-sulfophenyl)-5-[(phenylamino)-carbonyl]- <i>2H</i> -tetrazolium inner salt

LIST OF FIGURES

Figure 1.1: Death percentage caused by neoplasms in SA reported from year 2008 to 2011.....	8
Figure 1.2: The development of cancer from a single cell by undergoing multi-stage mutations.....	9
Figure 1.3: The process of metastasis inside the body.....	10
Figure 1.4: Chemical structures of spongouridine, spongothymidine, Ara-A and Ara-C.....	14
Figure 1.5: Chemical structure of ET-743.....	15
Figure 1.6: Chemical structures of halichondrin B, and its derivative eribulin mesylate.....	16
Figure 1.7: Chemical structure of kahalalide F.....	17
Figure 1.8: Chemical structures of didemnin B and dehydrodidemnin B.....	18
Figure 1.9: A diagram showing the pathways of apoptosis.....	22
Figure 1.10: Photographs of <i>P. tuberculosis</i>	25
Figure 1.11: Chemical structure of PLTX.....	29
Figure 1.12: Chemical structures of mycosporine-Gly, palythine, palythanol and palythene.....	30
Figure 1.13: Chemical structures of palythazine and isopalythazine.....	31
Figure 1.14: Chemical structures of 24 β -methylcholesta-5,22-dien-3 β -ol, cholest-5-en-3 β -ol, 24 β -methylcholest-5-en-3 β -ol, 24-ethylcholest-5-en-3 β -ol and gorgosterol.....	32
Figure 1.15: Chemical structures of chimyl alcohol and batyl alcohol.....	34

Figure 1.16: Chemical structures of 6-bromo-5,9-eicosadienoic acid, Palythoalones A and Palythoalones B.....	35
Figure 2.1: TLC profile of the main fractions of <i>P.tuberculosis</i> in visible and under UV light.....	45
Figure 2.2: TLC of sub-fractions of main fraction XXII.....	46
Figure 2.3: HPLC chromatogram of sub-fraction XXII ₁	47
Figure 2.4: HPLC chromatogram of sub-fraction XXII ₂	48
Figure 2.5: HPLC chromatogram of XXII ₂₋₁	48
Figure 2.6: HPLC chromatogram of main fraction XXV.....	49
Figure 2.7: HPLC chromatogram of sub-fraction XXV ₁	50
Figure 2.8: Collective TLC of main fraction XXVI.....	51
Figure 2.9: HPLC chromatogram of sub-fraction isolated from XXVI ₁₋₁	51
Figure 2.10: HPLC chromatogram of sub-fraction XXVII ₁	52
Figure 2.11: Chemical structure of palysterol A.....	56
Figure 2.12: ¹ H NMR of palysterol A	56
Figure 2.13: ¹³ C NMR of palysterol A	57
Figure 2.14: gCOSY of palysterol A.....	57
Figure 2.15: Multiplicity-edited gHSQC of palysterol A	58
Figure 2.16: Selected gHMBC correlations observed for palysterol A.....	58
Figure 2.17: gHMBC of palysterol A	59
Figure 2.18: Chemical structure of palysterol B.....	60

Figure 2.19: ^1H NMR of palysterol B	60
Figure 2.20: ^{13}C NMR of palysterol B	61
Figure 2.21: gCOSY of palysterol B	61
Figure 2.22: Multiplicity-edited gHSQC of palysterol B	62
Figure 2.23: Selected gHMBC correlations observed for palysterol B.....	62
Figure 2.24: gHMBC of palysterol B	63
Figure 2.25: ROESY of palysterol B	63
Figure 2.26: Chemical structure of palysterol C.....	64
Figure 2.27: ^1H NMR of palysterol C	65
Figure 2.28: ^{13}C NMR of palysterol C	65
Figure 2.29: gCOSY of palysterol C	66
Figure 2.30: Multiplicity-edited gHSQC of palysterol C.....	66
Figure 2.31: gHMBC of palysterol C	67
Figure 2.32: ROESY of palysterol C	67
Figure 2.33: Chemical structure of palysterol D.....	68
Figure 2.34: ^1H NMR of palysterol D	69
Figure 2.35: ^{13}C NMR of palysterol D	69
Figure 2.36: gCOSY of palysterol D	70
Figure 2.37: Multiplicity-edited gHSQC of palysterol D	70
Figure 2.38: Selected gHMBC correlations observed for palysterol D.....	71

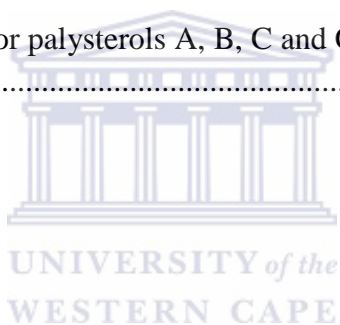
Figure 2.39: gHMBC of palysterol D	71
Figure 2.40: ROESY of palysterol D	72
Figure 2.41: Chemical structure of palysterol E.....	73
Figure 2.42: ^1H NMR of palysterol E	73
Figure 2.43: ^{13}C NMR of palysterol E	74
Figure 2.44: gCOSY of palysterol E	74
Figure 2.45: Multiplicity-edited gHSQC of palysterol E	75
Figure 2.46: gHMBC of palysterol E	75
Figure 2.47: ROESY of palysterol E	76
Figure 2.48: Chemical structure of palysterol F.....	77
Figure 2.49: ^1H NMR of palysterol F	77
Figure 2.50: ^{13}C NMR of palysterol F	78
Figure 2.51: Multiplicity-edited gHSQC of palysterol F	78
Figure 2.52: gHMBC of palysterol F	79
Figure 2.53: Chemical structure of palysterol G.....	80
Figure 2.54: ^1H NMR of palysterol G	80
Figure 2.55: ^{13}C NMR of palysterol G	81
Figure 2.56: gCOSY of palysterol G	81
Figure 2.57: Multiplicity-edited gHSQC of palysterol G	82
Figure 2.58: gHMBC of palysterol G	82

Figure 2.59: ROESY of palysterol G	83
Figure 3.1: The effect of the total methanolic extract of <i>P. tuberculosis</i> on the cell viability as determined by WST-1 assay.....	94
Figure 3.2: Percentage of live, dead and apoptotic cells induced by palysterols B and G.....	96
Figure 3.3: Photographs showing the apoptotic effect of the two compounds on MCF-7 cells.....	97



LIST OF TABLES

Table 1.1: Possible mechanisms to overcome the low supply of marine products.....	6
Table 1.2: Number of reported cancer cases and deaths worldwide in 2012 according to IARC.....	8
Table 2.1: Solvent system used for fractionation of the total extract of <i>P.tuberculosis</i> .	43
Table 2.2: Fractions obtained upon fractionation of the total extract of <i>P.tuberculosis</i>	44
Table 2.3: ¹ H and ¹³ C NMR spectral data of palysterols A-G.....	84
Table 3.1: Cell lines used in this study.....	88
Table 3.2: IC ₅₀ and SI values for palysterols A, B, C and G as determined by WST-1 assay.....	95



LIST OF SCHEMES

Scheme 2.1: A flow diagram for the isolated compounds from *P. tuberculosa*..... 53



Outline of Chapter One: Introduction and Literature Review

1.1 Introduction

1.1.2 Background on marine natural products

1.1.3 Background on cancer

1.1.3.1 Definition of cancer

1.1.3.2 Cancer statistics

1.1.3.3 Progression of cancer

1.1.3.4 Metastasis of cancer

1.1.3.5 Aetiology of cancer

1.1.3.6 Marine natural products in cancer treatment

1.1.3.6.1 ET-743 (Yondelis™)

1.1.3.6.2 Eribulin mesylate

1.1.3.6.3 Kahalalide F (KF)

1.1.3.6.4 Didemnin B

1.1.3.7 Cell death mechanisms

1.1.3.7.1 Apoptosis

1.2 Literature review on *Palythoa tuberculosa*

1.2.1 Taxonomy

1.2.2 Ecological background

1.2.3 Chemical studies on the species *P. tuberculosa*

1.2.4 Chemical studies on the genus *palythoa*

1.3 Statement of research problem

1.4 Problem identification

1.5 Research aim

CHAPTER ONE

INTRODUCTION AND LITERATURE REVIEW

1.1 Introduction

The medicinal use of natural products (NPs) (i.e. secondary metabolites) of terrestrial plants, marine organisms, or any natural source has captured human's interest throughout the ages. Interestingly, palaeoanthropological (the scientific study of human fossils) studies conducted by Solecki at the cave site of Shanidar (Northern Iraq) were able to uncover several pollen grains which were buried, presumably intentionally, in a grave containing the remains of a Neanderthal dating back to more than 60,000 years ago (Solecki, 1975). These pollen samples are known to have curative properties, as diuretics, stimulants, astringents as well as anti-inflammatory properties (Solecki, 1975). Moreover, the documented use of oils from *Papaver somniferum* (poppy juice) and *Commiphora* species (myrrh) dating back to 2600 BC has been written about in cuneiform scripts from Mesopotamia. These oils are still used today for treatment of coughs, colds and inflammation. Also, the Papyrus Ebers written in 1500 BC describes hundreds of drugs prepared from terrestrial plants in ancient Egypt (Cragg and Newman, 2005). The World Health Organization (WHO) estimates that 80% of the population in third world countries depend on folk medicine for medical treatment (Ahmad *et al.*, 1998).

However, proper scientific toxicological, microbial, pharmacological and chemical studies are needed to ensure the safe use of these alternative medicines (Nkunya *et al.*, 1990). NP chemists have been able to isolate and identify the chemicals or secondary

metabolites responsible for the biological effects of these natural sources. Morphine is the first drug isolated from a natural source, and the first to be sold commercially as well (Ji *et al.*, 2009). Merck started marketing morphine in 1826 as an opioid analgesic drug. The German pharmacist Friedrich Wilhelm Sertürner was the first person to isolate this compound from opium in 1806 (Sertürner, 1806).

Now NPs have become an integral part of modern drug manufacturing. A recent study looking into the sources of novel drugs identified between the period 1981 and 2010, shows that in the category of anticancer drugs alone, nearly half of the drug components used are either entirely from or derived from NPs (Newman and Cragg, 2012). The influence of NPs is even higher in other drug classes such as anti-infective drugs (Newman and Cragg, 2012). Well-known examples of NPs that are part of drugs currently in use include antibiotics (e.g. erythromycin and its derivatives, such as clarithromycin), immunosuppressive agents (e.g. cyclosporin A and FK 506), anticancer agents (e.g. paclitaxel and camptothecin and its derivatives, such as topotecan and irinotecan) and anticholesterolemic agents (e.g. lovastatin and its derivatives) (Hung *et al.*, 1996).

1.1.2 Background on marine natural products

For many years chemists focused mainly on terrestrial plants as a source of NPs, while no attention was given to marine organisms. It was only around the mid 20th century when marine inhabitants were investigated for their unique biological activities (Capon, 2010). Nonetheless, there is some evidence of the use of marine organisms in folk medicine, for

example, seaweed-based remedies were advocated by early Chinese pharmacopeia to treat numerous disorders like, pain, abscesses, menstrual difficulties and cancer (Ruggieri, 1976).

Most of the studies on Marine Natural Products (MNPs) were focused on marine invertebrates. These animals are soft-bodied and sessile, lacking morphological defence mechanisms, such as shells, claws or spines to ward off predators, hence they have adopted more subtle means to safeguard themselves against the extremely hostile marine environment by producing secondary metabolites that act as a chemical defence system to ensure their survival. These secondary metabolites can deter other organisms from feeding on some of the marine invertebrates (Blunt *et al.*, 2008). Moreover, these secondary metabolites can defend the organisms from infections or induce cell growth inhibition to protect the territory from competitors. Also, these chemicals can facilitate organisms' feeding process by immobilizing prey (Capon, 2010).

In general, the secondary metabolites isolated from marine organisms differ structurally from secondary metabolites present in their terrestrial counterparts (Capon, 2010). These marine secondary metabolites exhibit a unique structural skeleton with unusual carbon and heterocyclic skeletons (Capon, 2010). Of equal importance, marine organisms exhibit higher bioactivity compared to terrestrial organisms. A screening study conducted by the US National Cancer Institute (NCI) evaluating the cytotoxicity of NPs showed that approximately 2% of the tested marine samples exhibited significant cytotoxicity,

whereas less than 0.5% of the terrestrial samples showed similar activity (Munro *et al.*, 1999).

On the other hand, MNPs tend to be highly sensitive to light, temperature, oxygen and pH levels (Capon, 2010). Consequently, special precautions must be taken during their isolation and characterization. Separation methods such as acid and base extraction or steam distillation used to isolate secondary metabolites from terrestrial plants cannot be applied in the isolation of MNPs (Capon, 2010).

Moreover, the presence of MNPs at very low concentrations relative to the net weight of the organisms is a major challenge for MNP chemists. For instance, one metric tonne of the tunicate *Ecteinascidia turbinata* is required to isolate one gram of ecteinascidin-743, a promising anti-cancer compound (Mendola, 2000). Also, in order to isolate around 300 mg of potent cytostatic halichondrins, one metric tonne of the sponge *Lissodendoryx sp.* is required (Hart *et al.*, 2000).

There are, however, numerous approaches that can be adopted to overcome the availability issue of the MNPs (Table 1.1). Ecteinascidin-743, for example, was produced through mariculture and semi-synthesis (Cuevas *et al.*, 2000). Aplidin^R and Kahalalide F were also successfully produced by full chemical synthesis (Jou *et al.*, 1997) (López-Maciá *et al.*, 2001). Furthermore, since microbial symbionts are suggested to be the true source of the secondary metabolites formulated within the organisms, it is possible to control and manipulate their biosynthetic pathways to harvest their metabolites. For

example, the anticancer Salinosporamide A, which was first isolated from the marine-sediment actinomycete strain *S. tropica* (Fenical *et al.*, 2009), was supplied by means of saline-fermentation (Montaser and Luesch, 2011). In addition, the utilization of genetic engineering can also be used to supply MNPs, especially in case of uncultivated marine bacteria. For instance, the gamma-proteobacterium *Candidatus Endobugula sertula*, which is a symbiont of the marine bryozoan *Bugula neritina*, was found to be the true source of the anticancer compound bryostatin 1 (Hildebrand *et al.*, 2004), which was supplied through the costly aquaculture process. The genes responsible for the biosynthesis of bryostatin 1 were successfully identified and sequenced (Sudek *et al.*, 2007). Consequently, the cloning of the biosynthetic genes for bryostatin 1 and its heterologous expression (the expression of a gene or part of a gene in a host organism) can provide a more practical option for the compound's supply (Molinski *et al.*, 2009).

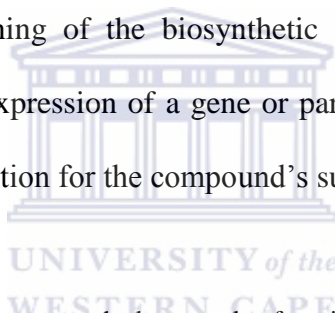


Table 1.1: Possible mechanisms to overcome the low supply of marine products (source: Jimeno *et al.*, 2004).

• Mariculture:	Farming the organism in its natural milieu
• Aquaculture:	Culture of the organism under artificial conditions
• Hemi synthesis:	Use of a parent / related compound as the starting point followed by a short / industrially effective synthetic process
• Synthesis	
• Microbial fermentation	
• Genetic intervention	

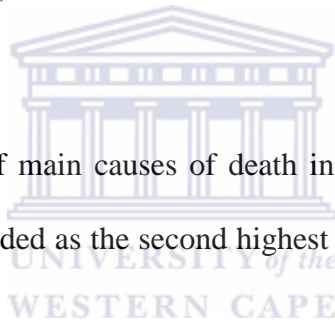
1.1.3 Background on cancer

1.1.3.1 Definition of cancer

Cancer results from the failure of cell cycle control, which allows mutated or injured cells to evade apoptosis (programmed cell death), leading to the uncontrolled accumulation of such cells with these defects (Story and Kodym 1998). These mutations usually occur in proto-oncogenes which can, upon mutation, promote tumour growth. In addition to proto-oncogenes, mutations can also take place in tumour suppressor genes, which in turn would promote uncontrolled cell cycle progression, hence promoting abnormal cell growth (Vermeulen *et al.*, 2003).

1.1.3.2 Cancer statistics

Cancer is considered as one of main causes of death in first-world countries. While in third-world countries it is regarded as the second highest cause of mortality (Jemal *et al.*, 2011).



The GLOBOCAN 2012 (globocan.iarc.fr), which is a statistical report of incidence and fatality rate of cancer worldwide issued by the International Agency for Research on Cancer (IARC), stated that in the year 2012 there were nearly 14.1 million new cancer cases worldwide, and around eight million deaths from cancer in the same year (globocan.iarc.fr). More than half of new cases and mortalities caused by cancer occurred in less developed countries. Compared to cervical and colon cancer, breast cancer was more frequent with over 1.6 million new cases worldwide, while colon cancer's fatality rate was higher with 694,000 deaths (Table 1.2).

Table 1.2: Number of reported cancer cases and deaths worldwide in 2012 according to IARC (globocan.iarc.fr).

Region	Number of new cases*				Number of deaths*			
	Overall	Breast	Colon	Cervical	Overall	Breast	Colon	Cervical
World	14090	1677	1361	528	8201	522	694	266
More developed regions	6076	794	737	83	2878	198	333	35
Less developed regions	8014	883	624	445	5323	324	361	230

*Numbers are in thousands.

There is also an increase in mortality rate caused by cancer in South Africa (SA). According to a report issued in 2014 by Statistics South Africa (Stats SA) (<http://beta2.statssa.gov.za/>), the annual percentage of deaths caused by neoplasms in SA in 2011 reached 7.3% of total 505 803 deaths registered in the same year. This is a 1.4% increase compared to the percentage registered in 2008 of total 595 624 deaths counted (Figure 1.1).

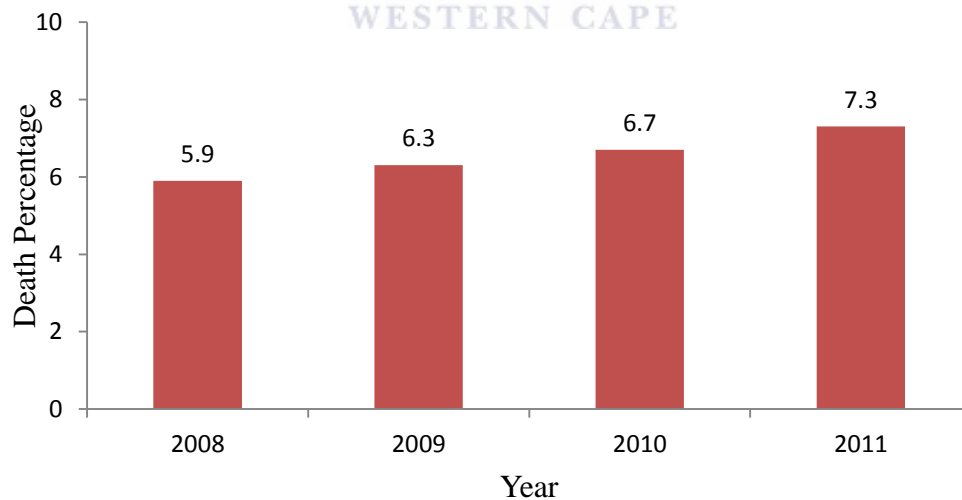


Figure 1.1: Death percentages caused by neoplasms in SA reported from the year 2008 to 2011.

1.1.3.3 Progression of cancer

In contrast to single-gene diseases, cancer is considered a multi-gene, multi-step disorder. First, the progression of cancer is ‘initiated’ by a DNA mutation of one somatic cell, followed by another or multiple stages of different mutations leading to the ‘promotion’ of several other cancerous cells until a tumour mass is established (Hejmadi, 2010). The latter step may take months or years before eventually tumour mass ‘progresses’ all over the body (metastasis) contributing to a detectable cancer (Figure 1.2) (Hejmadi, 2010).

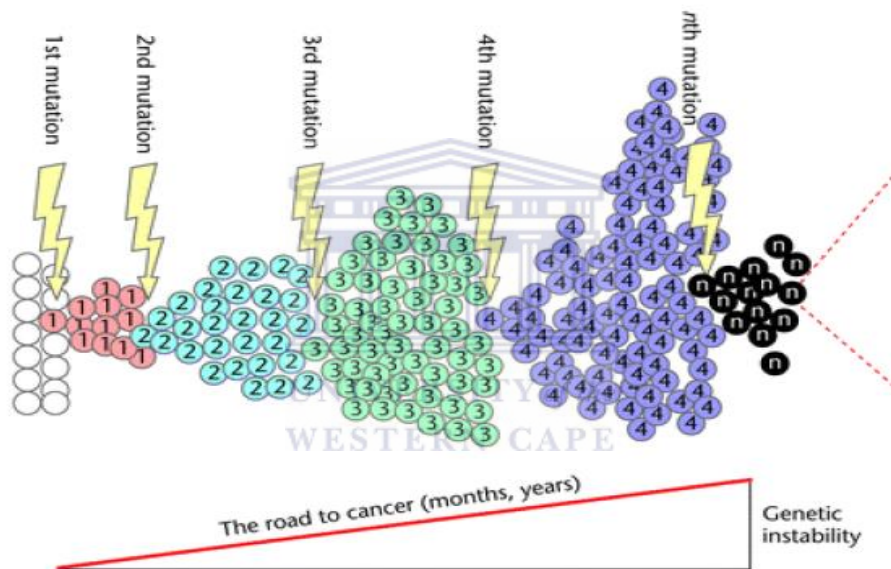


Figure 1.2: The development of cancer from a single cell by undergoing multi-stage mutations (Alison, 2001).

This “initiation, promotion, and progression” (IPP) model was presented to understand the genetic structure of cancer (Kopelovich, 1982; Trosko, 2010). Still, it is difficult to determine the exact number of mutations needed or genes involved for a cancer to become clinically manifested. “The six hallmarks of cancer” was described by Hanahan and Weinberg (2000) to help to discriminate cancer cells from normal or healthy cells. The six major hallmarks of cancer detail the exact sequence of mutations that must occur

for the cells to develop into clinical detectable cancer. These hallmarks include (1) the potential of having unlimited replications, (2) having self-sufficient growth signals, (3) resistance to anti-growth signals, (4) the ability to elude apoptosis, (5) angiogenesis: ability to grow new blood vessels and (6) the capability to metastasize and attack other tissues (Hanahan and Weinberg, 2000).

1.1.3.4 Metastasis of cancer

Metastasis is a fatal process in which the tumour cells invade other parts of the body after they exceed the capacity of their original environment to support their growth. In 2003, Fidler proposed his hypothesis “seed and soil” to explain how metastasis proceeds, where cells or “seeds” abandon their original tumour site, use blood vessels to spread, attack other favourable tissues “soil” (Figure 1.3).

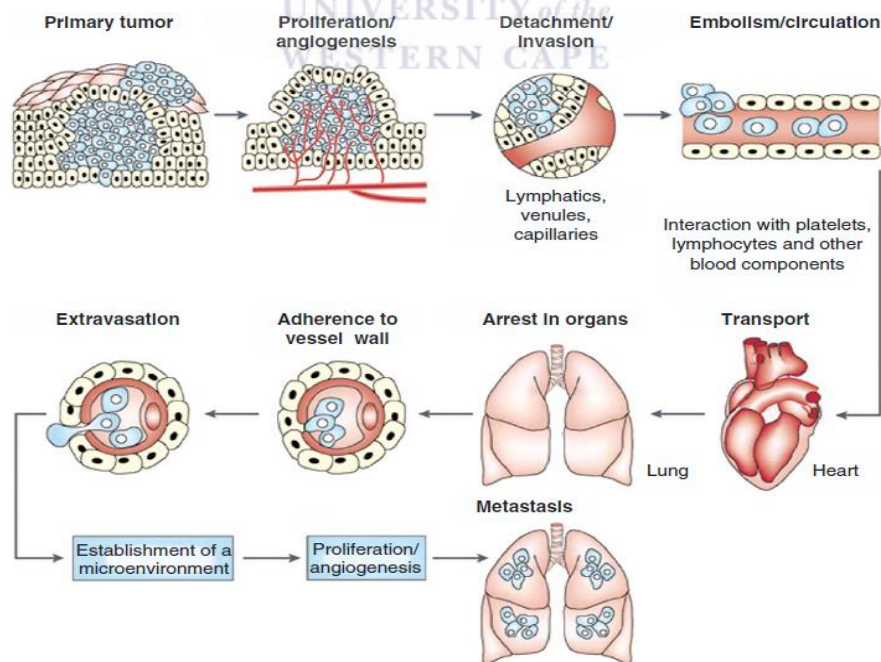


Figure 1.3: The process of metastasis inside the body (Withrow and Vail, 2007).

Firstly, growing of the tumour in size occurs by consumption of nutrients through simple diffusion, followed by manufacturing and secretion of angiogenic factors to build blood vessels, then invasion of the surrounding host stroma takes place, subsequently tumour cells escape into the circulation after detachment, these cells then get entrapped in the vessels beds of the distant organs, eventually extravasation occurs and the metastasis process is completed by the proliferation of the tumour cells within the attacked organ (Fidler, 2003) .

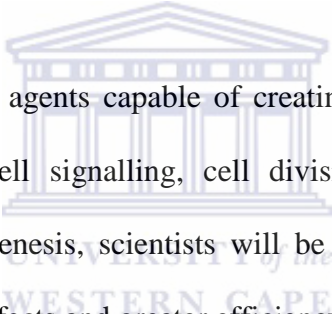
1.1.3.5 Aetiology of cancer

Although certain genetic factors (e.g. in retinoblastoma, familial adenomatosis coli, xeroderma pigmentosum and familial carcinoma syndrome) can predispose an individual to cancer (Demant, 2005), there are also environmental factors that can cause cancer. For instance, according to Hejmadi the prevalence of stomach cancer in Japan is 6-8 fold higher compared to the incidence rate in the USA. Yet, young Japanese migrants to USA follow the same incidence rate as the USA population (Hejmadi, 2010). This change in incidence rate can be attributed to the differences in environmental and lifestyle factors and highlight the effect of these factors on the development of cancer (Hejmadi, 2010).

An unhealthy diet can also be a major contributing factor. For example, high fat and low fibre intake is linked to bowel, pancreatic, prostate and breast cancer (Hejmadi, 2010). Moreover, some infectious agents can cause cancer, such as viruses [hepatitis B virus (HBV), human immunodeficiency virus (HIV)] or bacteria like *Helicobacter pylori* in the case of stomach cancer (Hejmadi, 2010). In addition, exposure to sunlight and ultraviolet rays is also associated with increased risk of skin cancer (Hejmadi, 2010).

1.1.3.6 Marine natural products in cancer treatment

Besides surgical approaches, chemotherapy and radiotherapy are the backbone of cancer treatment. Yet for their many limitations, there is a need to find alternative ways to treat cancer. Chemotherapy possesses narrow therapeutic index associated with significant toxicity and is more often counteracted by the development of resistance (Vanneman and Dranoff, 2012). Furthermore, radiation is limited for many reasons; (1) the resistance of many tumours is sometimes higher than the normal surrounding tissue, (2) lack of clear patho-anatomical borders in some of the tumours, (3) difficulty of adjusting the treatment dose (Orth *et al.*, 2014).

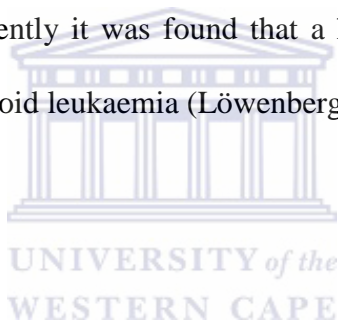


Through the discovery of new agents capable of creating new ways of killing tumour cells by means of altering cell signalling, cell division, energy metabolism, gene expression or affecting angiogenesis, scientists will be able to unveil tumour-specific treatments with minimal side effects and greater efficiency (Nagle *et al.*, 2004).

Many previously isolated MNPs were found to have cytotoxic effects. These effects may be attributed to the ecological evolutionary need that led to the formation of some sort of chemical defence (McClintock *et al.*, 2001) as discussed in section 1.1.2. Currently, more than 30 MNPs and their derivatives are studied in clinical trials as possible anticancer agents (Newman and Cragg, 2014).

The anticancer use of MNPs began in the middle of the last century with the isolation of spongouridine and spongothymidine (Figure 1.4) from the Caribbean sponge *Cryptotheca*

crypta by the American scientist Werner Bergmann (Jimeno *et al.*, 2004). Unlike most compounds of that class, spongouridine and spongothymidine possessed arabinose residues instead of the ribose and deoxyribose. This discovery was followed by the development of the antiviral [arabinoadenine (Ara-A, Vidarabine)] and anticancer [arabinocytosine (Ara-C, Cytarabine)] agents (Figure 1.4) (Stonik, 2009). Cytarabine is known to affect DNA replication and synthesis by blocking DNA polymerase (Uemura *et al.*, 1985). It is a well-known chemotherapeutic agent and has been in use for the past four decades. Cytarabine is also considered to be a drug of choice for the treatment of Hodgkin's lymphoma, acute lymphoblastic leukaemia and chronic myelogenous leukaemia (Cohen, 1976). Recently it was found that a high dose of cytarabine can be used in treatment of acute myeloid leukaemia (Löwenberg, 2013).



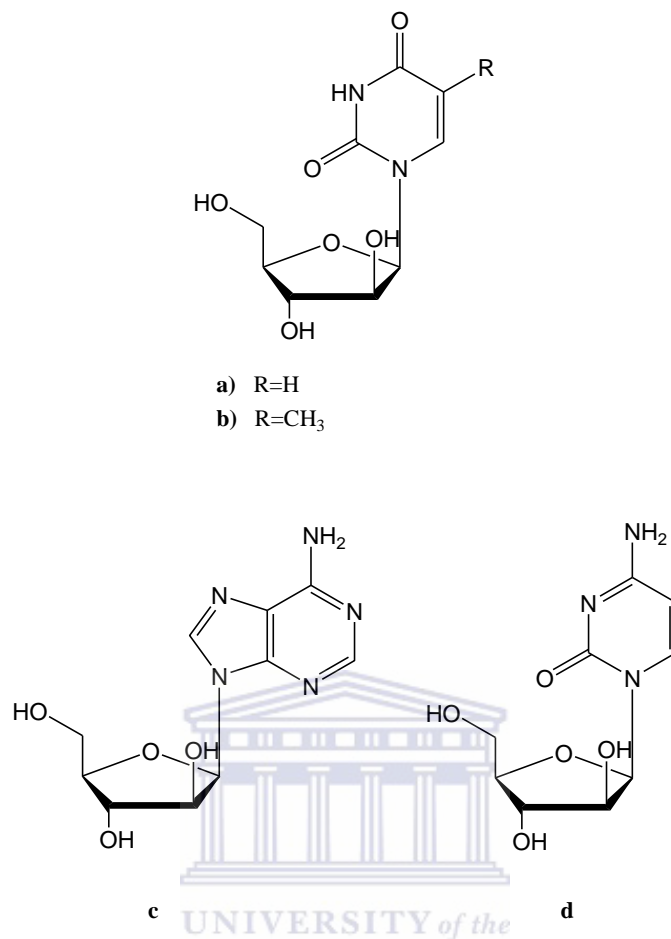


Figure 1.4: Chemical structures of spongouridine (a), spongothymidine (b), Ara-A (c) and Ara-C (d).

1.1.3.6.1 Ecteinascidin-743 (ET-743, Yondelis™)

Ecteinascidin-743 (ET-743) (Figure 1.5) is a tetrahydroisoquinoline alkaloid, first isolated from the tunicate *Ecteinascidia turbinata* living in the waters of West Indies coral reefs and mangrove swamps in 1990 (Rinehart *et al.*, 1990; Wright *et al.*, 1990). ET-743 inhibits activated transcription without showing any effect on the constitutive transcription (Minuzzo *et al.*, 2000), which improves the targeting of the compound towards the highly active dividing cancer cells in comparison to the normal cells which exhibit normal rates of transcription and translation. ET-743 also prevents the tumour cells from becoming resistant to chemotherapy as it interferes with the gene that produces

P-glycoprotein (Kanzaki *et al.*, 2002), which is a protein that induces resistance of cancer cells towards other anticancer drugs such as doxorubicin and taxanes. ET-743 does not cause cytotoxic side effects such as, hair loss, mucositis, neurotoxicity or diarrhoea associated with other anticancer drugs (Lopez Martin *et al.*, 2002). The drug was developed by the Spanish marine pharmaceutical company (pharmaMar), and marketed as Yondelis™. In 2014, pharmaMar reported that the net sale of Yondelis™ in the first quarter increased by 18% compared to the same period from the previous year, reaching almost 20 million euro (www.zeltia.com).

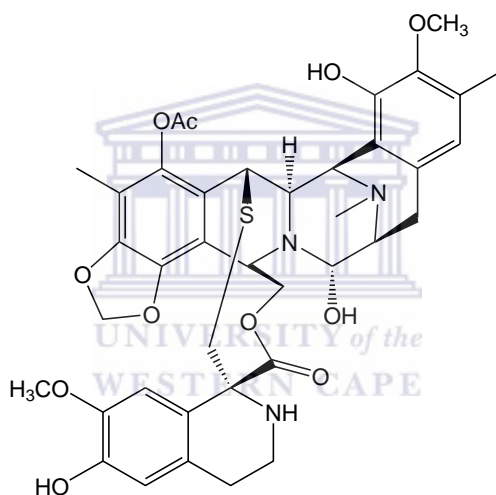


Figure 1.5: Chemical structure of ET-743.

1.1.3.6.2 Eribulin mesylate

In 1986, a very potent cytotoxic compound, halichondrin B (Figure 1.6) was isolated from the sponge *Halichondria okadai* (Hirata and Uemura., 1986). The compound was found to bind to tubulin on the same site as vinca-alkaloids applied in clinical treatment (Bai *et al.*, 1991). The low yield of this compound from *H. okadai* limited further clinical evaluation. Moreover, due to the compound's complex structure, chemical synthesis of this compound was also unattainable (Aicher *et al.*, 1992). It was not until much later

when scientists were able to obtain 310 mg of halichondrin B from the sponge *Lissodendoryx* sp. produced by aquaculture (Munro *et al.*, 1999), which enabled the initiation of preclinical studies with halichondrin B. A new simpler derivative, eribulin mesylate (Figure 1.6), was developed by the Japanese Eisai company in 2010, which was approved as anticancer drug and launched onto market under trade name Halaven™ (www.eisai.com). According to the company's reports, the drug recorded 10.9 billion yen sales in 2011 compared to 0.4 billion yen when it was released in 2010.

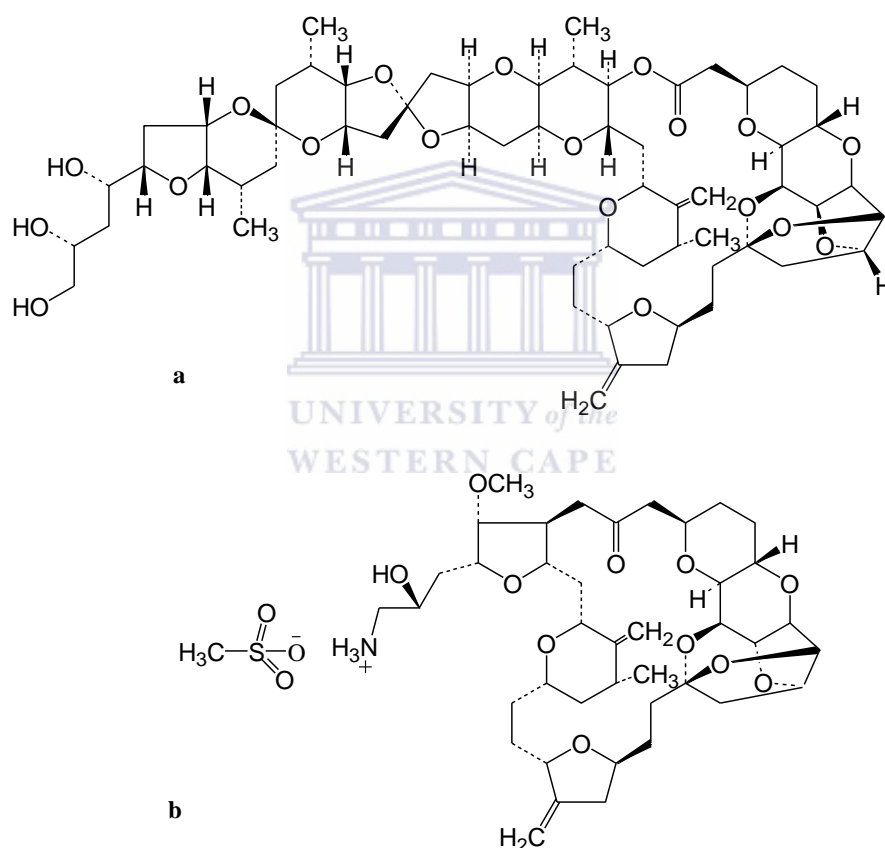


Figure 1.6: Chemical structures of halichondrin B (a) and its derivative eribulin mesylate (b).

1.1.3.6.3 Kahalalide F (KF)

Kahalalide F (Figure 1.7) was isolated from the mollusc (sea slug) *Elysia rufescens* gathered from Hawaii (Hamann *et al.*, 1996). Kahalalide F is a C₇₅ cyclic tridecapeptide that contains unusual amino-acid residues, including a rare Z-dehydroaminobutyric acid (Molinski *et al.*, 2009). The mollusc feeds on the green algae *Bryopsis* sp., which is believed to be the source of KF (Hamann *et al.*, 1996).

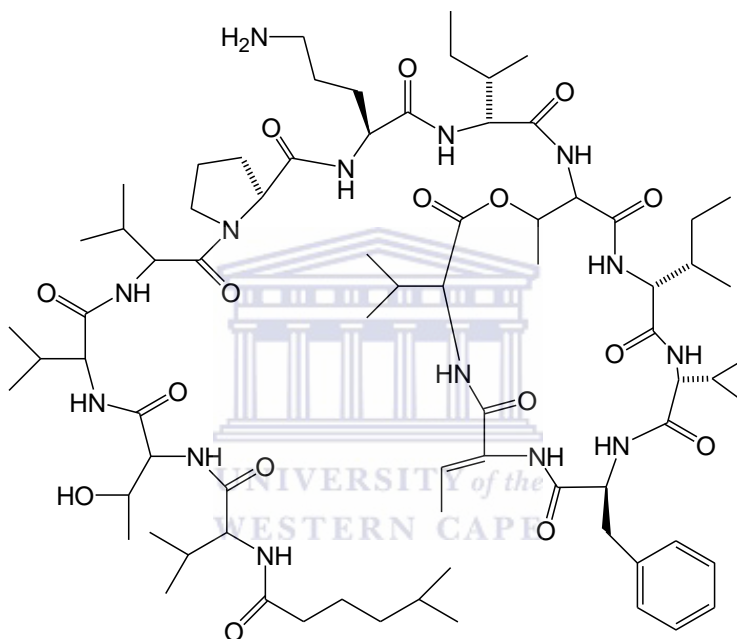


Figure 1.7: Chemical structure of kahalalide F.

KF exhibits both *in vivo* and *in vitro* cytotoxicity against several tumour models, such as colon, breast, non-small cell lung and prostate cancer (Faircloth *et al.*, 2001). Mechanistic studies of KF shows that it acts on lysosomal membranes by disrupting them and in turn forms large vacuoles, this mechanism is considered unique compared to other antitumor agents, which increase acidification of the intra-cellular space leading to apoptosis (Garcia-Rocha *et al.*, 1996).

1.1.3.6.4 Didemnin B

Didemnin B (Figure 1.8) is a cyclic depsipeptide isolated from the Caribbean tunicate *Trididemnum solidum* (Rinehart *et al.*, 1981), it was the first MNP to be subjected to clinical trials. The depsipeptide showed strong antiproliferative effect against several human tumour cell lines *in vitro*. Mechanistically, it was found that it acts as GTP-binding protein elongation factor (Nuijen *et al.*, 2000). Phase I and phase II clinical trials were conducted for the compound. However, the trials were ceased as didemnin B exhibited high toxicity, low solubility, and a short lifespan (Newman and Cragg 2004). More research into marine invertebrates led to isolation of dihydrodidemnin B (Figure 1.8) from the Mediterranean tunicate *Aplidium albicans*. Dihydrodidemnin B showed similar effect to didemnin B, but with lower toxicity and higher solubility. Currently, synthetically derived dehydrodidemnin B is being subjected to phase II clinical studies under trade name Aplidine[®] (APL) (Menna, 2009).

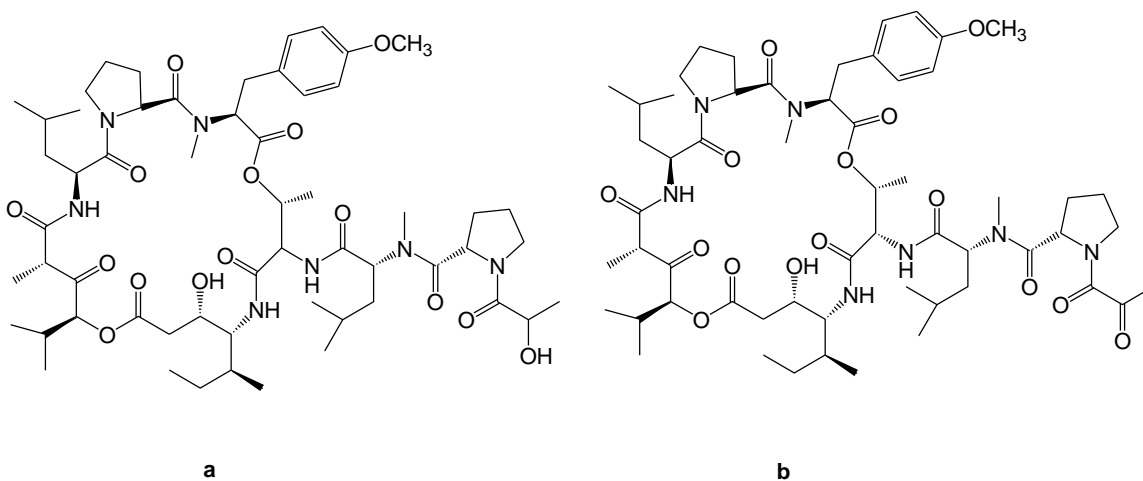
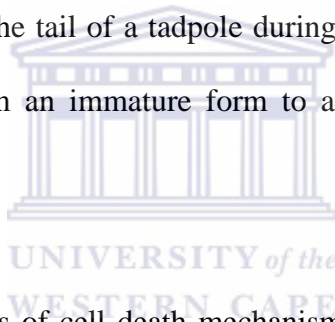


Figure 1.8: Chemical structures of didemnin B (a) and dehydrodidemnin B (b).

1.1.3.7 Cell death mechanisms

Irregular cell death is a common factor in many human diseases such as cancer, stroke and neurodegenerative disorders (Kepp *et al.*, 2011). Hence the regulation of cell death is an important approach for effective therapeutic strategy. For instance, anticancer agents induce cell death (Brown and Attardi, 2005), whereas cytoprotective drugs are used to avoid cell death in case of stroke, myocardial infarction or neurodegenerative disorders (Degterev *et al.*, 2005). Controlled cell death is a vital biological mechanism that takes part in various physiological processes within any living organisms. It sculpts organs or separate fingers and toes (Penaloza *et al.*, 2006). It also eliminates body structures that are no longer needed such as the tail of a tadpole during amphibian metamorphosis (the process of transformation from an immature form to an adult form) (Penaloza *et al.*, 2006).



Generally, there are three types of cell death mechanisms namely apoptosis, autophagy and necrosis. **Apoptosis** (type I cell death) is morphologically characterized by the condensation of both the nucleus and the cytoplasm of the cell in addition to the fragmentation of the DNA. It involves cell shrinkage, blebbing of plasma membrane and formation of apoptotic bodies containing nuclear or cytoplasmic material (Clarke, 1990). **Autophagy** (type II cell death) is defined as an intracellular self-defence mechanism through which the accumulation of damaged or unwanted components of any cell are recycled by their sequestration into autophagic vesicles that subsequently are eliminated through fusion with lysosomes (Amaravadi *et al.*, 2011). **Necrosis** (type III cell death) is described by Penaloza and co-workers as uncontrolled death that occurs as a result of cell

injury, leading to lysis of the cell. In necrosis, the cell membrane bursts, allowing the leakage of cellular contents. Unlike apoptosis or autophagy, necrosis triggers an inflammatory response due to the release of intracellular material, including the invasion of mast cells, phagocytes and natural killer cells (Penaloza *et al.*, 2006). Therefore, massive necrosis can be threatening to the organism and can contribute to an autoimmune reaction (Penaloza *et al.*, 2006).

1.1.3.7.1 Apoptosis

Apoptosis is a Greek word which depicts the process of falling of leaves from trees or petals from flowers. The term was inspired by the release of apoptotic bodies from the apoptotic cells (Reed, 2000). Kerr and co-workers first introduced the term to the scientific community in 1972 (Kerr *et al.*, 1972). Apoptosis is considered to be a programmed cell-suicide functioning to remove unwanted or irreversibly damaged cells. Apoptosis is an important factor in development, taking part in morphogenesis (the sculpting of the form of embryos) and in sexual differentiation (Jacobson *et al.*, 1997). Apoptosis is also involved in the growth of the immune and nervous systems of our body (Ameisen, 2002). Moreover, apoptosis is crucial for tissue homeostasis cells (Ameisen, 2002).

Any alteration in the levels of apoptosis can lead to many disease states. For instance, increased levels of apoptosis can lead to Alzheimer's disease (Honig and Rosenberg, 2000) and is also implicated in HIV/AIDS (Badley *et al.*, 1997). On the other hand, decreased levels of apoptosis can lead to the development of cancer (Hejmadi, 2010), and

can also contribute to inflammation, persistent infections and autoimmune diseases (Reed and Pellecchia, 2005).

Apoptosis is initiated by highly complex mechanisms (Figure 1.9) which involve several pathways; extrinsic or death receptor, which can be activated by extracellular ligands, intrinsic or mitochondrial, which is activated by various extra and intracellular stresses such as DNA damage, hypoxia and accumulation of undesired proteins (Kumar and Robbins, 2007), and perforin/granzyme (A or B) pathways, which are signalled by the immune system cells (Elmore, 2007). These pathways activate a family of intracellular enzymes known as caspases (Cysteine Aspartyl specific Proteases) which are present as inactive forms in all animal cells (Reed, 2000). A specific initiator caspase (caspase-8, -9 or -10) is activated by each pathway and consequently activate the executioner caspase-3, resulting in DNA fragmentation, degradation of cytoskeleton and nuclear protein of the cell leading to its death. Conversely, the granzyme A pathway acts in a caspase-independent manner which induces single stranded DNA damage (Reed, 2000). The final step of apoptosis is the fragmentation of the nucleus into numerous smaller fragments. These fragments are encapsulated by apoptotic bodies which -in contrast to non-apoptotic cells- have their phosphatidylserines in the outer leaflet of their plasma membrane (Kumar and Robbins, 2007). The relocation of phosphatidylserine to the outer layer of the plasma membrane of the apoptotic bodies acts as a death signal that allow macrophages to recognise the apoptotic cells/bodies resulting in the macrophages engulfing and destroying the apoptotic cell (Ameisen, 2002).

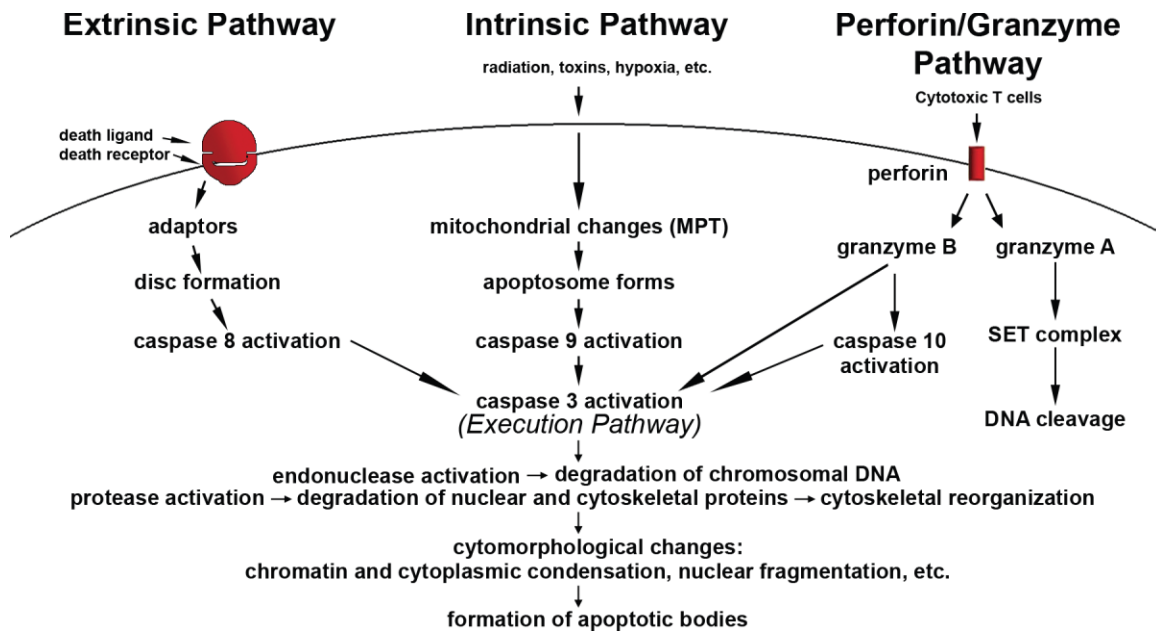


Figure 1.9: A diagram showing the pathways of apoptosis (source: Elmore, 2007).

In conclusion, apoptosis plays a key role in the prevention of cancer (Hejmadi, 2010). The ability to elude apoptosis is a common feature in the development of cancer in living cells (Hanahan and Weinberg, 2000). Therefore, the targeted activation of apoptosis in cancer cells is a feasible therapeutic strategy to treat cancer. Many MNPs were found to induce cell death *via* apoptosis (Nagle *et al.*, 2004). Such therapeutic agents can target cancer with minimal toxicity to normal cells and without the initiation of inflammatory reaction that can be induced by necrosis (Nagle *et al.*, 2004).

1.2 Literature review on *Palythoa tuberculosa*

1.2.1 Taxonomy

Kingdom: Animalia

Phylum: Cnidaria

Class: Anthozoa

Subclass: Hexacorallia

Order: Zoantharia

Suborder: Brachycnemina

Family: Sphenopidae

Genus: *Palythoa*

Species: *Palythoa tuberculosa* (Esper, 1791).



1.2.2 Ecological background

Zoanthids (Anthozoa: Hexacorallia: Zoantharia) are common shallow reef benthic organisms. Some zooxanthellate genera, such as *Palythoa* (family: Sphenopidae) and *Zoanthus* (family: Zoanthidae), are aggressive benthic competitors in specific environmental conditions (Suchanek and Green, 1981; Sebens, 1982). Species of the genera *Zoanthus* and *Palythoa* within the suborder Brachycnemina are usually dominant components of live reef cover, particularly on coral reef tops and reef edges (Burnett *et al.*, 1997; Swain, 2010; Irei *et al.*, 2011). Species of the genus *Palythoa* are colonial and commonly found in shallow coral reefs worldwide.

Presently, there are more than 100 nominal species of *Palythoa* cited in the literature (Reimer, 2014). Nonetheless, for the high levels of morphological variation within the species it is believed that the exact number is much lower (Burnett *et al.*, 1997; Reimer *et al.*, 2004). Morphologically, *Palythoa sp.* have their tentacles arranged in two rows around their oral disk, and are enclosed with sand detritus, with foreign materials constituting up to 65% of their body weight (Haywick & Mueller, 1997), which makes it resistant to strong wave energy (Suchanek and Green, 1981; Irei *et al.*, 2011).

The tropical zoanthid *Palythoa tuberculosa* (Esper, 1791) has been shown to form extensive mats in the shallow inter- and intra-tidal zones. Its wide Indo-Pacific distribution includes the reefs of Japan, Saipan (Micronesia), Indonesia, Madagascar, and the Red Sea (Reimer *et al.*, 2006). *P. tuberculosa* is an active planktonivore (feeds on planktons) (Fabricius and Metzner, 2004). *P. tuberculosa* also hosts a generalist *Symbiodinium* type (Reimer *et al.*, 2006; Hibino *et al.*, 2013). Moreover, during bleaching events the species can survive *via* heterotrophy (Reimer, 1971a, b) which, unlike many other bleaching-susceptible anthozoans, allows them to have low mortality during bleaching events (Jiménez, 2001).

There is an observable increase in the number of *P. tuberculosa* recently in the Gulf of Suez (Red Sea, Egypt), particularly at Ras Za'farana and Ras Muhammed (Sharm El-Sheikh, Egypt), forming extensive rubber mats covering large areas of coral reefs and overgrowing the reef-building corals in these areas (Figure 1.10). The rapidly growing, encrusting form of *P. tuberculosa* causes massive damage to the coral reefs in the Gulf of

Suez and the Egyptian Red Sea coast. This increased coverage of *P. tuberculosa* may be attributed to the recent change in the environmental conditions along the Egyptian Red Sea coast. Ras Za'farana marine environment is characterized by strong wave energy, high turbidity and increased nutrient enrichment (Ali and Hamed, 2006), these stresses may be tolerated by *P. tuberculosa* (Irei *et al.* 2011) and give it a competitive advantage over the true corals. Furthermore, under increased anthropogenic stress, these reef communities may shift from corals-dominated reef to aggressive and rapidly growing benthic zoanthid *P. tuberculosa*. However, there is little information about the factors responsible for the rapid growth of *P. tuberculosa* in the Gulf of Suez in the recent years. Much work is needed to understand the relationship between the increased coverage of the benthic zoanthid *P. tuberculosa* and the changing environmental conditions.

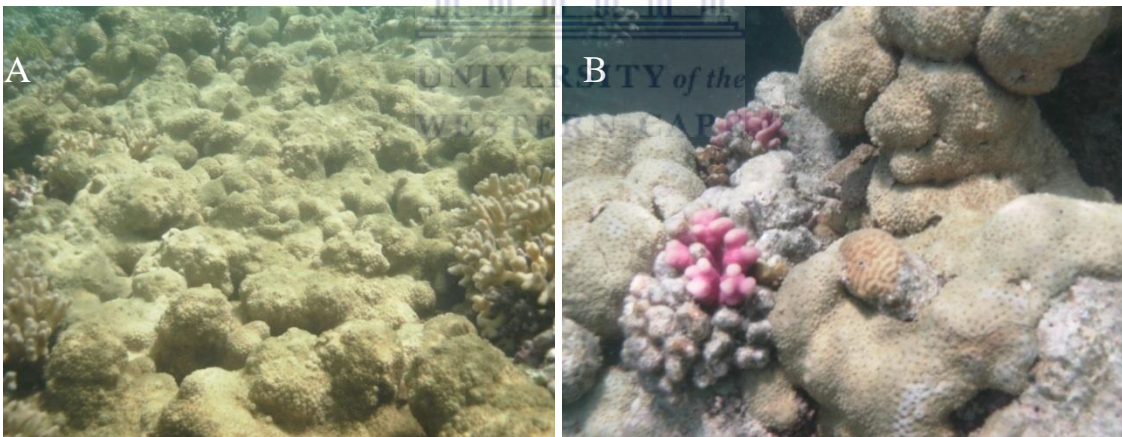


Figure 1.10: The zoanthid rubber mat *P. tuberculosa* dominating the benthic substrate and overgrowing the corals at Ras Za'farana, Gulf of Suez, Egypt. Depth ~ 1 to 5 m (A). And at Ras Muhammed, Sharm E-Sheikh, Egypt. Depth ~ 3 to 5 m (B).

1.2.3 Chemical studies on the species *P. tuberculosa*

Even before the chemistry of genus *Palythoa* was studied, it was well-known for its toxicity. In Hawai'i, the zoanthid was deeply incorporated in the Hawaiian people's myths and legends, it was known as '*limy-make-o-Hana*' which can be translated to deadly seaweed of Hana (Uemura, 2010). One of these stories was about a sacred pool containing seaweed which when applied to the soldiers' spears will bring certain death to foes, the pool became a sacred place and it was told that a curse will fall on anyone who dare to enter the site (Uemura, 2010).

A study conducted between 1965 and 1967 in the same area identified a new species *P. toxica* (Walsh and Bowers, 1971). Subsequently, another study by Moore and Scheuer (1971) on *P. toxica* led to isolation of Palytoxin (PLTX) (Figure 1.11), which is one of the most toxic NP ever discovered (Pettit *et al.*, 1982a). PLTX's intravenous LD₅₀ on dogs, rabbits, monkeys, guinea pigs, rats, and mice ranges between 0.033 and 0.45 µg/kg (Wiles *et al.*, 1974). By extrapolation, its toxic dose in humans was predicted to be in the range of 2.3 to 31.5 µg (Uemura, 1991). Being a large molecule, PLTX was first reported to have a molecular weight of 3300 and molecular formula of C₁₄₅H₂₆₄N₄O₇₈ with no repetition of sugar or amino acid units (Moore and Scheuer, 1971).

In 1973, a study conducted on the gut content of filefish *Aluterus scriptus* in Japan revealed the presence of *P. tuberculosa* and a compound of similar character to PLTX (Kimura and Hashimoto, 1973). In his article published in 2010, Uemura stated that his group started working on the Okinawan *P. tuberculosa* in 1974 and was successful in

isolating PLTX which was found to be amphipathic (water and fat soluble) and was found to be 50 times more toxic than tetrodotoxin (one of the most powerful marine toxin) (Uemura, 2010). The 263 nm chromophore part (Figure 1.11) of the compound was identified by means of spectroscopy, chemical degradation and synthesis (Moore *et al.*, 1975). A later study showed, using mass spectrometric analysis, that the exact molecular weight of PLTX was 2,681 and its molecular formula is $C_{129}H_{222}N_3O_{54}$ with eight double bonds (Macfarlane *et al.*, 1980).

Researchers continued their efforts to elucidate PLTX's outstandingly large structure. Two different research groups proposed a planar structure for PLTX. A Japanese group studied the PLTX isolated from the Okinawan *P. tuberculosa* and reported a hydroxyl substituent at C44 and a hemiketal functionality at C47 (Figure 1.11) (Uemura *et al.*, 1981a and 1981b), whereas the chemical study of the compound isolated from a *Palythoa* *sp.* collected from Tahiti by Moore and Bartolini (1981) reported a ketal bond between C44 and C47 (Figure 1.11). PLTX's stereostructure was described a year later (Klein *et al.*, 1982; Ko *et al.*, 1982; Fujioka *et al.*, 1982; Cha *et al.*, 1982).

In 1984, it was shown that PLTX induces both coronary artery contraction and peripheral vessel contraction by easing the absorption of sodium ions by neurons (Muramatsu *et al.*, 1984 and 1988). It was also found that PLTX was not an antagonist to tetrodotoxin, suggesting the existence of a yet unidentified sodium channel (Muramatsu *et al.*, 1984 and 1988). It was later suggested that Na^+ , K^+ -ATPase was the target molecule and it was

proposed that a channel structure existed within the ion pump. This channel structure was later confirmed (Artigas and Gadsby, 2003).

The cytotoxic action of PLTX was also studied. PLTX was found to control murine Ehrlich ascites carcinoma in mice at a dose of 84 ng/kg (Quinn *et al.*, 1974). The inhibitory effect of PLTX on the tumour was observed at doses as low as 5.25 ng/kg (Quinn *et al.*, 1974), but the extreme toxicity of the compound hindered its usefulness as an anticancer agent.

Further studies on *P. tuberculosa* led to the isolation of several PLTX-like compounds. In 1985, homopalytoxin, bishomopalytoxin, neopalytoxin and deoxypalytoxin were isolated (Uemura *et al.*, 1985). Ostreocin-D (Ukena *et al.*, 2001) and ovatoxin-A (Ciminiello *et al.*, 2012) are also PLTX-like structures which were isolated from the dinoflagellates *Ostreopsis* sp. In 2009, a new PLTX analogue, 42-hydroxypalytoxin (Figure 1.11), was isolated from both *P. toxica* and *P. tuberculosa* collected off the Hawaiian coast. The analogue showed similar biological activity to the PLTX (Ciminiello *et al.*, 2009). Secondary metabolites like PLTX which are derived from marine sources and contain long carbon chains were named “super-carbon-chain compounds” (Uemura, 2006).

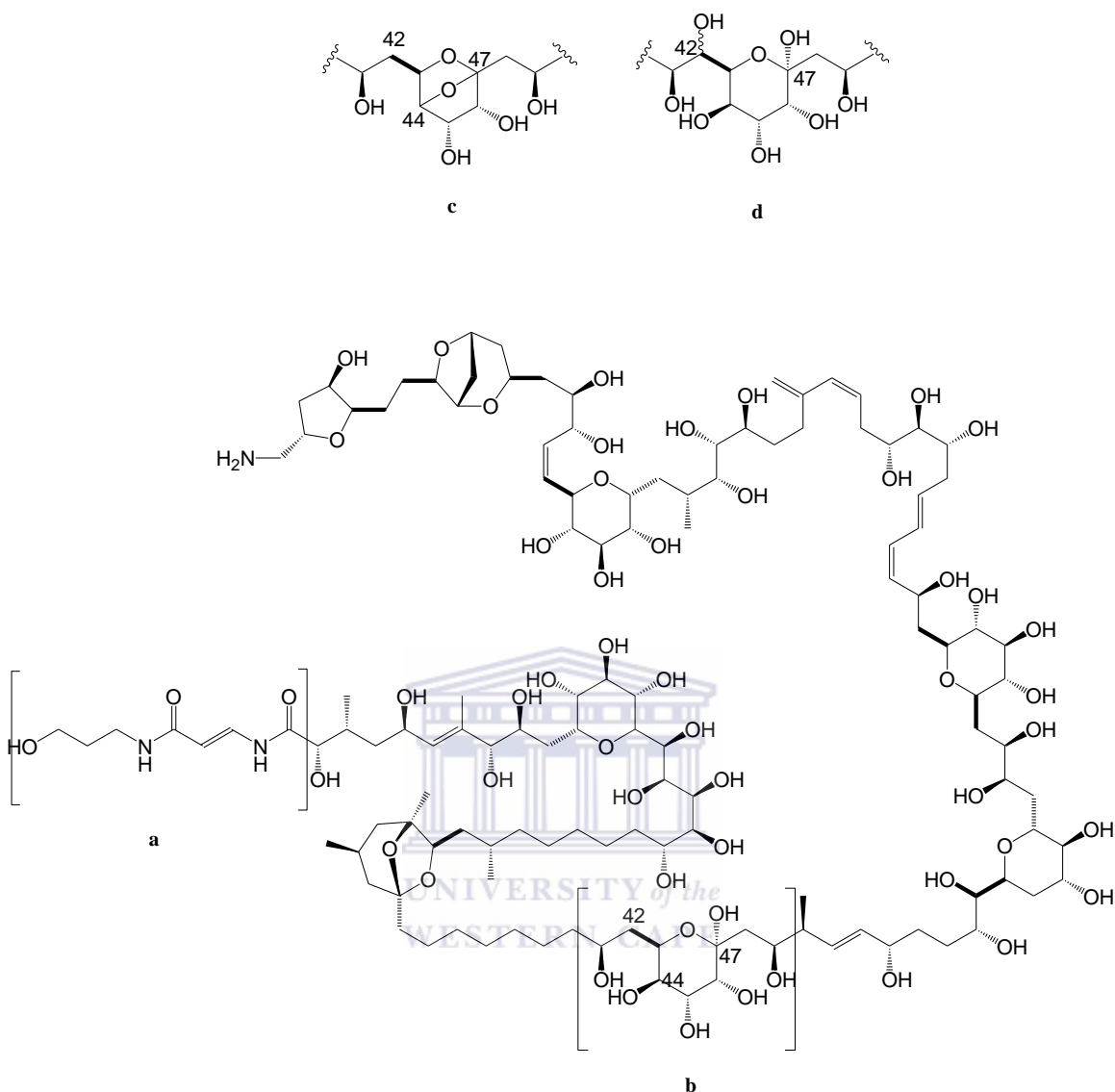


Figure 1.11: Chemical structure of PLTX*.

*The figure illustrates **a**) Chromophore part of 263 nm, **b**) The part of PLTX reported by Uemura *et al.* (1981) showing hydroxyl substituent at C44 and a hemiketal functionality at C47, **c**) The part of PLTX showing the ketone bond between C44 and C47 which was reported by Moore and Bartolini (1981), **d**) The part of PLTX showing the hydroxyl group at C42 in the reported structure of 42-hydroxypalytoxin by Ciminiello *et al.* (2009).

Several other water-soluble compounds (Figure 1.12) with strong absorption maxima were successfully isolated in several studies conducted on *P. tuberculosis*; mycosporine-Gly (Ito and Hirata, 1977), palythine (Takano *et al.*, 1978a), palythanol and palythene (Takano *et al.*, 1978b). These compounds, named mycosporine like amino acids or MAA,

are widely spread among marine inhabitants and believed to protect these organisms against UV radiation (Dunlap and Chalker, 1986). MAAs, in particular mycosporine-Gly, were found to have moderate antioxidant activity which may suggest their role as photo-oxidative stress protection caused by oxygen radicals in photoautotrophic symbiosis (Dunlap and Yamamoto, 1995).

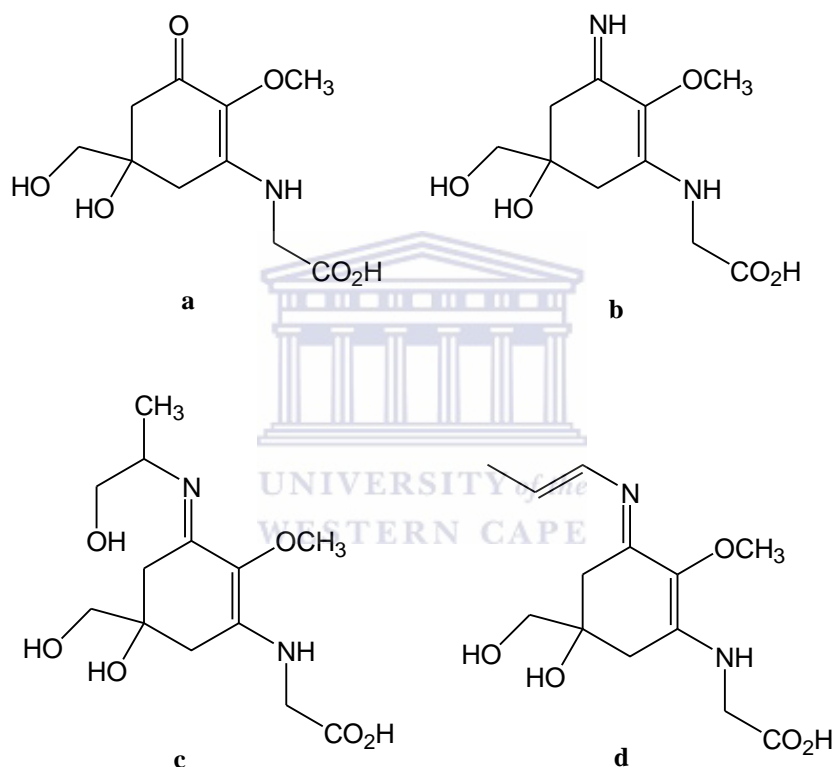


Figure 1.12: Chemical structures of mycosporine-Gly (a), palythine (b), palythanol (c), and palythene (d).

Further studies on *P. tuberculosis* led to the isolation of two isomeric compounds containing pyrazine rings; palythazine and isopalythazine (Figure 1.13). These compounds were found to be optically active and share the same molecular formula $C_{12}H_{16}N_2O_4$ (Uemura *et al.*, 1979). The structures of these compounds were confirmed by means of chemical derivatization.

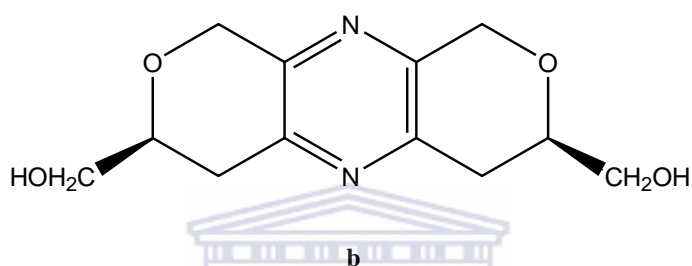
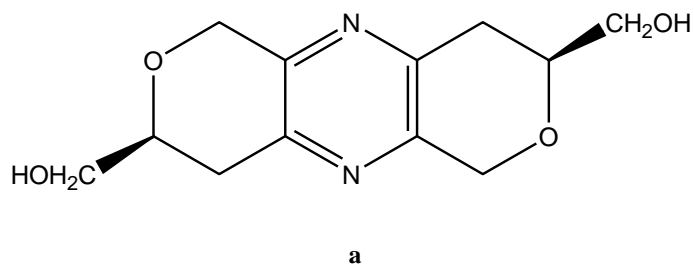


Figure 1.13: Chemical structures of palythazine (**a**) and isopalythazine (**b**).

In 1969, Gupta and Sheuer reported the isolation of a mixture of sterols from *P. tuberculosa* (Gupta and Sheuer, 1969). The physical constant of the sterol mixture was found to be similar to previously isolated sterol from *P. mamnzilosa* by Bergmann and co-workers in 1951 (Bergmann *et al.*, 1951). Bergmann's sterol was different from all other sterols identified at that time, and was thus given the name palysterol (Bergmann *et al.*, 1951). The major sterol identified by Gupta and Sheuer was 22,23-dihydrobrassicasterol (24 β -methylcholest-5-en-3 β -ol) (Figure 1.14), which had never before been identified from marine or natural source (Gupta and Sheuer, 1969). The other minor sterols were 24 β -methylcholesta-5,22-dien-3 β -ol, cholest-5-en-3 β -ol, 24-ethylcholest-5-en-3 β -ol and gorgosterol (Figure 1.14) (Gupta and Sheuer, 1969).

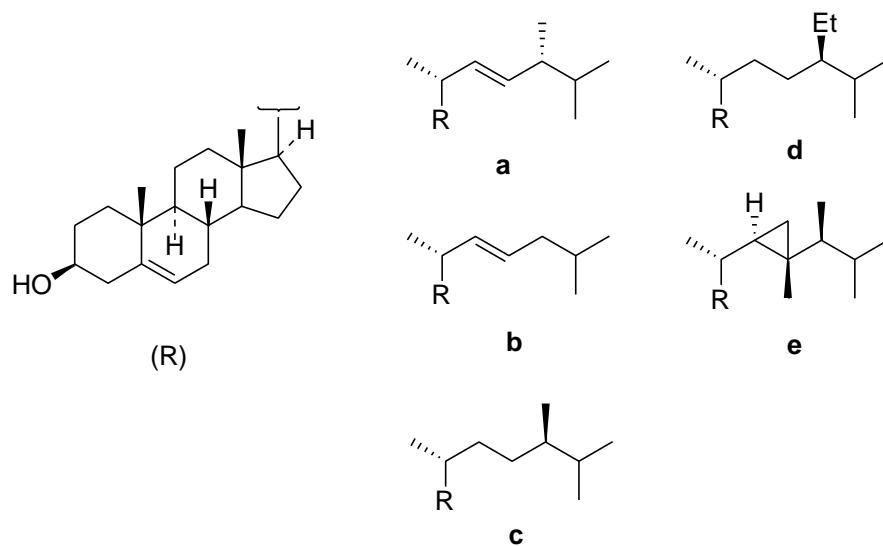


Figure 1.14: Chemical structures of 24 β -methylcholesta-5,22-dien-3 β -ol (**a**), cholest-5-en-3 β -ol (**b**), 24 β -methylcholest-5-en-3 β -ol (**c**), 24-ethylcholest-5-en-3 β -ol (**d**) and gorgosterol (**e**).

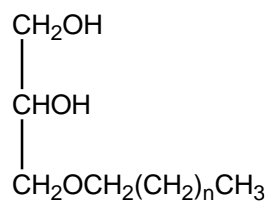


1.2.4 Chemical studies on the genus *Palythoa*

Several studies conducted on *Palythoa liscia*, collected from Mauritius, were successful in isolating various anticancer agents. Pettit and co-worker (1982a) isolated three cell growth inhibitor proteins with a higher mass than PLTX, namely palystatin 1 (mol. wt. $128,000 \pm 12,000$), palystatin 2 (mol. wt. 5×10^5) and palystatin 3 (mol. wt. $> 2 \times 10^7$). The three proteins exhibited anticancer activity when tested against murine P388 lymphocytic leukaemia, both palystatin 2 and 3 showed similar results (ED_{50} 0.01 $\mu\text{g/ml}$) where palystatin 1 exhibited higher potency (ED_{50} $1.3-5.5 \times 10^{-4}$ $\mu\text{g/ml}$) (Pettit *et al.*, 1982a).

The same group also reported the isolation of several lower molecular weight peptides from the same species named 'palystatin A-D' of molecular weights 4,500, 4,000, 3,300 and 3,000, respectively. The peptides exhibited anticancer activity and with ED_{50} values of 0.0023 (palystatin A), 0.020 (palystatin B), 0.0018 (palystatin C) and 0.022 $\mu\text{g/ml}$ (palystatin D) (Pettit *et al.*, 1982b).

In the same year, Pettit and Fujii (1982) reported the isolation of several glycerol ethers from the same species. Two of these glycerols were pure; 1-*O*-hexadecylglycerol (chimylyl alcohol) and 1-*O*-octadecylglycerol (batyl alcohol) (Figure 1.15). Batyl alcohol, in particular, was reported to have anti-inflammatory effects similar to that of hydrocortisone, to accelerate wound healing and afford protection against radiation sickness (Pettit and Fujii, 1982).



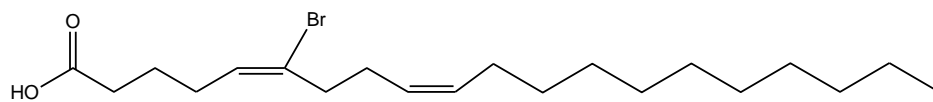
a) $n = 14$

b) $n = 16$

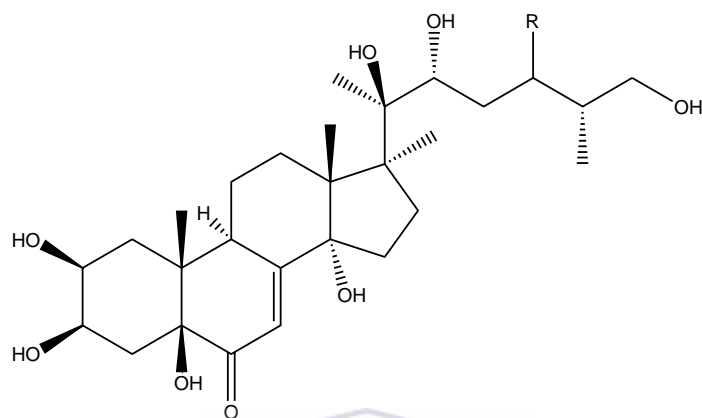
Figure 1.15: Chemical structures of chimyl alcohol (**a**) and batyl alcohol (**b**).

The chemical study of the phospholipids of the Puerto Rican zoanthid *Palythoa caribaeorum* revealed the presence of a new brominated fatty acid; 6-bromo-5,9-eicosadienoic acid (Figure 1.16), along with several $\Delta^{5,9}$ fatty acids; 5,9-octadecadienoic acid, 5,9-eicosadienoic acid, 5,9-docosadienoic acid and 5,9-tetracosadienoic acid. This study proved that phospholipid fatty acids were not only confined to marine sponges as previously suggested (Carballeira and Reyes, 1995).

Also, two new ectasteroids, palythoalones A and B (Figure 1.16), were isolated and identified by spectroscopic and chemical means from the methanolic extract of *P. australiae* collected from Okinawa (Shigemori *et al.*, 1999).



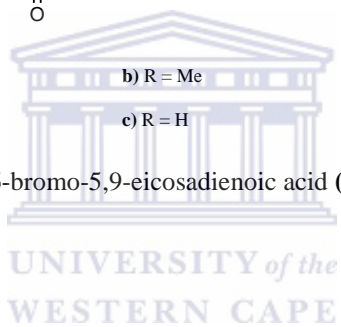
a



b) R = Me

c) R = H

Figure 1.16: Chemical structures of 6-bromo-5,9-eicosadienoic acid (**a**), palytholones A (**b**) and palytholones B (**c**).



1.3 Statement of research problem

For many decades the oceans and seas drew the attention of biologists and chemists for the search of marine natural products formulated within the inhabitants of these vast and harsh environments. The chemical and biological nature of marine natural products is expected to be unique and different from natural products isolated from terrestrial sources. This uniqueness can mainly be attributed to the aqueous nature of the surroundings that the marine organisms find themselves in. Sessile creatures such as soft corals, sponges and zoanthids, had to develop alternative ways to protect their existence from predators and diseases. These organisms may therefore produce secondary metabolites with very unique cytotoxic activities. Cytotoxic natural products are important lead compounds for the discovery of new anticancer agents.

Several chemical studies of the genus *Palythoa* (Coelenterata, Zoanthidae) and in particular the species of *P. tuberculosa* led to the isolation of several unique compounds. Many of these compounds have been shown to be extremely cytotoxic. However, no previous studies have been conducted on *P. tuberculosa* collected from Red sea. It is well known that there is a link between geographical location and both bio- and chemo-diversity. It is therefore possible that chemical composition of *P. tuberculosa* collected from Red sea could be different from *P. tuberculosa* collected from other locations.

1.4 Problem identification

What type of secondary metabolites exists within the *P.tuberculosis* collected from Red Sea? How can we isolate them? Are these metabolites cytotoxic and if they are cytotoxic can they induce apoptosis in human cancer cells?

1.5 Research aim

The aim of this study is to perform both chemical and biological characterization of the marine zoanthoid *P. tuberculosis*. The selected specimen will be extracted using suitable polar organic solvents. The extract will then be subjected to different chromatographic techniques using both simple [Thin Layer Chromatography (TLC) and Open Column Chromatography] and advanced chromatography [High Pressure Liquid Chromatography (HPLC)]. Subsequently, the isolated compounds will be investigated to determine their chemical structures using several spectroscopic techniques including, 1D and 2D NMR and MS. The purified compounds will undergo cytotoxicity evaluations using colorimetric *in vitro* assays on various human cancer cell lines.

Outline of Chapter Two: Chemical study of *Palythoa tuberculosa*

2.1 Abstract

2.2 Methodology of chemical isolation

2.2.1 Reagents and solvents

2.2.2 Solvent evaporation

2.2.3 Chromatography

2.2.3.1 Thin layer chromatography (TLC)

2.2.3.2 Column chromatography

2.2.3.3 High pressure liquid chromatography (HPLC)

2.2.4 Spectroscopy

2.2.4.1 Nuclear magnetic resonance (NMR) spectroscopy

2.2.4.2 Mass spectroscopy (MS)

2.2.4.3 Infrared (IR) spectroscopy

2.2.4.4 Optical rotation measurements

2.3 Sample collection and identification

2.4 Extraction of the marine sample

2.5 Fractionation of the total extract

2.6 Isolation of the pure compounds

2.6.1 Isolation of palysterols C, E and G

2.6.2 Isolation of palysterol F

2.6.3 Isolation of palysterol B

2.6.4 Isolation of palysterols A and D

2.7 Spectroscopic data of the isolated compounds

2.8 Results and discussion

2.8.1 Analysis of palysterols A

2.8.2 Analysis of palysterols B

2.8.3 Analysis of palysterols C

2.8.4 Analysis of palysterols D

2.8.5 Analysis of palysterols E

2.8.6 Analysis of palysterols F

2.8.7 Analysis of palysterols G

CHAPTER TWO

CHEMICAL STUDY OF *Palythoa tuberculosa*

2.1 Abstract

The chemistry of *P. tuberculosa* attracted the attention for its structurally complex and highly toxic content, in particular PLTX. Red Sea is a unique marine source which contains highly diversified marine fauna including *P. tuberculosa*. Neither chemical nor biological studies have been conducted on *P. tuberculosa* growing in the Red Sea. These factors provided the justification to chemically and biologically evaluate the constituents of the *P. tuberculosa* from the Red Sea. The chemical study of *P. tuberculosa* resulted in the isolation of seven polyhydroxylated sterols viz; 24-methylenecholest-5-ene-1 α ,3 β ,11 α -triol (palysterol A), 24-methylenecholest-5-ene-1 α ,3 β ,11 α ,18-tetrol-1-acetate (palysterol B), 24-methylene-1 α ,3 β ,11 α -trihydroxycholest-5-en-18-al-1-acetate (palysterol C), cholesta-5,22(23),24(28)-trien-1 α ,3 β ,11 α -triol (palysterol D), cholesta-5,22(23),24(28)-trien-1 α ,3 β ,11 α -triol 1-acetate (palysterols E), cholesta-5,22(23),24(28)-trien-1 α ,3 β ,11 α ,18-tetrol-1,18-diacetate (palysterol F), and cholesta-5,22(23),24(28)-trien-1 α ,3 β ,11 α ,trihydroxy-18-al 1-acetate (palysterols G). The presence of polyhydroxylated sterols in *P. tuberculosa* was reported early in 1961 as mentioned in section 1.2.3. In this study, no compounds related to PLTX were detected as indicated by the extensive NMR measurements of the different main fractions obtained from the methanolic extract of *P. tuberculosa*. This chemical difference highlights the effect of the environmental and ecological factors on determining the chemical contents of *P. tuberculosa*.

2.2 Methodology of chemical isolation

2.2.1 Reagents and solvents

Ethanol.....	Crest Chemicals (SA)
Methanol.....	Crest Chemicals (SA)
Hexane.....	Crest Chemicals (SA)
Ethyl acetate.....	Kimix (SA)
Dichloromethane.....	Kimix (SA)
Sulphuric acid.....	Kimix (SA)
Deuterated chloroform.....	Merck, Germany
Vanillin.....	Merck-Schuchardt, Germany.

2.2.2 Solvent evaporation

Rotavapor model Buchi Rotavapor RE 111 was used for solvent evaporation at 40 °C and 14 mbar.

2.2.3 Chromatography

2.2.3.1 Thin layer chromatography (TLC)

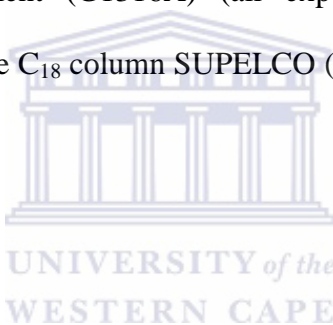
Pre-coated plates of silica gel 60 F₂₅₄ (Merck, Germany) was used for TLC analysis. Visualization of TLC plates was done by observing the bands “spots” under UV at λ_{254} nm and λ_{366} nm using UV lamp (CAMAG, Switzerland), and by spraying with the vanillin/sulphuric acid reagent according to Wagner *et al.*, (1984).

2.2.3.2 Column chromatography

Glass columns (different diameters) packed with either silica gel 60 (0.063-0.0200 mm) (Merck), or alumina (Aluminium oxide Fluka typ 507C from Fluka AG, Buchs SG, Switzerland) were used for column chromatography. Size-exclusion chromatography was carried out using Sephadex[®] LH-20 (Pharmacia).

2.2.3.3 High Pressure Liquid Chromatography (HPLC)

Sample purification was carried out using Agilent Technologies 1200 series, equipped with UV detector, manual injector, quaternary pump (G1311A), vacuum degasser (G1322A), column compartment (G1316A) (all experiments were done at room temperature) and reversed phase C₁₈ column SUPELCO (25 x 1 cm, 5 μm). The flow rate was set at 1.5 mL/min.



2.2.4 Spectroscopy

2.2.4.1 Nuclear magnetic resonance (NMR) spectroscopy

NMR spectra were recorded at 25 °C, using CDCl₃ as solvent, on a Varian SYSTEM 500 NMR spectrometer (¹H 500 MHz, ¹³C 125 MHz) equipped with a 5-mm HCN cold probe. Chemical shifts of ¹H (δ_H) and ¹³C (δ_C) in ppm were determined relative to tetramethylsilane.

2.2.4.2 Mass spectroscopy (MS)

High resolution mass spectroscopy (HRMS) analysis were conducted using an Agilent 1200 LC binary pump coupled to an Agilent QTOF. Accurate Mass mass spectrometer using electrospray ionization (ESI) interface working in the positive mode.

2.2.4.3 Infrared (IR) spectroscopy

Attenuated total internal reflectance FTIR measurements were carried out using Spectrum 100 (PerkinElmer). Spectra recording were accomplished using the interface “Spectrum”. Dichloromethane was used to dissolve the samples.

2.2.4.4 Optical rotation measurements

Optical activity measurements were conducted using Anton Paar MCP 200 Polarimeter. The following conditions were used: sample concentration: 0.1g/mL in dichloromethane; wavelength: 589 nm; cell temperature: 25 °C.

2.3 Sample collection and identification

The Red Sea *Palythoa tuberculosa* was collected in May 2010, at depth of 2-3 meters from Hurghada, Egypt. The tissue was kept in MeOH. The material was collected by Dr. A. Ali (National Institute of Oceanography and Fisheries, Suez City, Egypt) and identified by Dr. S. Parker-Nance (Zoology department, Nelson Mandela Metropolitan University) and Dr. A. Ali. A voucher specimen is kept at Institute of Oceanography and Fisheries (Suez, Egypt).

2.4 Extraction of the marine sample

The fresh sliced bodies of ~1.0 kg of the collected species were blended with MeOH. The extract was filtered using Whatman filter paper, the residue was washed twice with fresh MeOH. The total extract was concentrated under vacuum and partitioned between EtOAc and H₂O. The water fraction was dried and the residue was washed with methanol and combined to the EtOAc fraction.

2.5 Fractionation of the total extract

The extract (20 g) was applied to silica gel column (5 x 30 cm) and eluted using mixture of hexane/EtOAc/methanol (Table 2.1).

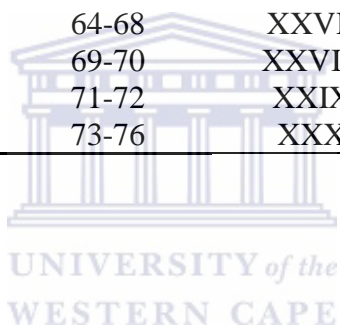
Table 2.1: Solvent system used for fractionation of the total extract of *P. tuberculosa*.

Solvent volume	Solvent system	Fractions collected
1 L	Hexane	1-4
1 L	Hexane : Ethyl acetate 95:5	5-8
1 L	Hexane : Ethyl acetate 90:10	9-12
1 L	Hexane : Ethyl acetate 85:15	13-16
2 L	Hexane : Ethyl acetate 80:20	17-24
1 L	Hexane : Ethyl acetate 75:25	25-28
2 L	Hexane : Ethyl acetate 70:30	29-36
1 L	Hexane : Ethyl acetate 65:35	37-40
2 L	Hexane : Ethyl acetate 60:40	41-48
1 L	Hexane : Ethyl acetate 55:45	49-52
2 L	Hexane : Ethyl acetate 50:50	53-60
1 L	Hexane : Ethyl acetate 40:60	61-64
1 L	Hexane : Ethyl acetate 30:70	65-68
1 L	Hexane : Ethyl acetate 20:80	69-72
1 L	Hexane : Ethyl acetate 10:90	73-76
1 L	Ethyl acetate 100%	77-80
1 L	Ethyl acetate : Methanol 95:5	81-84
1 L	Ethyl acetate : Methanol 80:20	85-88
1 L	Ethyl acetate : Methanol 50:50	89-92
1.5 L	Methanol 100 %	93

93 different fractions (volume = 250 mL) were collected. The fractions were concentrated on the rota-evaporator and chromatographed on TLC plates using different solvent systems; hexane:EtOAc 9:1 and DCM:MeOH 5%. The fractions were pooled together according to their TLC profiles (Figures 2.1) and were designated roman numbers (Table 2.2).

Table 2.2: Fractions obtained upon fractionation of the total extract of *P.tuberculosis*.

Fractions collected	Designated number	Fractions collected	Designated number	Fractions collected	Designated number
1-4	I	37-38	XVI	77, 78	XXXI
5-7	II	39-40	XVII	79-81	XXXII
8-9	III	41-42	XVIII	82-83	XXXIII
10	IV	43-45	XIX	84-85	XXXIV
11	V	46-47	XX	86-88	XXXV
12-14	VI	48-49	XXI	89-91	XXXVI
15-16	VII	50-51	XXII	92-93	XXXVII
17-19	VIII	52-53	XXIII		
20-22	IX	54-56	XXIV		
23-24	X	57-58	XXV		
25-27	XI	59-63	XXVI		
28-30	XII	64-68	XXVII		
31-32	XIII	69-70	XXVIII		
33-34	XIV	71-72	XXIX		
35-36	XV	73-76	XXX		



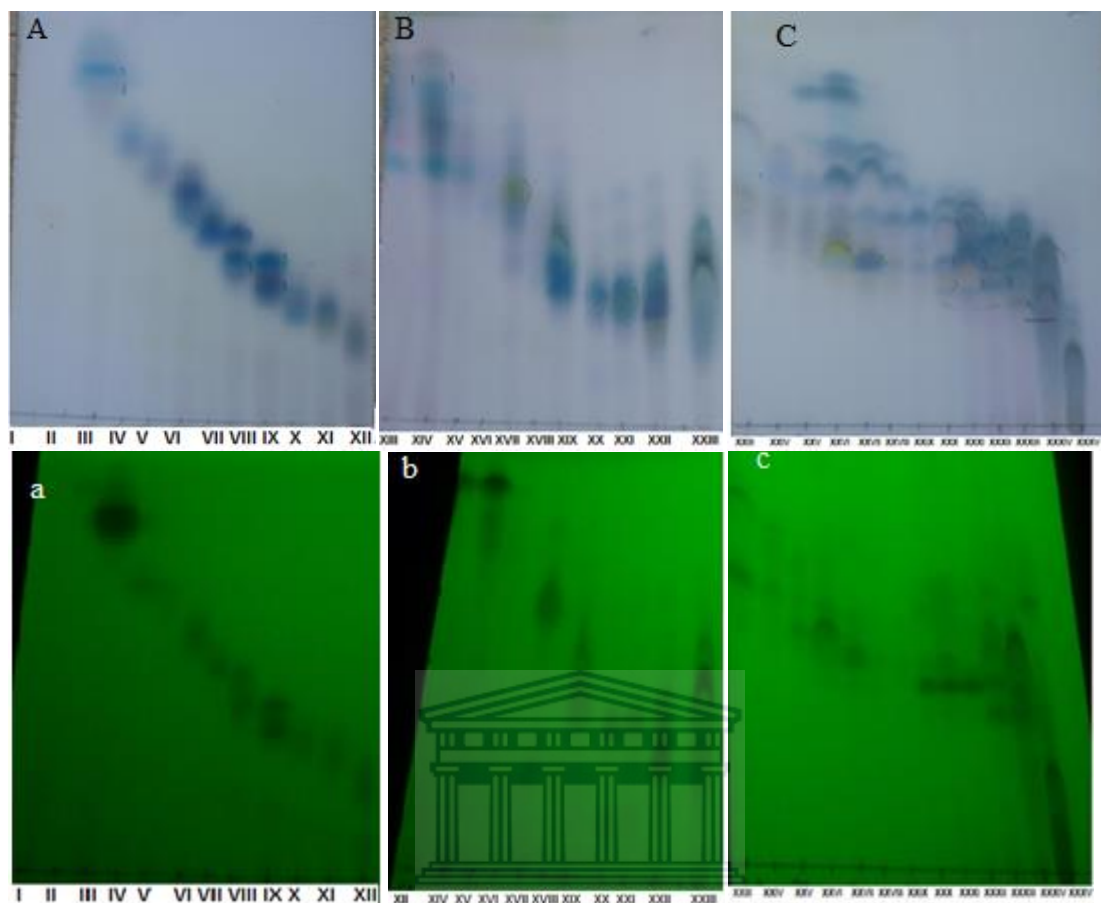


Figure 2.1: TLC profile of the main fractions after spraying with H₂SO₄/vanillin (A, B and C) and under UV light (a, b and c).

*TLC plate (A) of main fractions (I-XII) was developed using hexane:EtOAc 70:30

*TLC plate (B) of main fractions (XII-XXIII) was developed using hexane:EtOAc 50:50

*TLC plate (C) of main fractions (XXIII -XXXVI) was developed using DCM:MeOH 7%.

2.6 Isolation of the pure compounds

2.6.1 Isolation of palysterols C, E and G.

Main fraction XXII (100 mg) was adsorbed on silica gel and fractionated on an open column using gradient solvent system of hexane:EtOAc (80:20 to 0:100). The sub-fractions collected were combined together according to the TLC profile (Figure 2.2).

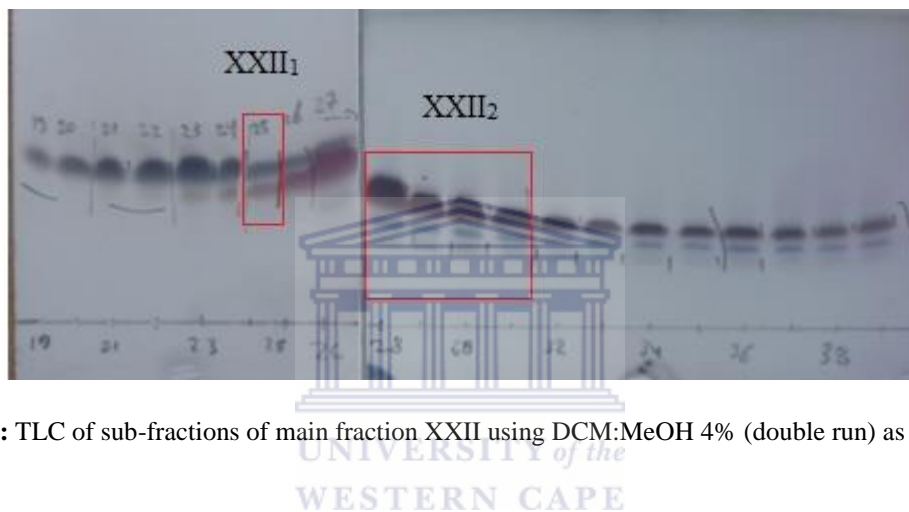


Figure 2.2: TLC of sub-fractions of main fraction XXII using DCM:MeOH 4% (double run) as mobile phase.

sub-fraction XXII₁ (Figure 2.2) was injected to the HPLC and eluted using gradient solvent system of MeOH and de-ionized water (DIW) (90:10 to 100% MeOH in 20 min, then 100% MeOH for 10 min). The peak at 25.5 min (Figure 2.3) was collected and gave palysterol E (1.8 mg). The sub-fraction XXII₂ (Figure 2.2) was also injected to the HPLC and eluted using gradient solvent system of MeOH:DIW (85:15 to 95:5 in 20 min, then 95:5 to 100% MeOH in 15 min). Two quantifiable peaks, at 25.2 and 27.1 min (Figure 2.4), were collected. The first peak gave palysterol G (6.6 mg). While the second peak (XXII₂₋₁) (41.6 mg) was injected to the HPLC using gradient solvent system of MeOH:DIW (90:10 to 100% MeOH in 10 min). The peak at 16.9 min (Figure 2.5) was collected and gave palysterol C (30 mg).

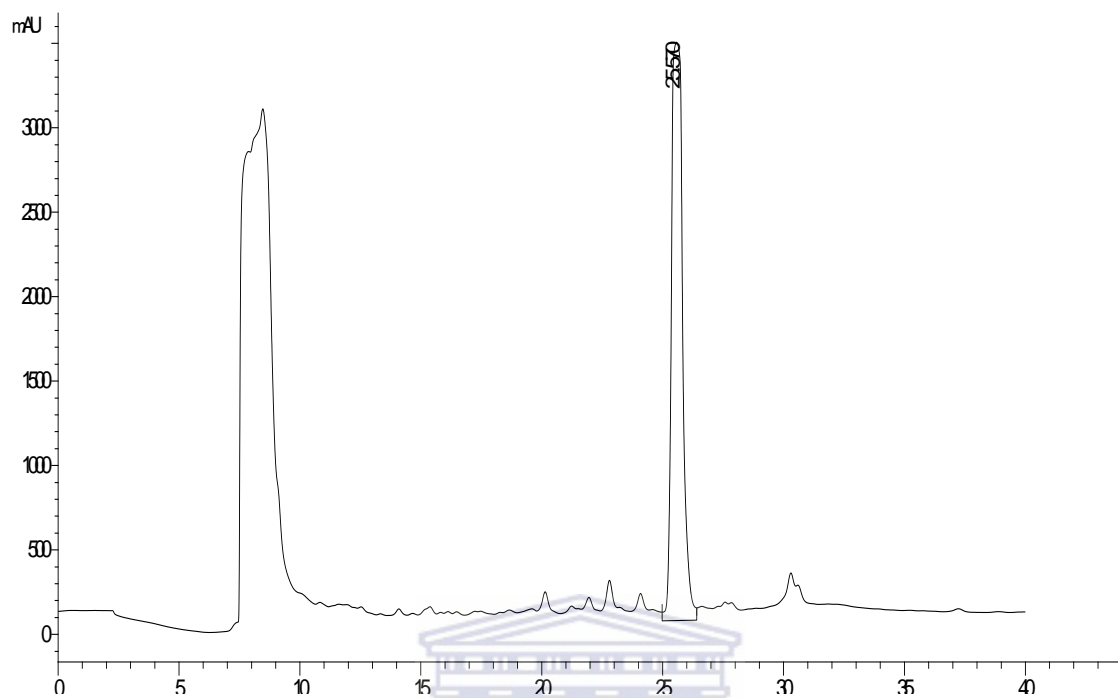


Figure 2.3: HPLC chromatogram of sub-fraction XXII₁*.

*Conditions:

Solvent	MeOH:DIW 90:10 to 100% MeOH in 20 min
Column	SUPELCO, RP18 (25X2.1 cm)
Flow rate	1.5 mL/min
Detection	UV at λ 220 nm

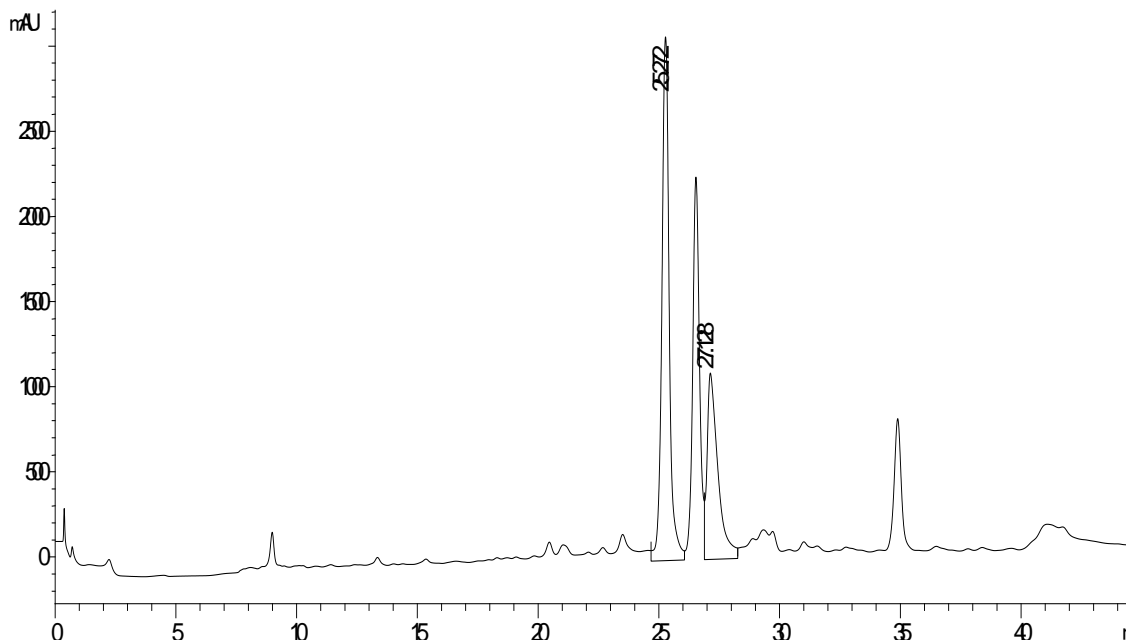


Figure 2.4: HPLC chromatogram of sub-fraction XXII₂*.

*Conditions:

Solvent	MeOH:DIW (85:15 to 95:5 in 20 min, then from 95:5 to 100% MeOH in 15 min)
Column	SUPELCO, RP18 (25X2.1 cm)
Flow rate	1.5 mL/min
Detection	UV at λ 220 nm

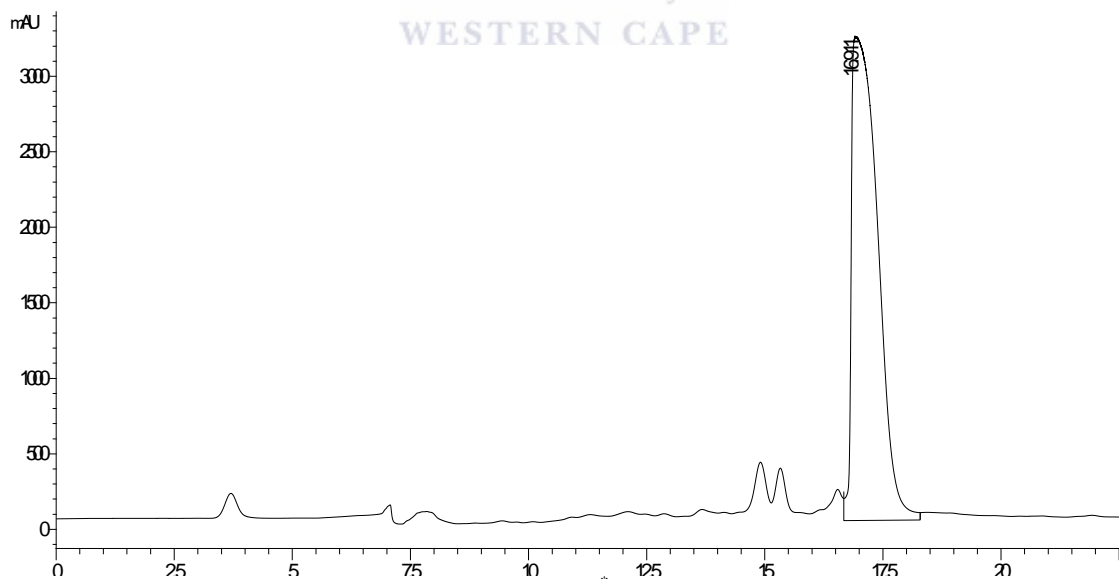


Figure 2.5: HPLC chromatogram of sub-fraction XXII₂₋₁*.

*Conditions:

Solvent	MeOH:DIW (90:10 to 100% MeOH in 10 min)
Column	SUPELCO, RP18 (25X2.1 cm)
Flow rate	1.5 mL/min
Detection	UV at λ 220 nm

2.6.2 Isolation of palysterol F

Main fraction XXV (90 mg) was injected to the HPLC and eluted using gradient solvent system of MeOH:DIW (80:20 to 85:15 in 20 min, then to 90:10 in 10 min, then to 100% MeOH in 10 min). The peak (XXV₁) (20 mg), eluted at 32.2 min (Figure 2.6), was re-injected to the HPLC using gradient solvent system of MeOH:DIW (80:20 to 85:15 in 5 min, then to 95:5 in 30 min, then to 100% MeOH in 5 min). The peak eluted at 37.3 min (Figure 2.7) was collected and gave palysterol F (6 mg).

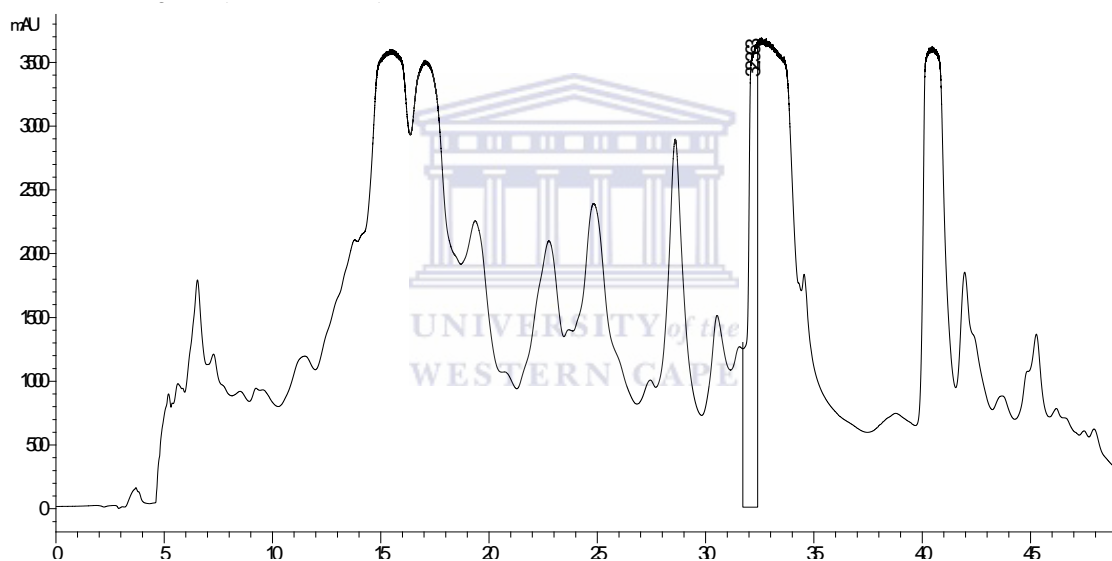


Figure 2.6: HPLC chromatogram of main fraction XXV*.

*Conditions:

Solvent	MeOH:DIW (80:20 to 85:15 in 20 min, then from 85:15 to 90:10 in 10 min, followed by increase to 100% MeOH in 10 min)
Column	SUPELCO, RP18 (25X2.1 cm)
Flow rate	1.5 mL/min
Detection	UV at λ 220 nm

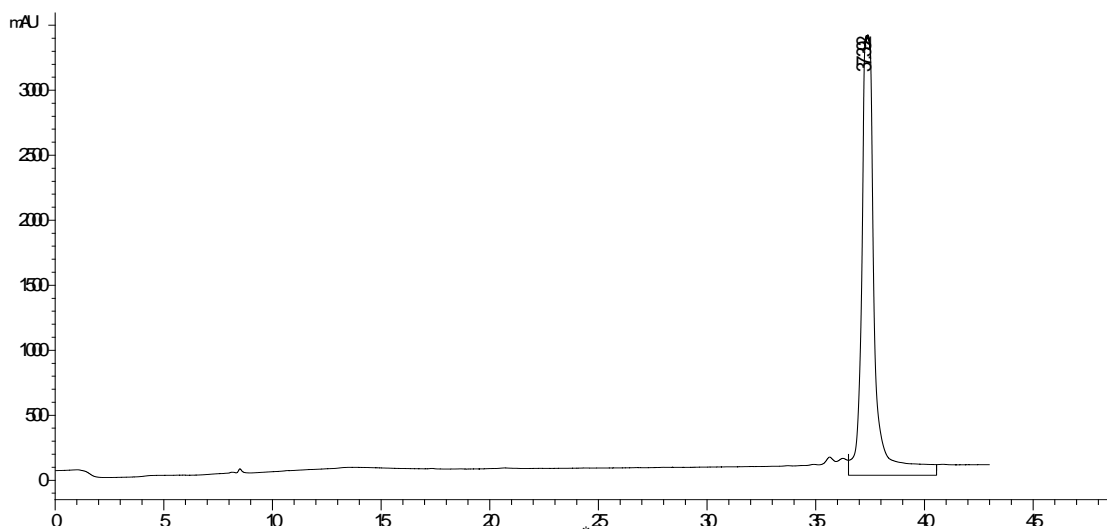


Figure 2.7: HPLC chromatogram of sub-fraction XXV₁.*

*Conditions:

Solvent	MeOH:DIW (80:20 to 85:15 in 5 min, then to 95:5 in 30 min, followed by increase to 100% MeOH in 5 min)
Column	SUPELCO, RP18 (25X2.1 cm)
Flow rate	1.5 mL/min
Detection	UV at λ 220 nm

2.6.3 Isolation of palysterol B

Main fraction XXVI (300 mg) was adsorbed on alumina and fractionated on an open column and eluted using gradient solvent system of DCM/MeOH of increasing polarity (0 to 10% MeOH). The sub-fractions were concentrated and developed in a TLC plate. The sub-fraction XXVI₁ (100 mg) (Figure 2.8) was adsorbed on silica gel and fractionated on a column using solvent system of hexane:EtOAc (55:45). Sub-fraction XXVI₁₋₁ (46 mg) was collected from the column and injected to the HPLC using gradient solvent system of MeOH:DIW (80:20 to 100% MeOH in 30 min). The peaks eluted from 30.0 to 35.5 min (Figure 2.9) were collected and gave Palysterol B (5.3 mg).

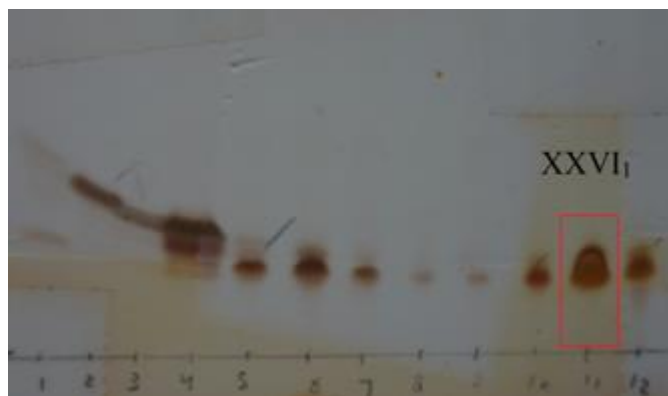


Figure 2.8: Collective TLC of main fraction XXVI, developed using DCM:MeOH 6%.

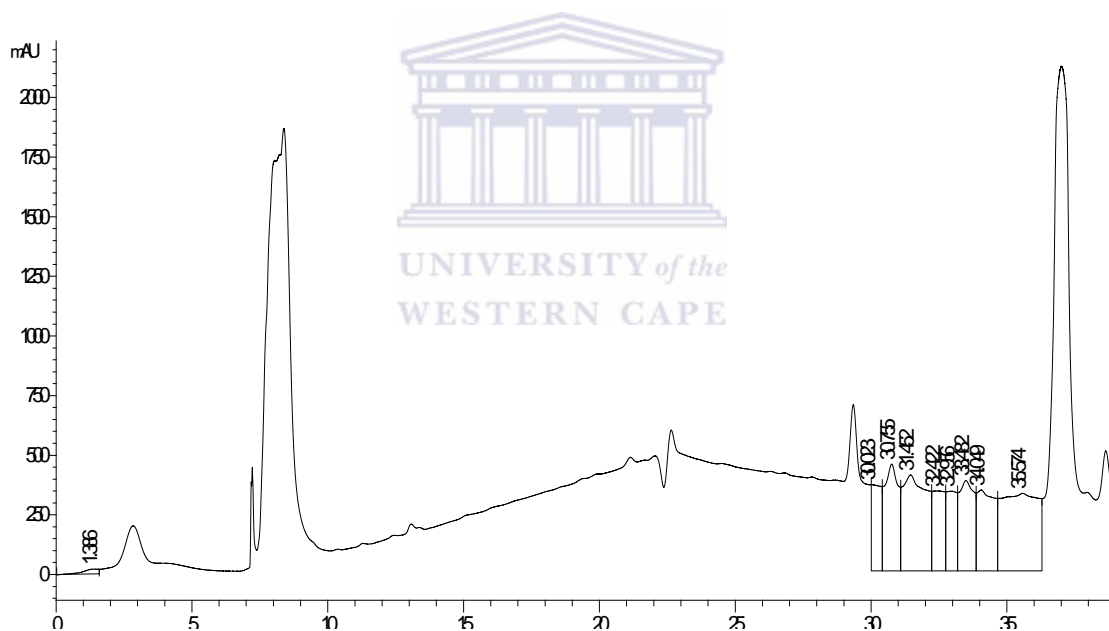


Figure 2.9: HPLC chromatogram of sub-fraction XXVI_{1.1}.

*Conditions:

Solvent	MeOH:DIW (80:20 increasing to 100% MeOH in 30 minutes)
Column	SUPELCO, RP18 (25X2.1 cm)
Flow rate	1.5 mL/min
Detection	UV at λ 220 nm

2.6.4 Isolation of palysterol A and D

Main fraction XXVII (188 mg) was adsorbed on alumina oxide and fractionated on an open column using gradient solvent system of DCM:MeOH (from 0.1% DCM to 3%). The sub-fraction XXVII₁ (35 mg) was collected and then injected to the HPLC using gradient solvent system of MeOH:DIW (80:20 to 100% MeOH in 30 min) to give palysterol D (3.8 mg) at 36.9 min and palysterol A (3.5 mg) at 38.7 min (Figure 2.10).

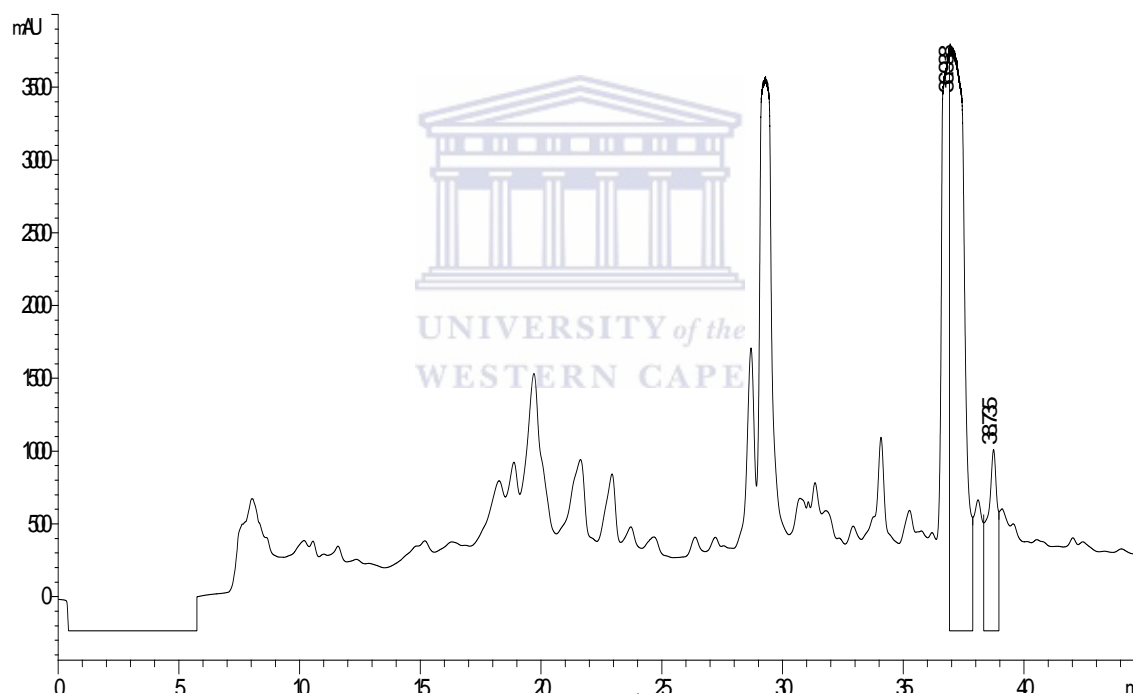
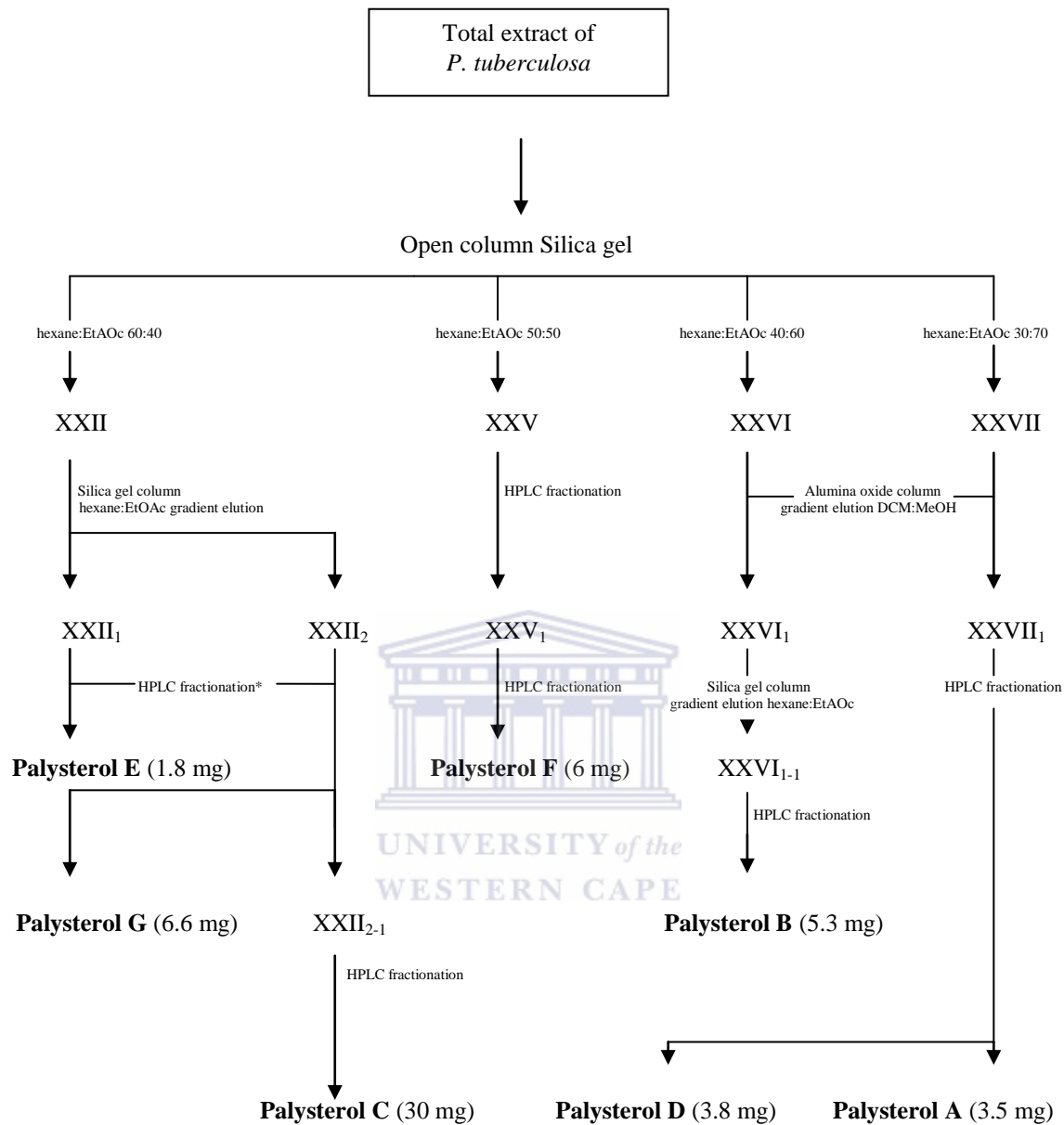


Figure 2.10: HPLC chromatogram of sub-fraction XXVII₁.*

*Conditions:

Solvent	MeOH:DIW (80:20 to 100% MeOH in 30 min)
Column	SUPELCO, RP18 (25X2.1 cm)
Flow rate	1.5 mL/min
Detection	UV at λ 220 nm



Scheme 2.1: A flow diagram for the isolated compounds from *P. tuberculosis*.

*All HPLC fractionations were done using different mixtures of MeOH:DIW.

2.7 Spectroscopic data of the isolated compounds

Palysterol A: white, amorphous powder; IR: 3308, 3054, 2942, 2305, 1640, 1421, 1265, 1051, 896, 739, 705 cm^{-1} ; ^1H NMR (CDCl_3) and ^{13}C NMR (CDCl_3): see table 2.3. HRMS m/z 430.3462 $[\text{M}]^+$ (calcd for $\text{C}_{28}\text{H}_{46}\text{O}_3$, 430.3447).

Palysterol B: white, amorphous powder; $[\alpha]_{\text{D}}^{25}$ -1.5 (c 0.1, DCM); IR: 3054, 2305, 1422, 1265, 1050, 895, 739, 705 cm^{-1} ; ^1H NMR (CDCl_3) and ^{13}C NMR (CDCl_3): see table 2.3. HRMS m/z 488.3510 $[\text{M}]^+$ (calcd for $\text{C}_{30}\text{H}_{48}\text{O}_5$, 488.3502).

Palysterol C: white, amorphous powder; $[\alpha]_{\text{D}}^{25}$ -2.5 (c 0.1, DCM); IR: 3944, 3424, 3054, 2962, 2305, 1713, 1421, 1375, 1265, 1049, 896, 739, 705 cm^{-1} ; ^1H NMR (CDCl_3) and ^{13}C NMR (CDCl_3): see table 2.3. HRMS m/z 486.3357 $[\text{M}]^+$ (calcd for $\text{C}_{30}\text{H}_{46}\text{O}_5$, 486.3345).

Palysterol D: white, amorphous powder; $[\alpha]_{\text{D}}^{25}$ -14 (c 0.1, DCM); IR: 3945, 3691, 3054, 2986, 2305, 1421, 1265, 896, 735, 705 cm^{-1} ; ^1H NMR (CDCl_3) and ^{13}C NMR (CDCl_3): see table 2.3. HRMS m/z 428.3309 $[\text{M}]^+$ (calcd for $\text{C}_{28}\text{H}_{44}\text{O}_3$, 428.3290).

Palysterol E: white, amorphous powder; $[\alpha]_{\text{D}}^{25}$ -9 (c 0.1, DCM); IR: 3054, 2986, 2305, 1421, 1265, 896, 753, 705 cm^{-1} ; ^1H NMR (CDCl_3) and ^{13}C NMR (CDCl_3): see table 2.3. HRMS m/z 470.3417 $[\text{M}]^+$ (calcd for $\text{C}_{30}\text{H}_{46}\text{O}_4$, 470.3396).

Palysterol F: white, amorphous powder; $[\alpha]_{\text{D}}^{25}$ 10.5 (c 0.1, DCM); IR: 3944, 3690, 3599, 3054, 2986, 2685, 2410, 2305, 1731, 1604, 1421, 1375, 1265, 1143, 1053, 1019, 896, 735, 705 cm^{-1} ; ^1H NMR (CDCl_3) and ^{13}C NMR (CDCl_3): see table 2.3. HRMS m/z 528.3451 $[\text{M}]^+$ (calcd for $\text{C}_{32}\text{H}_{48}\text{O}_6$, 528.3451).

Palysterol G: white, amorphous powder; $[\alpha]_D^{25}$ 18 (*c* 0.1, DCM); IR: 3463, 3054, 2985, 2305, 1719, 1422, 1374, 1265, 1051, 896, 739, 705 cm^{-1} ; ^1H NMR (CDCl_3) and ^{13}C NMR (CDCl_3): see table 2.3. HRMS m/z 484.3193 $[\text{M}]^+$ (calcd for $\text{C}_{30}\text{H}_{44}\text{O}_5$, 484.3189).

2.8 Results and discussion

The isolated palysterols were fully characterized by 1D (^1H and ^{13}C) and 2D NMR experiments, including gCOSY, TOCSY, multiplicity-edited gHSQC and gHMBC. ^1H and ^{13}C NMR chemical shifts observed are summarized in table 2.3.

2.8.1 Analysis of Palysterol A

The molecular formula of Palysterol A (Figure 2.11) was determined by HRMS as $\text{C}_{28}\text{H}_{46}\text{O}_3$. The ^1H NMR spectrum of palysterol A (Figure 2.12) exhibited the signals for five methyls at δ 1.03 (3H, d, $J = 6.8$ Hz, H-26), 1.02 (3H, d, $J = 6.8$ Hz, H-27), 0.96 (3H, d, $J = 6.6$ Hz, H-21), 1.13 (3H, s, H-19), and 0.67 (3H, s, H-18); an olefinic proton at δ 5.56 (1H, td, $J = 5.6, 2.0$ Hz, H-6), a methylene terminal group at δ 4.71 and 4.65 (2H, brd, H-28) and three oxygenated methines at δ 4.21 (1H, t, $J = 3.3$ Hz, H-1), 4.07 (1H, td, $J = 10.3, 5.6$ Hz, H-11) and 3.97 (1H, tt, $J = 11.6, 4.7$ Hz, H-3). The ^{13}C NMR spectroscopic data (Figure 2.13) (Table 2.3) together with analysis of its multiplicity-edited gHSQC spectrum (Figure 2.15) indicated 28 carbons, including five methyls, ten methylenes (one olefinic), nine methines (three oxygenated and one olefinic), and four quaternary carbons (two olefinic). From the gHMBC spectrum correlations (Figures 2.16 and 2.17), the structure of this compound was fully established. The relative stereochemistry of palysterol A was mainly assigned by a ROESY spectrum. Relevant correlations showed, mainly between Me-19 (δ 1.13) and H-1 and H-11, and between H-4 α (δ 2.65) and H-3,

as well as between Me-18 (δ 0.67) and H-8, H-11 and H-20. These led us to establish the structure as 24-methylenecholest-5-ene-1 α ,3 β ,11 α -triol. The structure was confirmed by comparing the data with those published by Jagodzinska *et al.* (1985).

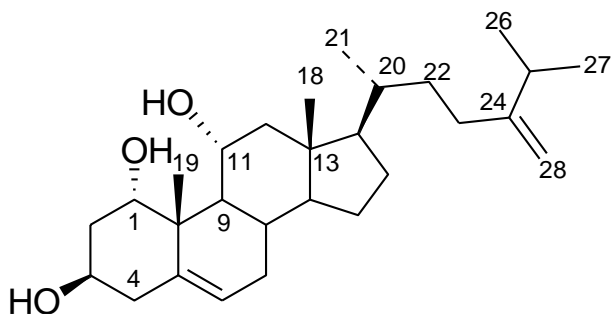


Figure 2.11: Chemical structure of palysterol A.

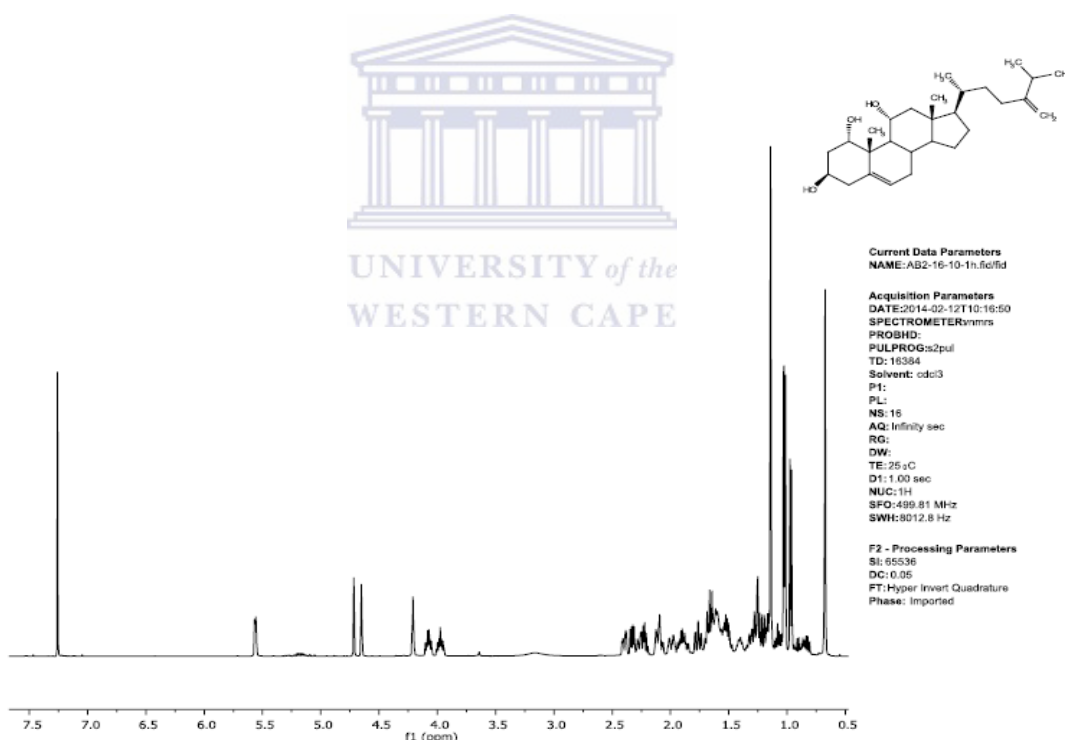


Figure 2.12: ^1H NMR (500 MHz, CDCl_3) of palysterol A.

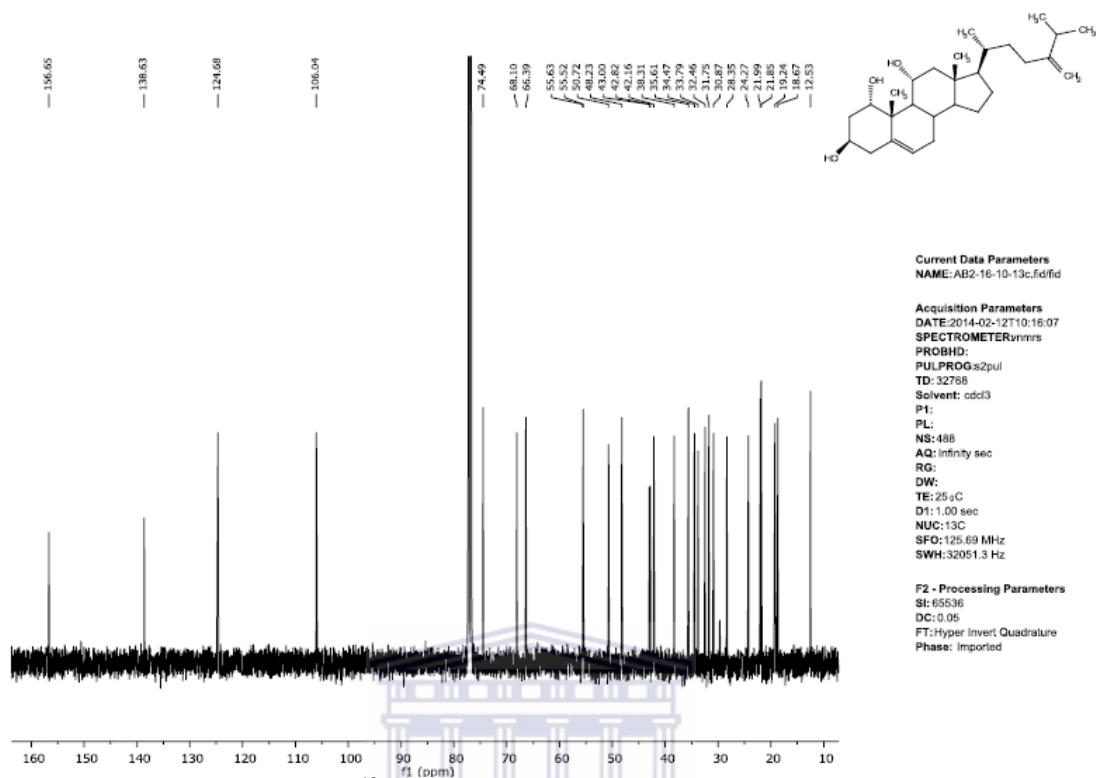


Figure 2.13: ^{13}C NMR (125 MHz, CDCl_3) of palysterol A.

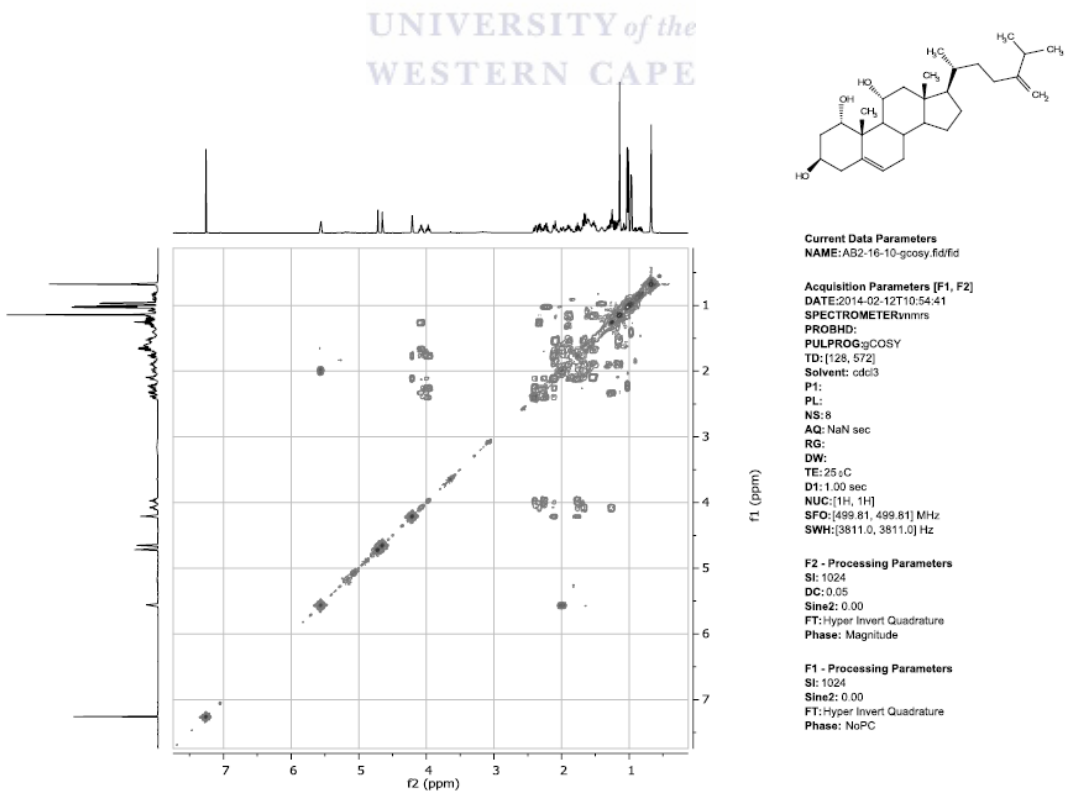


Figure 2.14: gCOSY (500 MHz, CDCl_3) of palysterol A.

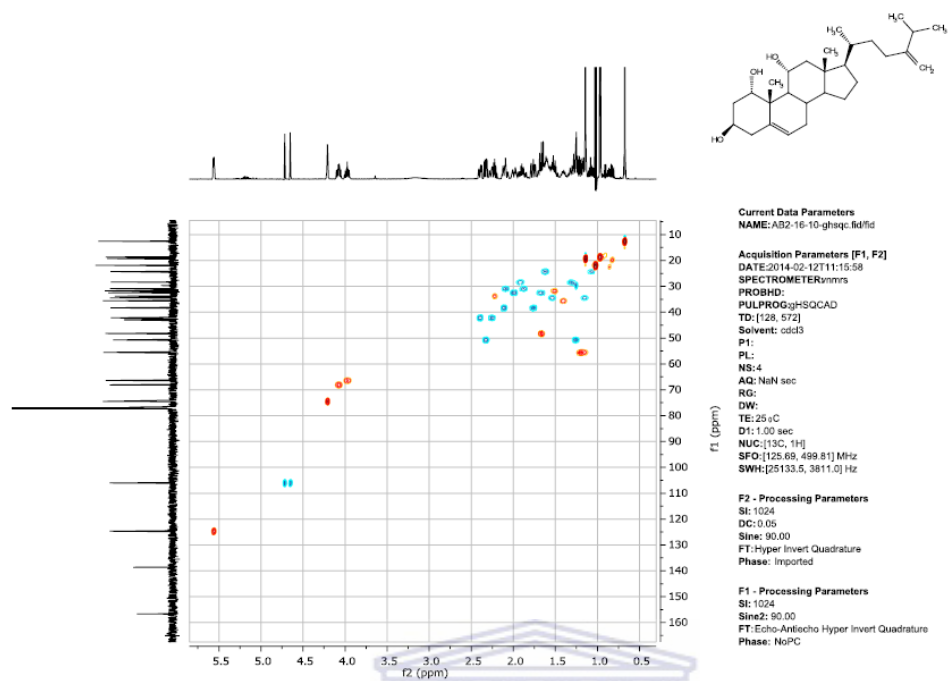


Figure 2.15: Multiplicity-edited gHSQC (methylene: blue cross peaks; methyl and methine: red cross peaks) (500 MHz, CDCl₃) of palysterol A.

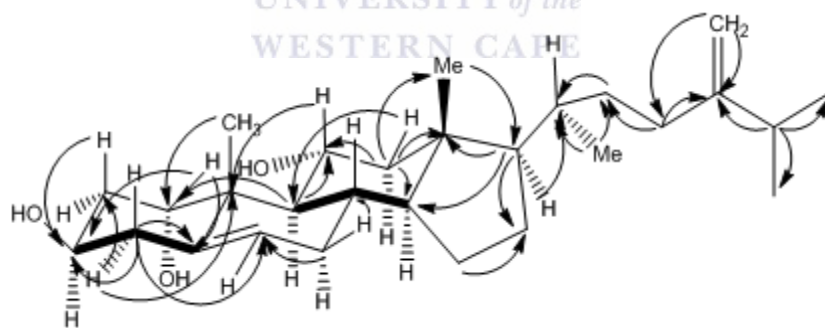


Figure 2.16: Selected gHMBC correlations observed for palysterol A.

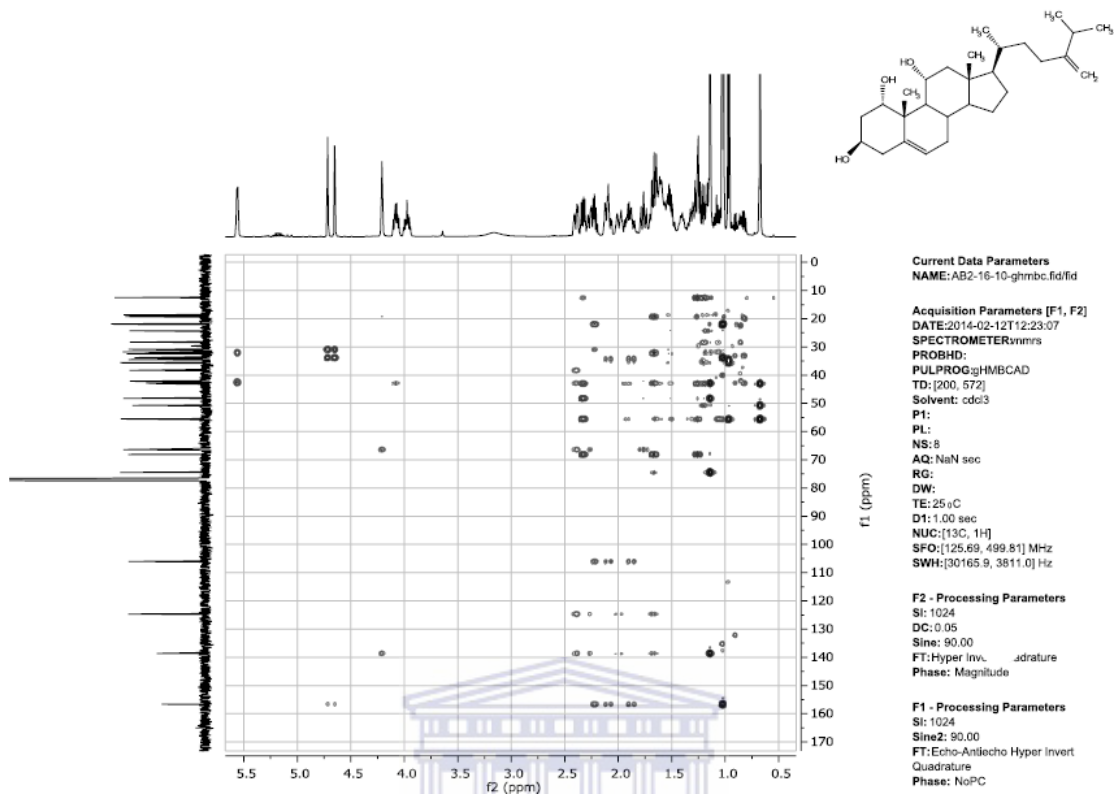


Figure 2.17: gHMBC (500 MHz, CDCl₃) of palysterol A.

UNIVERSITY of the
WESTERN CAPE

2.8.2 Analysis of palysterol B

The NMR spectroscopic data (Figures 2.19 and 2.20) of palysterol B (C₃₀H₄₈O₅) (Figure 2.18) showed similar spectra with those of palysterol A. The ¹³C NMR data (Table 2.3) together with analysis of its multiplicity-edited gHSQC spectrum (Figure 2.22) indicated 30 carbons, including five methyls, eleven methylenes (one oxygenated and one olefinic), nine methines (three oxygenated and one olefinic) and five quaternary carbons (two olefinic and one carbonyl carbons). The COSY spectrum (Figure 2.21) showed correlations between H-2/H-1 and H-3; H-11/H-12; and H-6/H-7. The only differences with palysterol A were the lack of the Me-18 resonance and the presence of an acetoxy group (δ_{H} 2.05 s, 3H; δ_{C} 171.64 s and 21.55 q) and a new oxygenated-methylene group

(δ_H 3.59 s, 2H; δ_C 61.46 t). The gHMBC spectrum (Figures 2.23 and 2.24) showed, in essence, the same relevant correlations of palysterol A (Figure 2.17). New correlations between the acetoxy-carbonyl carbon and H-1 and between the oxygenated-methylene carbon and H-12, H-14 and H-17 were observed. Finally, the ROESY spectrum (Figure 2.25) showed correlations between H-18 (δ_H 3.59) and H-8 (δ_H 1.45), H-11 (δ_H 3.99) and H-20 (δ_H 1.60). From the data above, the structure was identified as 24-methylenecholest-5-ene-1 α ,3 β ,11 α ,18-tetrol 1-acetate. To the best of our knowledge, palysterol B was not isolated before from any other natural source.

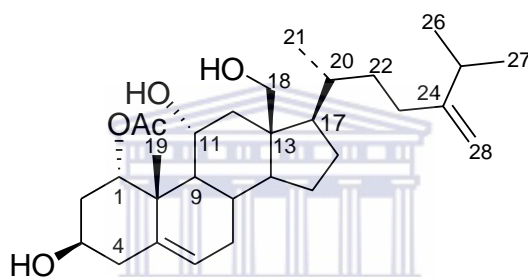


Figure 2.18: Chemical structure of palysterol B.

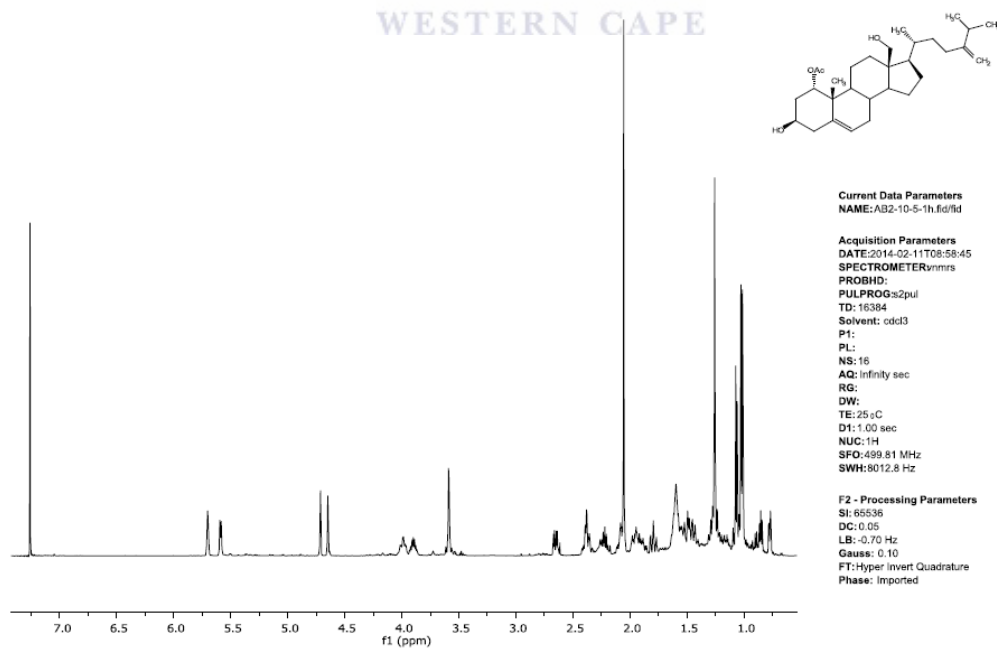


Figure 2.19: ¹H NMR (500 MHz, CDCl₃) of palysterol B.

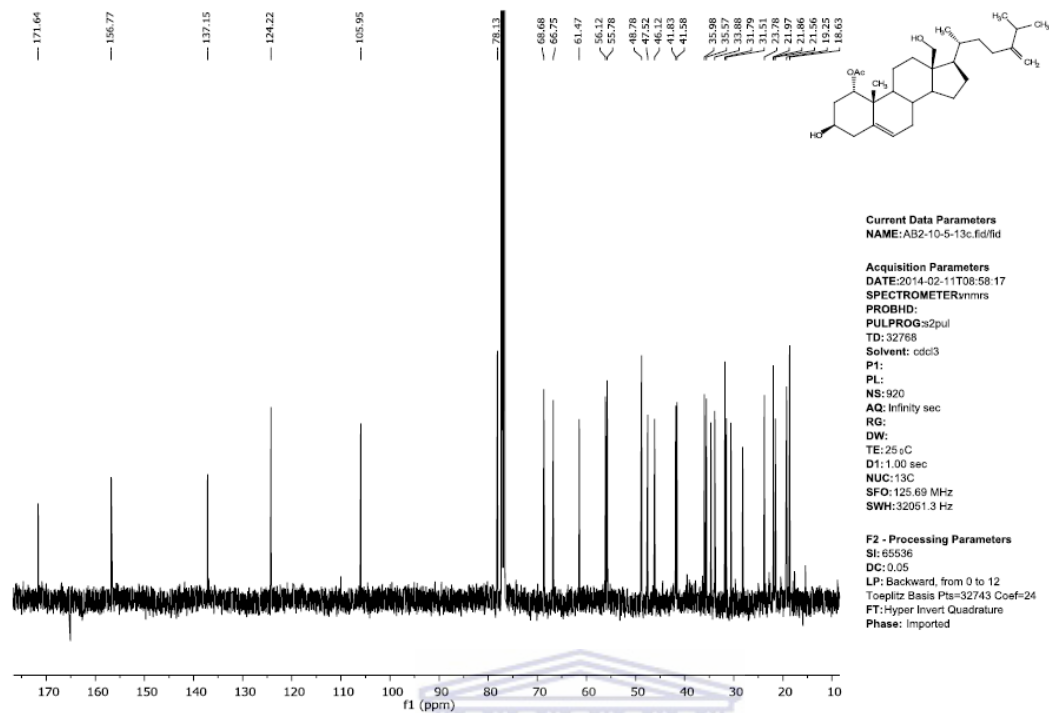


Figure 2.20: ^{13}C NMR (125 MHz, CDCl_3) of palysterol B.

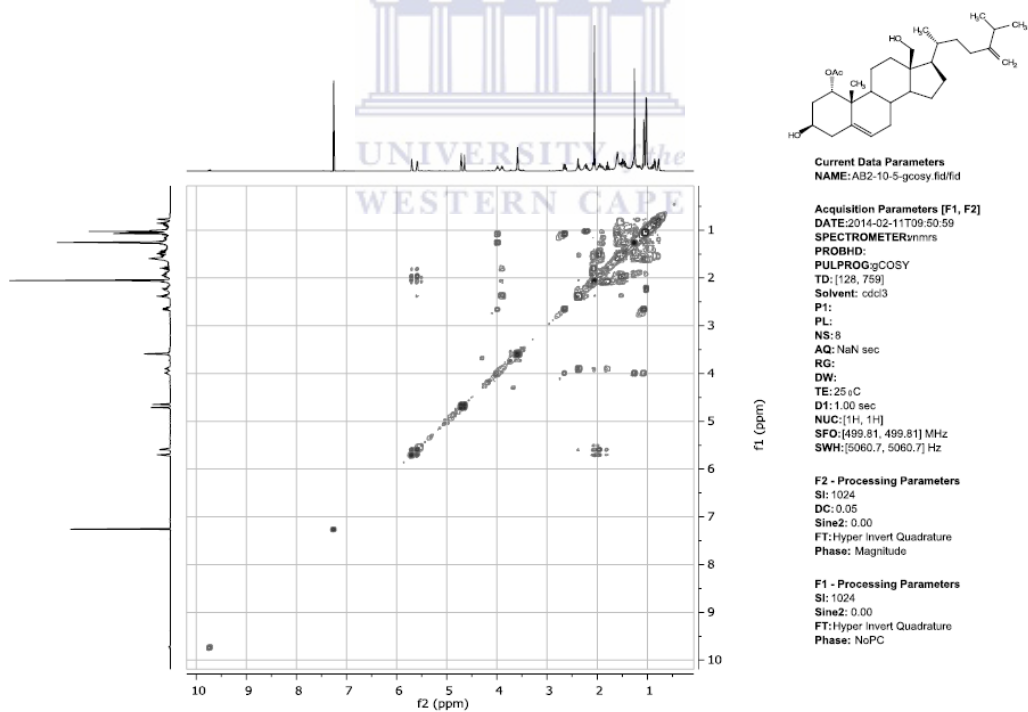


Figure 2.21: gCOSY (500 MHz, CDCl_3) of palysterol B.

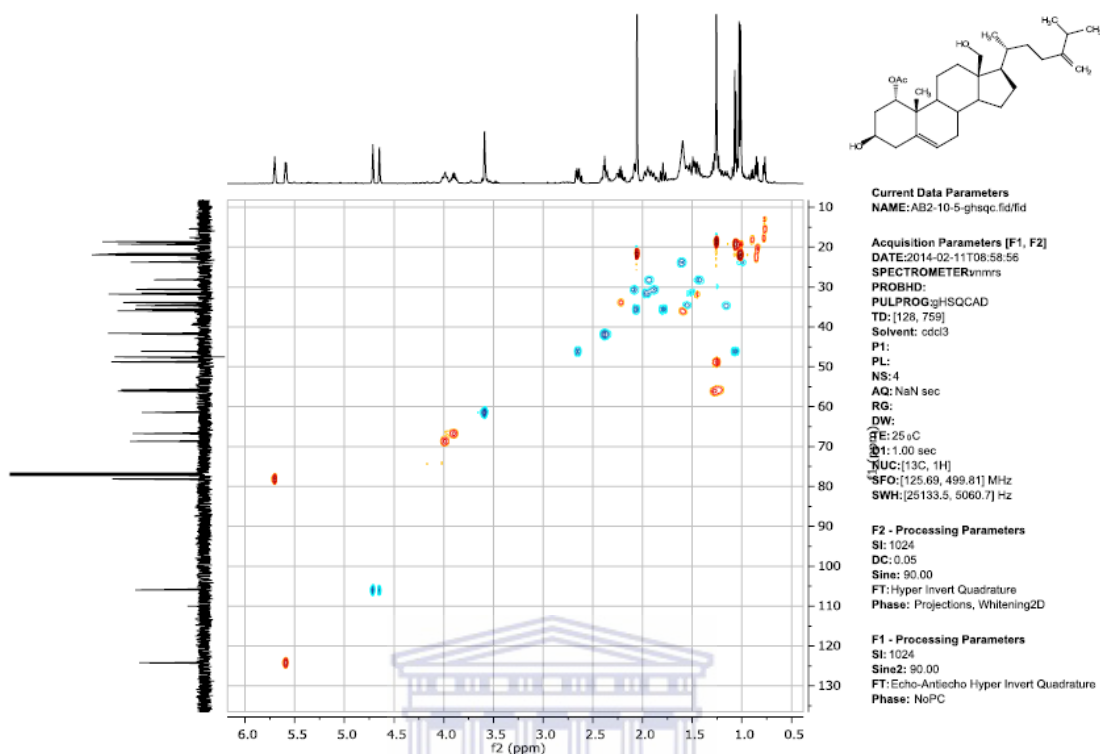


Figure 2.22: Multiplicity-edited gHSQC (methylene: blue cross peaks; methyl and methine: red cross peaks) (500 MHz, CDCl_3) of palysterol B.

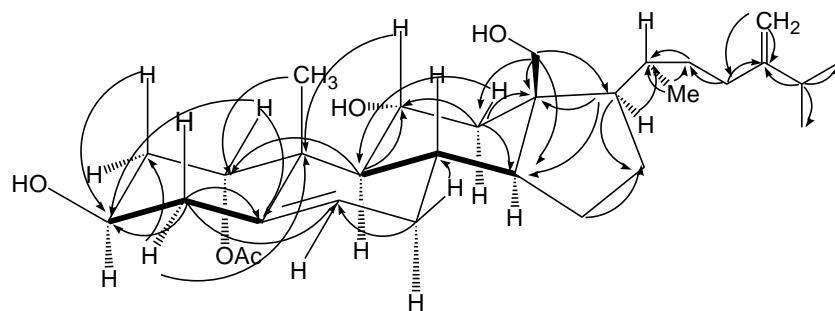


Figure 2.23: Selected gHMBC correlations observed for palysterol B.

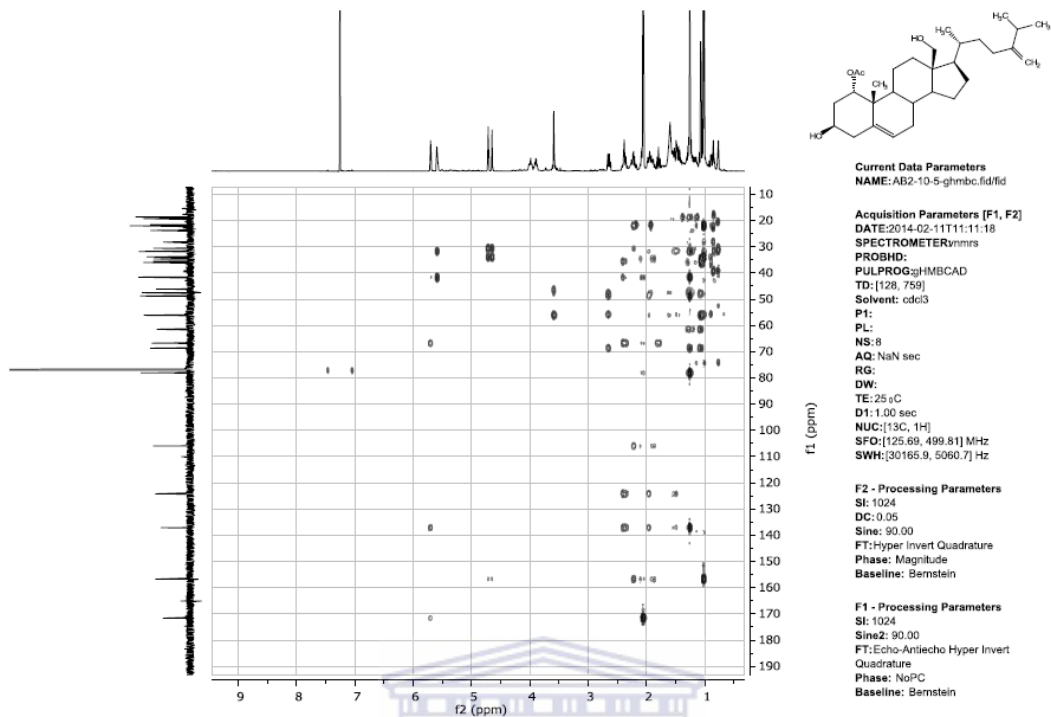


Figure 2.24: gHMBC (500 MHz, CDCl₃) of palysterol B.

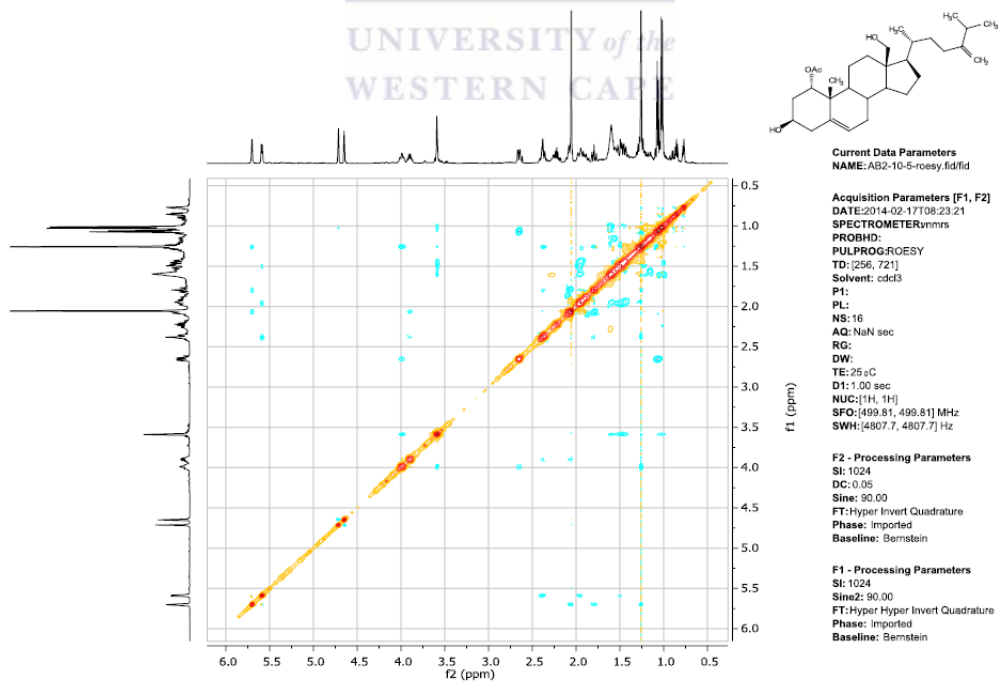


Figure 2.25: ROESY (500 MHz, CDCl₃) of palysterol B.

2.8.3 Analysis of palysterol C

The ^1H and ^{13}C NMR (Figures 2.27 and 2.28) spectra of palysterol C ($\text{C}_{30}\text{H}_{46}\text{O}_5$) (Figure 2.26) was similar to those of palysterol B. The disappearance of the Me-18 resonance and the presence of an acetoxy group (δ_{H} 2.02 s, 3H; δ_{C} 171.74 s and 21.53 q). In addition, a new formyl group (δ_{H} 9.77 s, 2H; δ_{C} 206.45 d) was observed. The gHMBC spectrum (Figure 2.31) showed the same relevant correlations of those showed for palysterol A (Figure 2.17) as well as some new relevant correlations between the acetoxy carbonyl carbon and H-1 and between the formyl carbon and H-12, H-14 and H-17. The COSY spectrum (Figure 2.29) showed correlations between H-2/H-1 and H-3; H-11/H-12; and H-6/H-7. Finally, the ROESY spectrum (Figure 2.32) showed correlations between the aldehyde proton (δ 9.77) and H-8, H-11 and H-20. From the data above, the structure was identified as 24-methylene-1 α ,3 β ,11 α -trihydroxycholest-5-en-18-al 1-acetate. To the best of our knowledge, palysterol C is isolated, in this study, for the first time from nature.

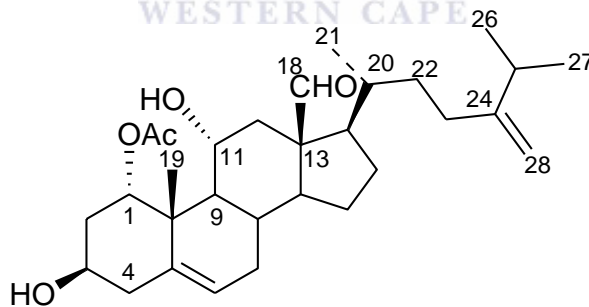


Figure 2.26: Chemical structure of palysterol C.

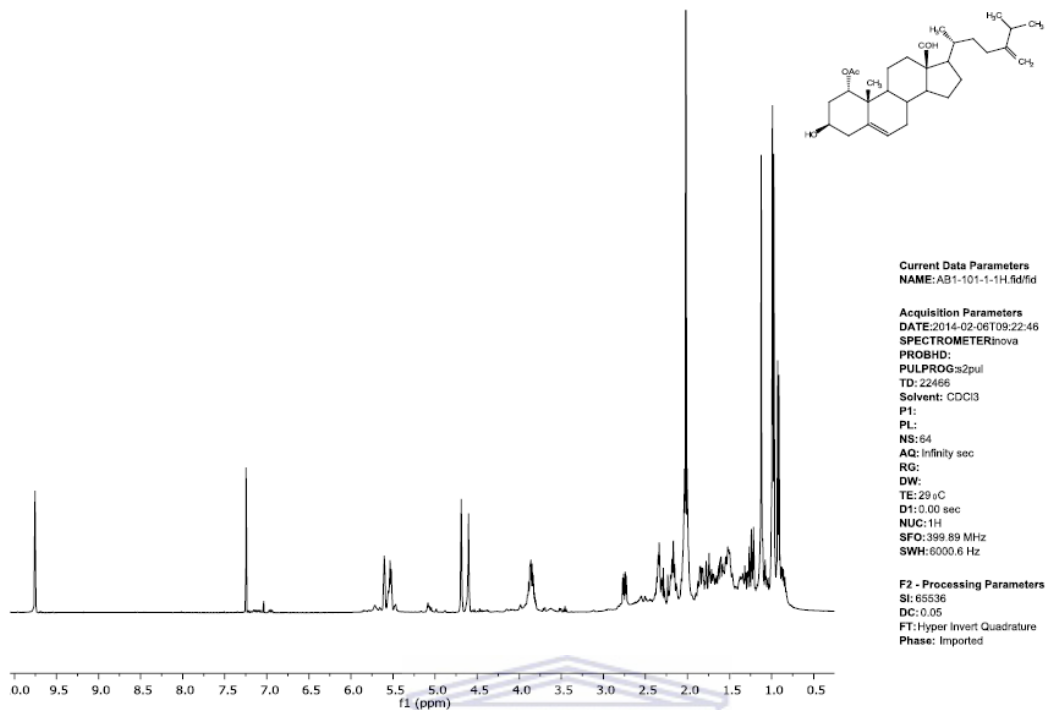


Figure 2.27: ^1H NMR (500 MHz, CDCl_3) of palysterol C.

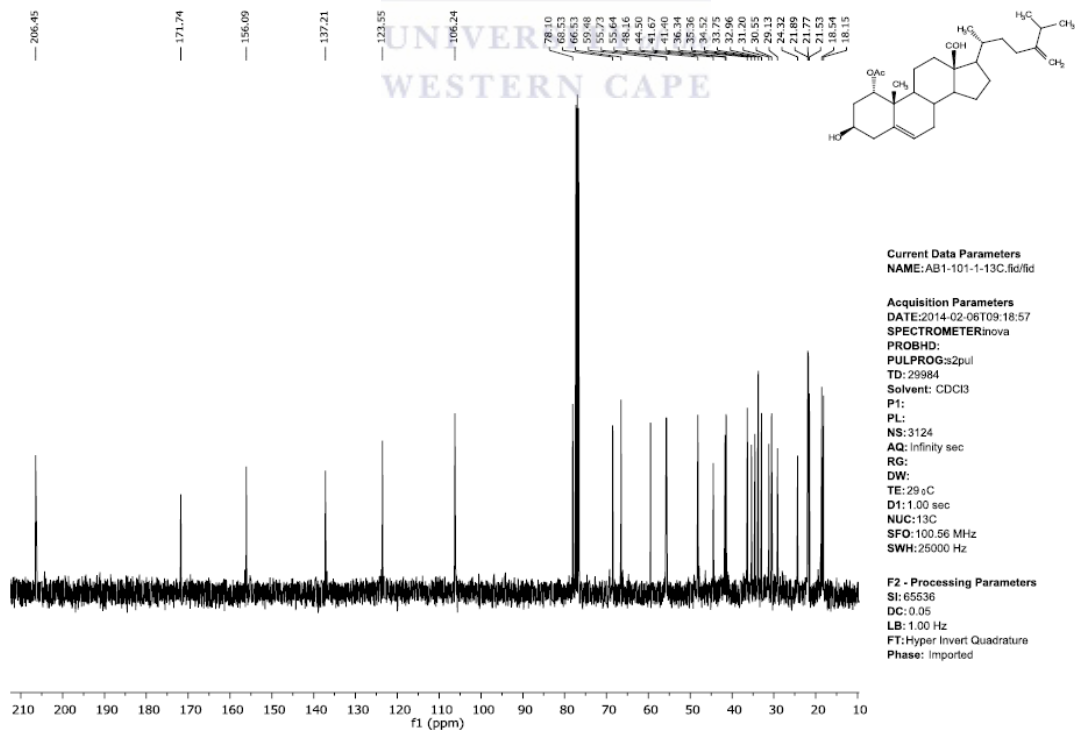


Figure 2.28: ^{13}C NMR (125 MHz, CDCl_3) of palysterol C.

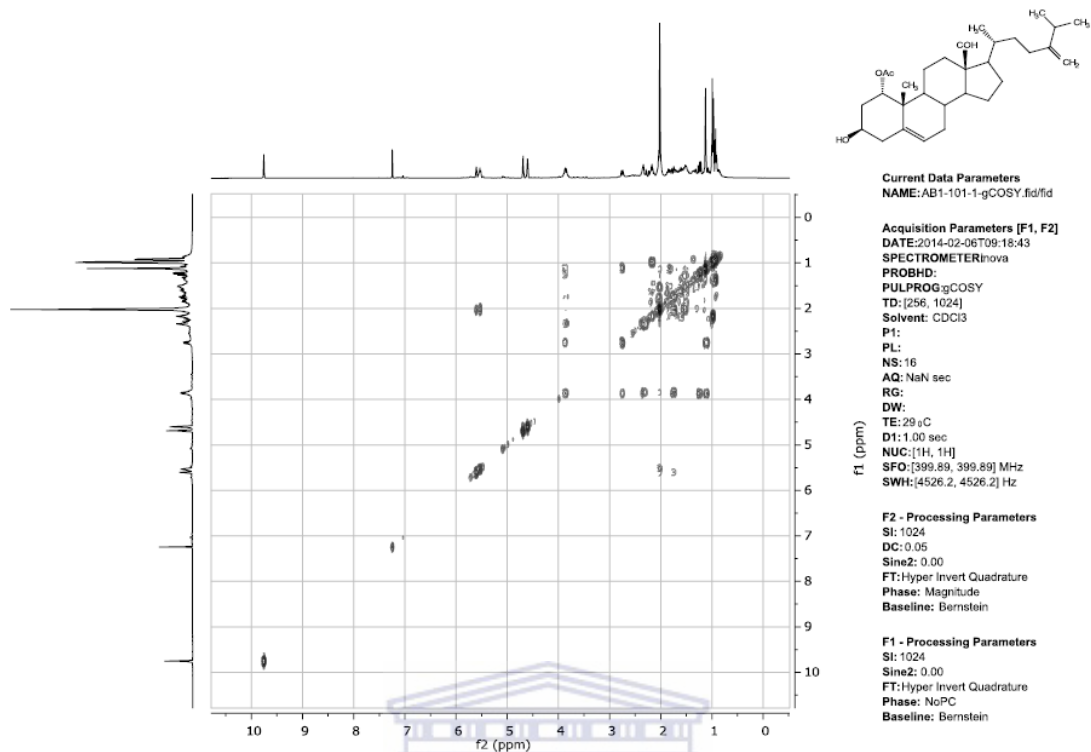


Figure 2.29: gCOSY (500 MHz, CDCl₃) of palysterol C.

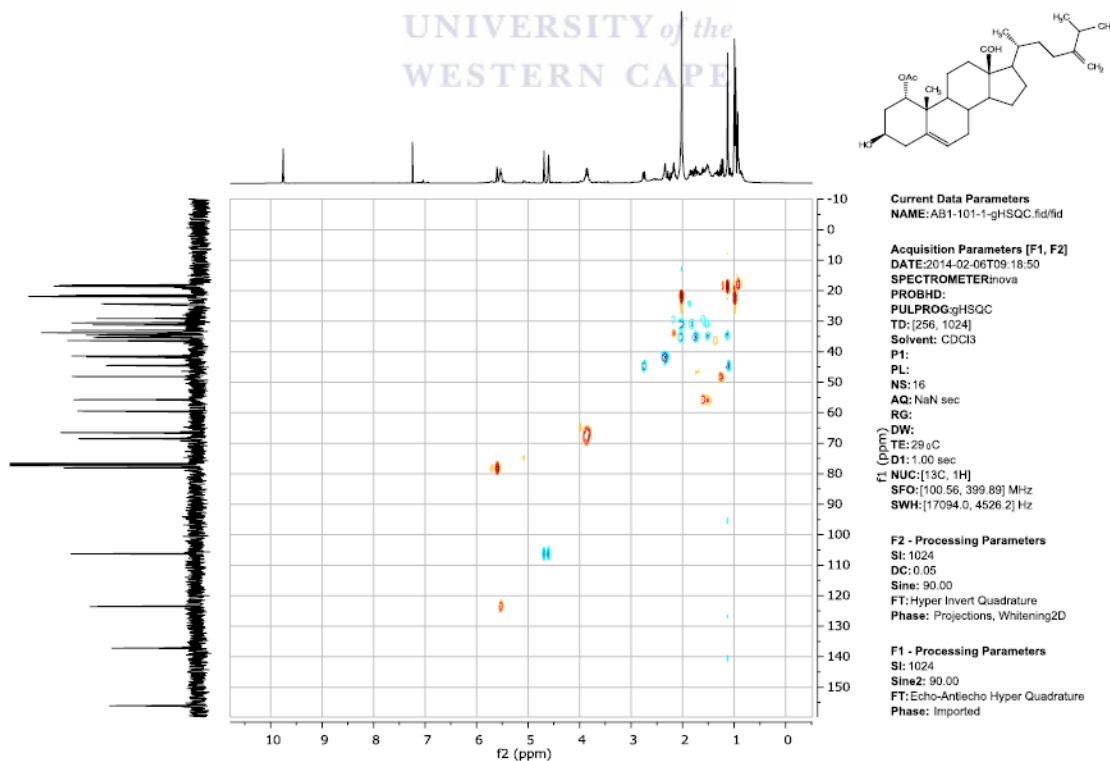


Figure 2.30: Multiplicity-edited gHSQC (methylene: blue cross peaks; methyl and methine: red cross peaks) (500 MHz, CDCl₃) of palysterol C.

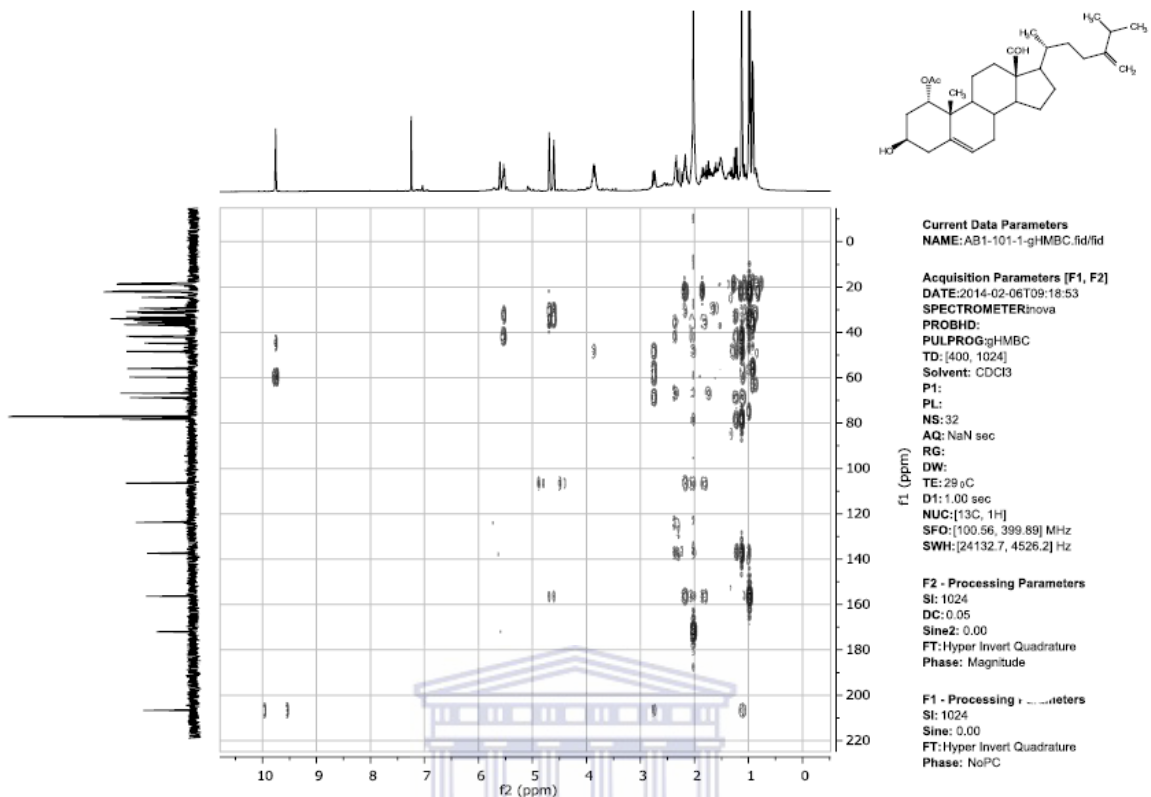


Figure 2.31: gHMBC (500 MHz, CDCl₃) of palysterol C.

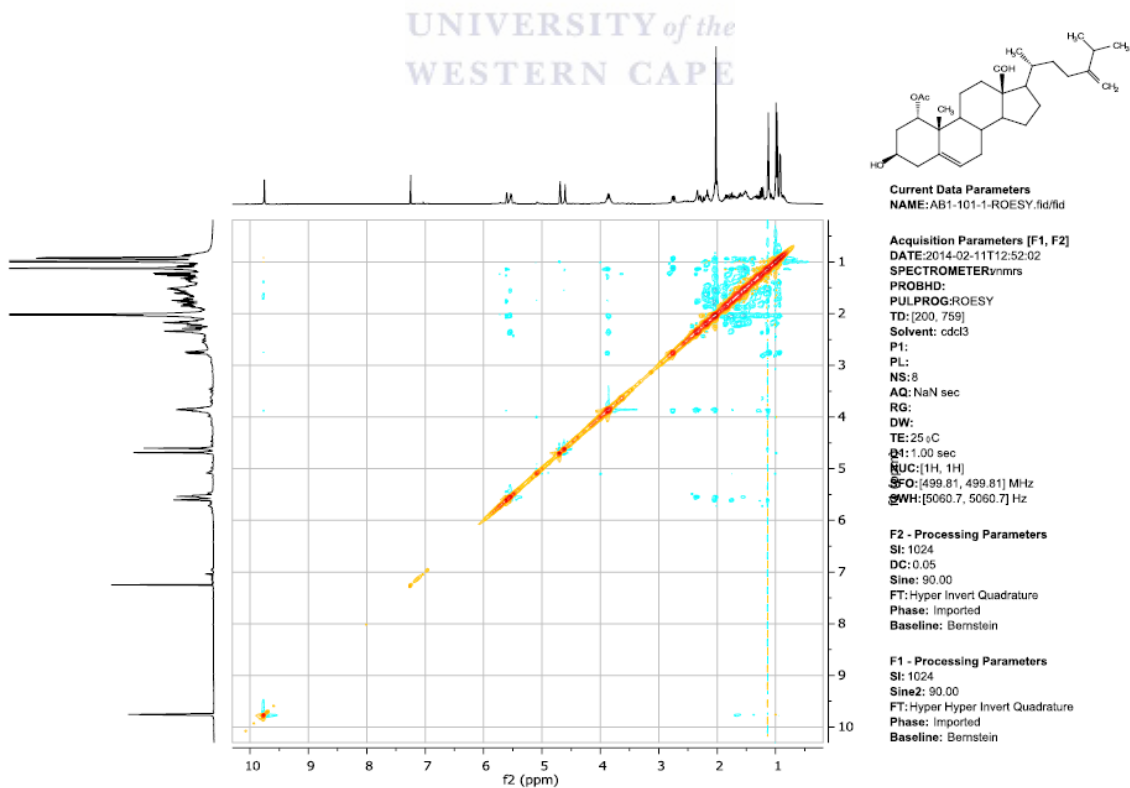


Figure 2.32: ROESY (500 MHz, CDCl₃) of palysterol C.

2.8.4 Analysis of palysterol D

The molecular formula of palysterol D (Figure 2.33) was determined by HRMS as $C_{28}H_{44}O_3$. The ^{13}C NMR spectroscopic data (Figure 2.35) (Table 2.3) together with analysis of its multiciplity-edited gHSQC spectrum (Figure 2.37) indicated 28 carbons, including five methyls, seven methylenes (one olefinic), twelve methines (three oxygenated and three olefinic) and four quaternary carbons (two olefinic). Its 1D NMR spectral data were similar to those of palysterol A except for the presence of two double bonds in the side-chain. The COSY spectrum (Figure 2.36) showed correlations between H-2/H-1 and H-3; H-11/H-12; H-6/H-7; and H-22/H-23 and H20. Additionally, the ROESY spectrum (Figure 2.40) showed correlations between Me-18/H-11, H-20 and H-8. The key gHMBC (Figure 2.38) correlations of the vinylic protons (H-22) with C-17, C-20, C-21, C-24 and H-23 with C-20, C-24, C-25 and C-28, led to the placement of the two double bonds at C-22 and C-24 of the side-chain, respectively. Thus, the structure of the palysterol D was proposed as Cholesta-5,22(23),24(28)-trien-1 α ,3 β ,11 α -triol. To the best of our knowledge, palysterol D is isolated, in this study, for the first time from nature.

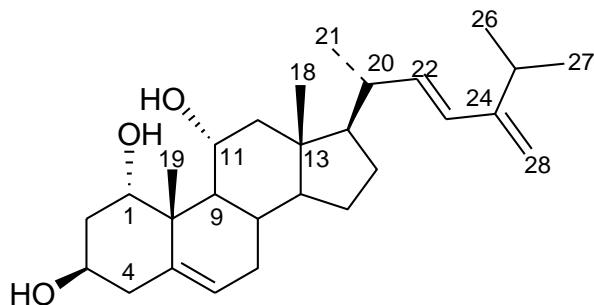


Figure 2.33: Chemical structure of palysterol D.

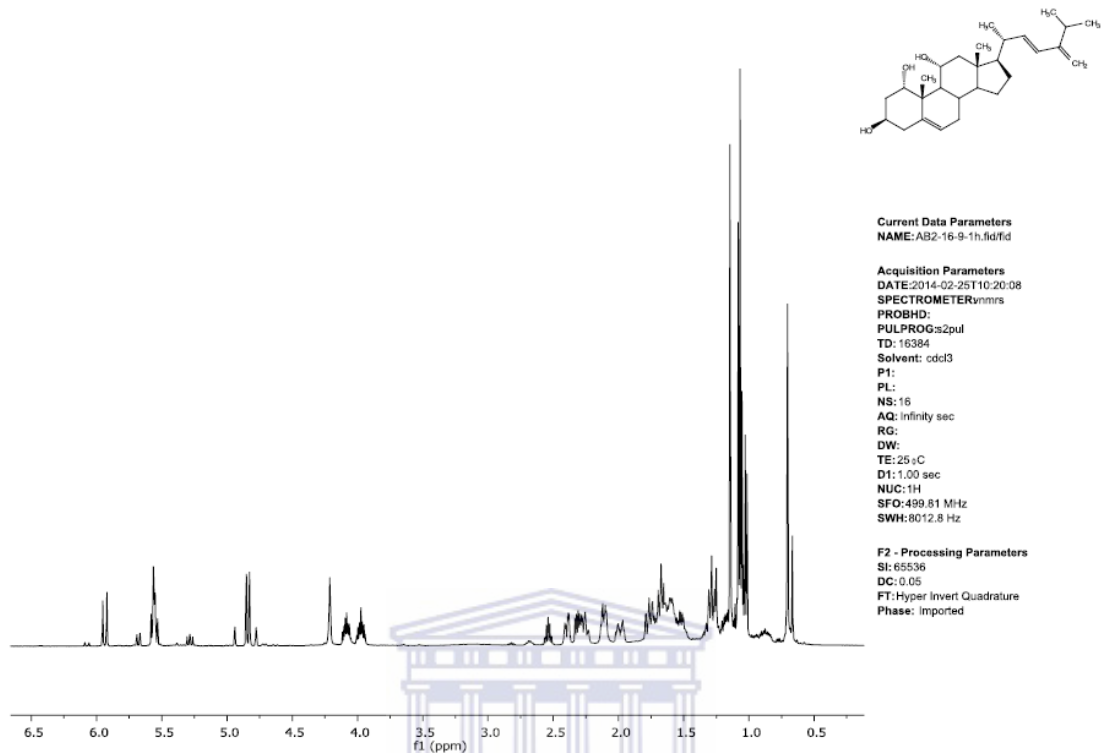


Figure 2.34: ^1H NMR (500 MHz, CDCl_3) of palysterol D.

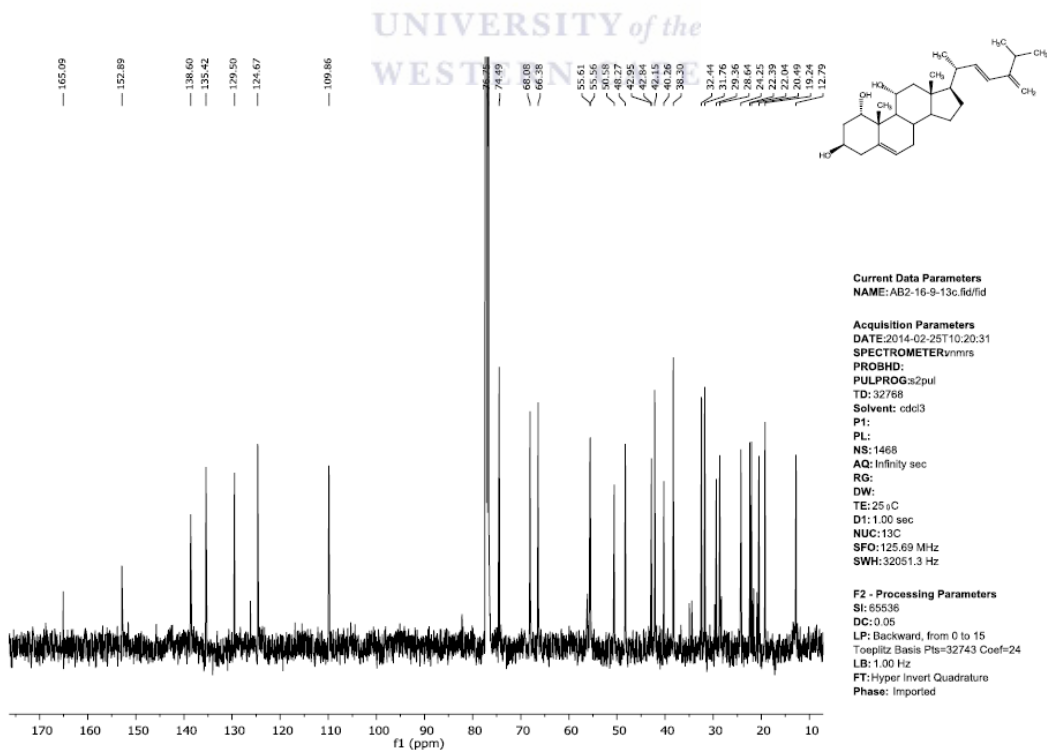


Figure 2.35: ^{13}C NMR (125 MHz, CDCl_3) of palysterol D.

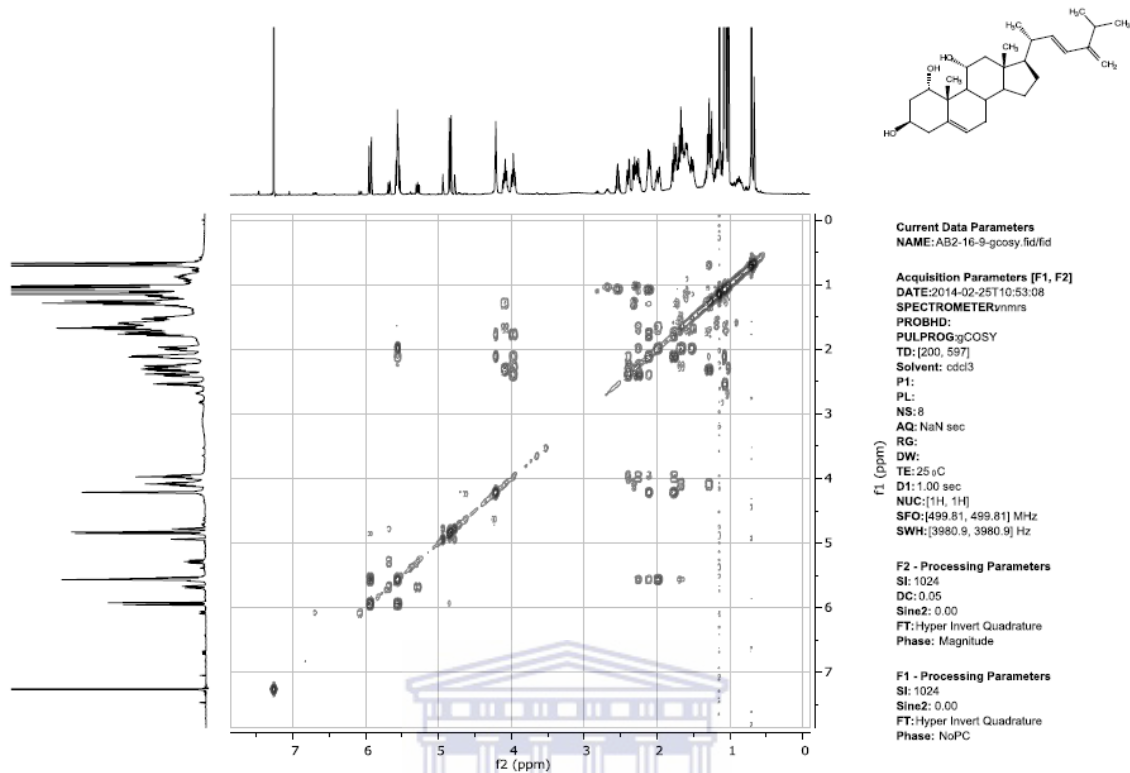


Figure 2.36: gCOSY (500 MHz, CDCl_3) of palysterol D.

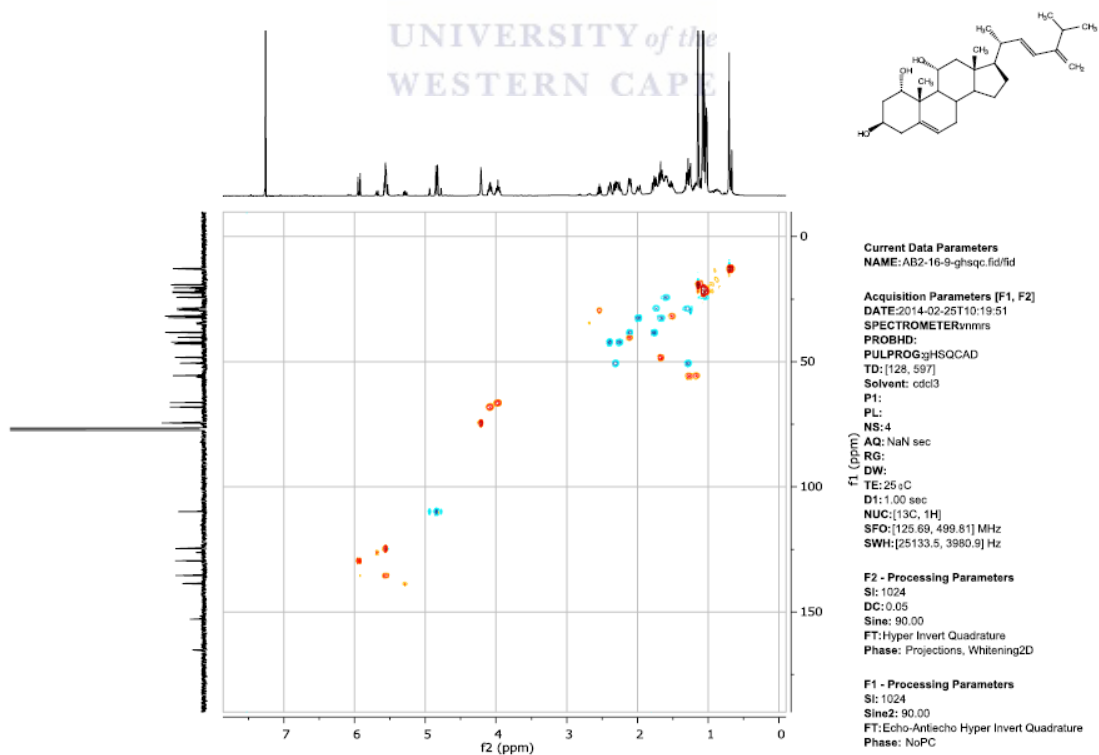


Figure 2.37: Multiplicity-edited gHSQC (methylene: blue cross peaks; methyl and methine: red cross peaks) (500 MHz, CDCl_3) of palysterol D.

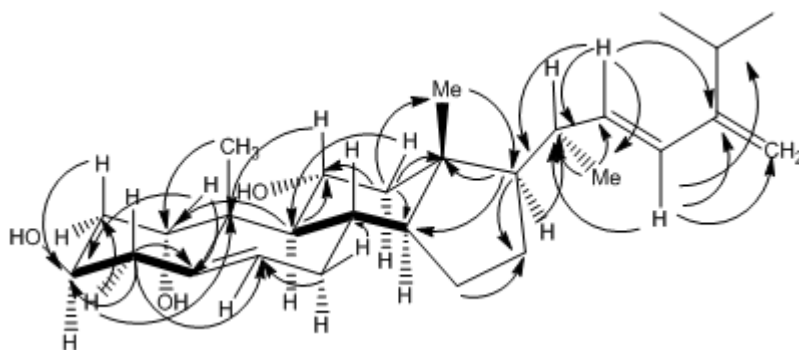


Figure 2.38: Selected gHMBC correlations observed for palysterol D.

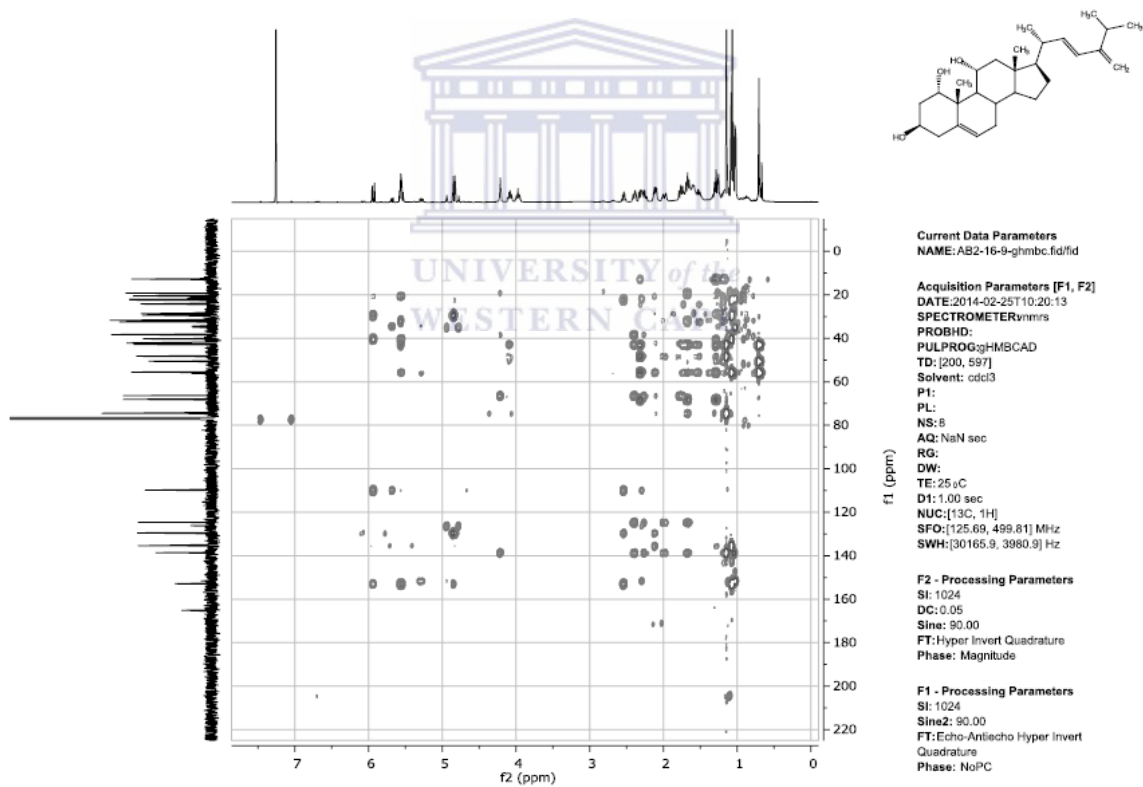


Figure 2.39: gHMBC (500 MHz, CDCl_3) of palysterol D.

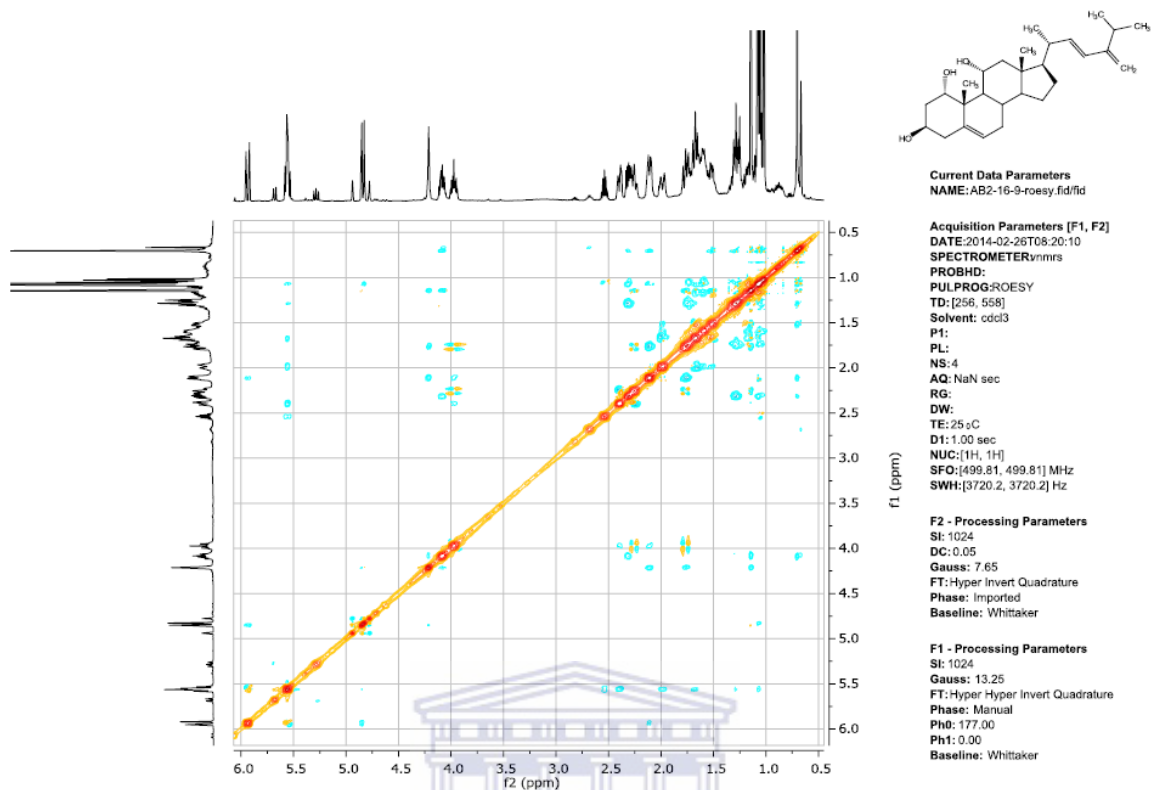


Figure 2.40: ROESY (500 MHz, CDCl₃) of palysterol D.

2.8.5 Analysis of palysterol E

¹³C NMR spectra (Figure 2.43) of palysterol E (C₃₀ H₄₆ O₄) (Figure 2.41) displayed 30 carbon signals. The ¹H and ¹³C NMR (Figures 2.42 and 2.43) spectra of palysterol E are consistent with those of palysterol D (Table 2.3). The only significant difference was the presence of an acetoxy group (δ_{H} 2.06 s, 3H; δ_{C} 171.71 s and 21.56 q). The COSY spectrum (Figure 2.44) showed correlations between H-2/H-1 and H-3; H-11/H-12; H-6/H-7; and H-22/H-23 and H20. Additionally, the ROESY spectrum (Figure 2.47) showed correlations between Me-18/H-11, H-20 and H-8. The gHMBC correlation between the acetoxy carbonyl carbon and H-1 (δ_{H} 5.70) confirmed the position of the acetyl group on C-1 (Figure 2.46). From the data above, the structure was identified as

Cholesta-5,22(23),24(28)-trien-1 α ,3 β ,11 α -triol 1-acetate. To the best of our knowledge, palysterol E was not isolated before from other natural sources.

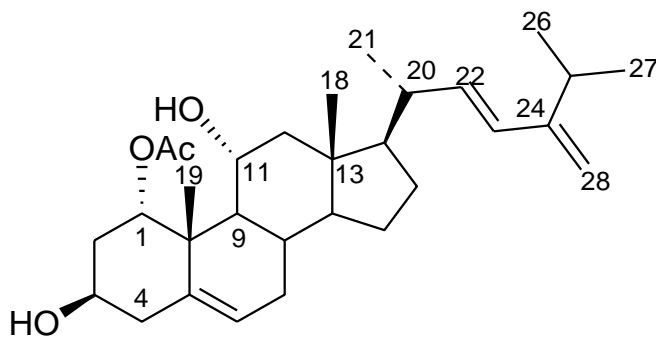


Figure 2.41: Chemical structure of palysterol E.

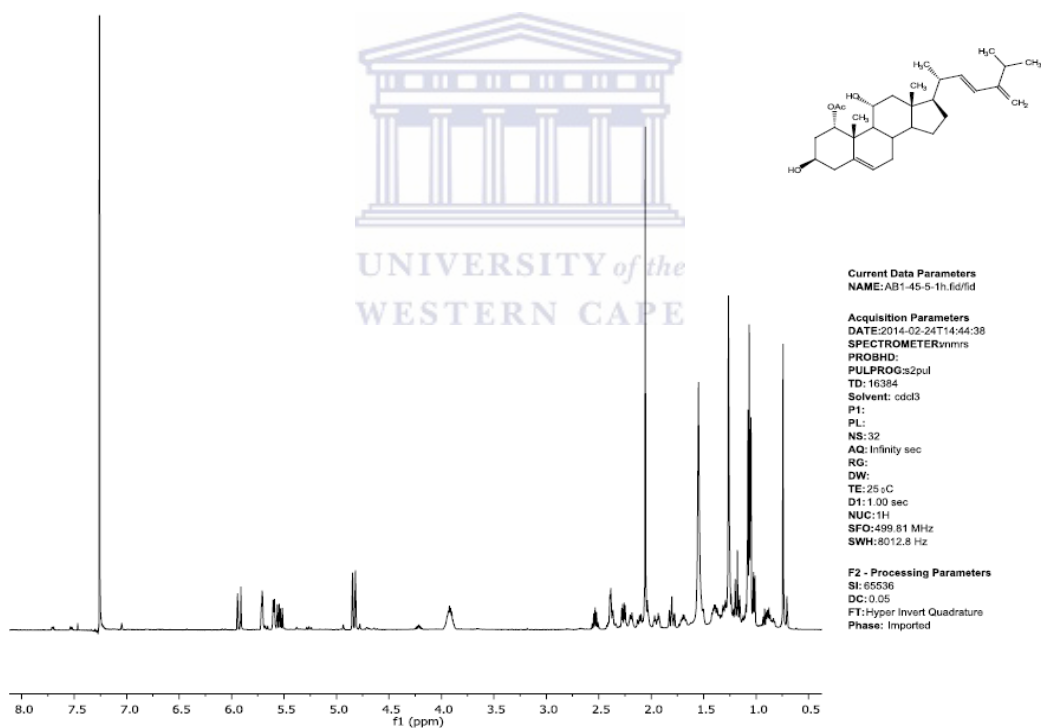


Figure 2.42: ^1H NMR (500 MHz, CDCl_3) of palysterol E.

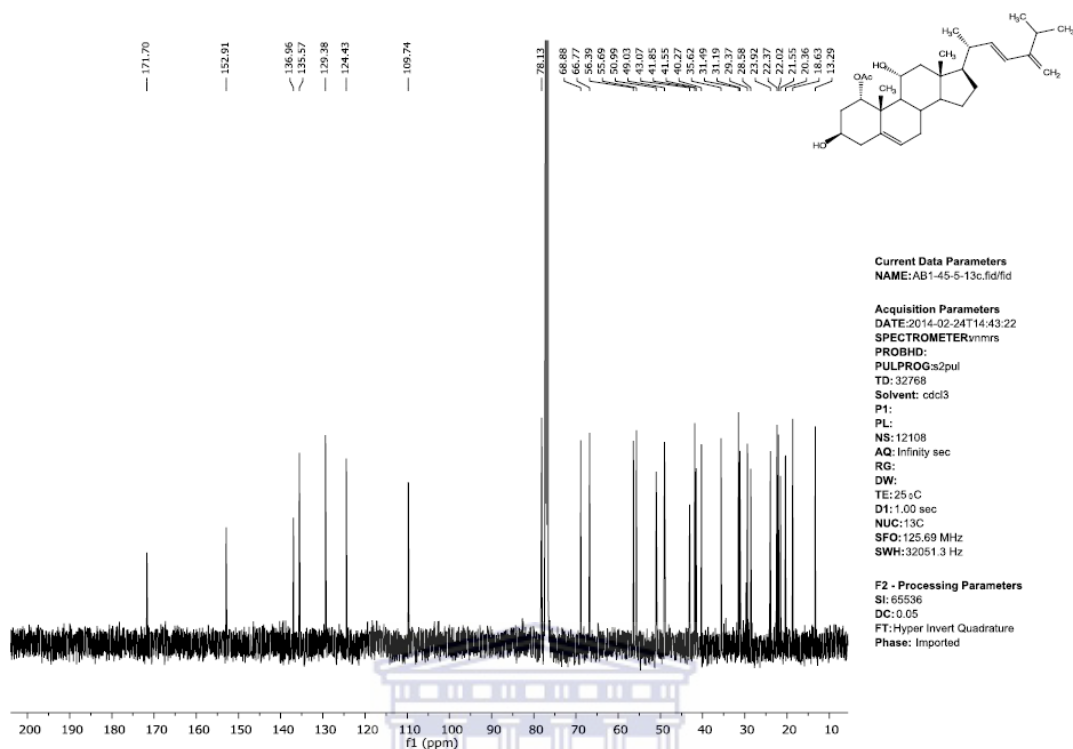


Figure 2.43: ^{13}C NMR (125 MHz, CDCl_3) of palysterol E.

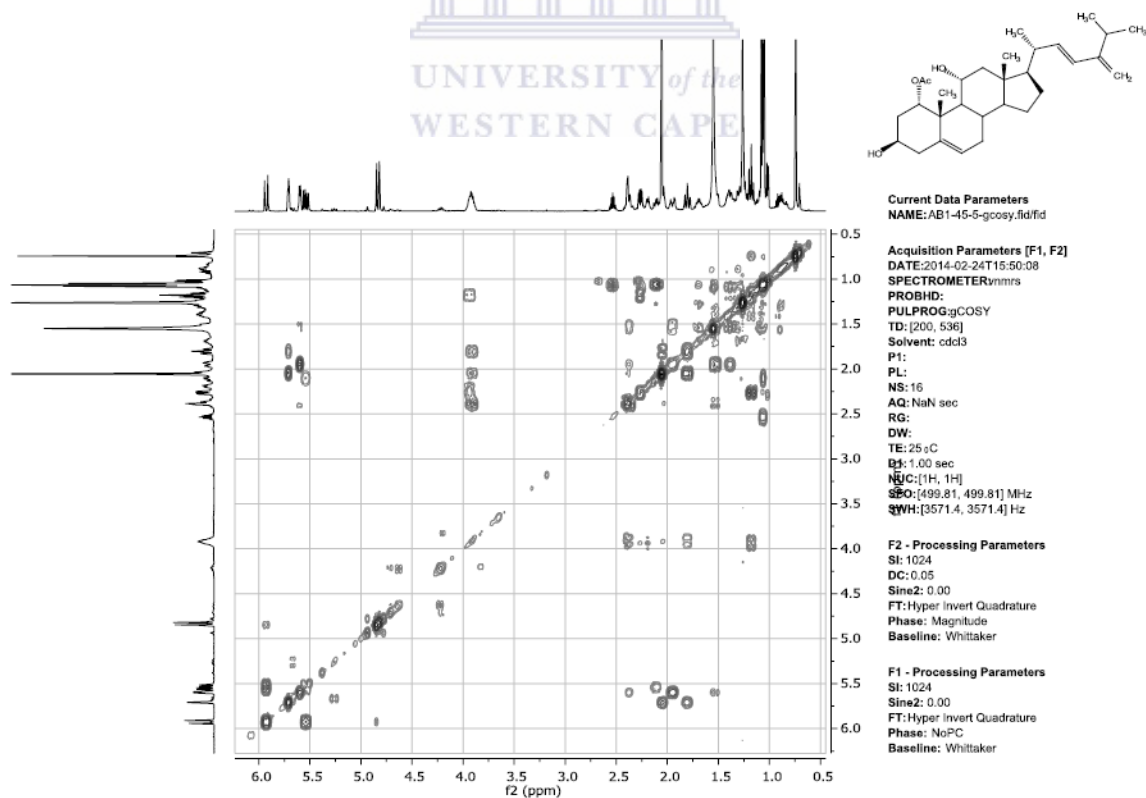


Figure 2.44: gCOSY (500 MHz, CDCl_3) of palysterol E.

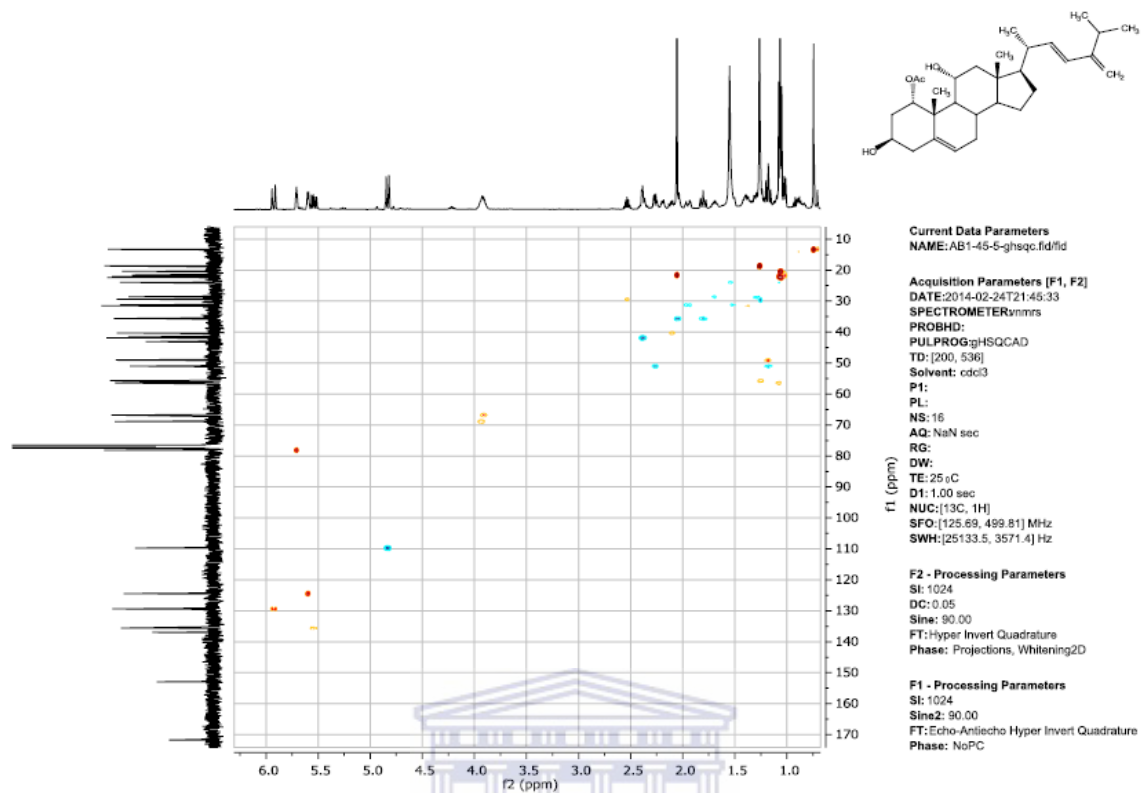


Figure 2.45: Multiplicity-edited gHSQC (methylene: blue cross peaks; methyl and methine: red cross peaks) (500 MHz, CDCl₃) of palysterol E.

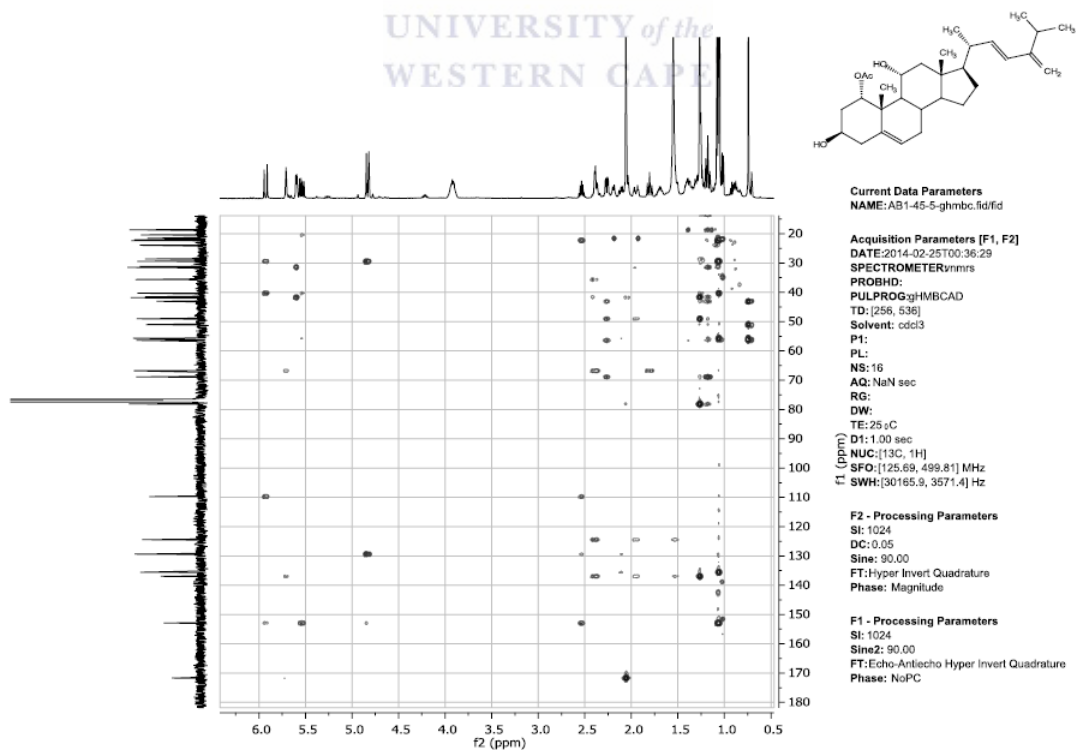


Figure 2.46: gHMBC (500 MHz, CDCl₃) of palysterol E.

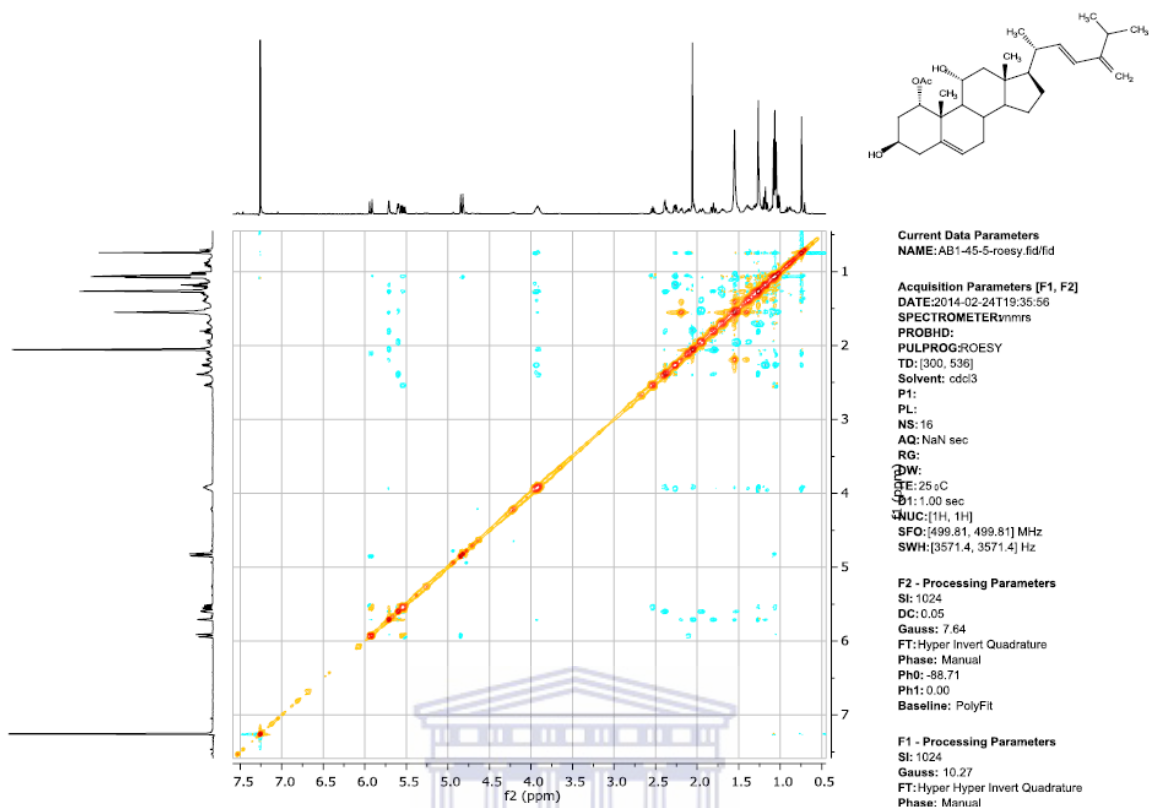


Figure 2.47: ROESY (500 MHz, CDCl₃) of palysterol E.

2.8.6 Analysis of palysterol F

Palysterol F (Figure 2.48) possessed the molecular formula C₃₂H₄₈O₆, as determined by its HRMS. The ¹³C NMR spectroscopic data (Figure 2.50) (Table 2.3) together with analysis of its gHSQC spectrum (Figure 2.51) indicated 32 carbons, including six methyls, eight methylenes (one oxygenated and one olefinic), twelve methines (three oxygenated and three olefinic), and six quaternary carbons (two olefinic and two carbonyl carbons). The significant differences with D were the presence of two acetoxy groups (δ_{H} 2.06 s, 3H; δ_{C} 171.87 s and 21.58 q) and (δ_{H} 2.10 s, 3H; δ_{C} 171.29 s and 21.17 q) and of a new oxygenated-methylene group (δ_{H} 4.02, 3.96, 2H; δ_{C} 63.06 t). Comprehensive analysis of the gHMBC spectra (Figure 2.52) suggested that the two acetoxy groups were located on C-1 and C-18. In addition, the gHMBC correlations

between the oxygenated-methylene carbon and H-12/C-18, H-14/C-18 and H-17/C-18, combined with ROESY correlations between the methylene protons H-8, H-11 and H-20, confirmed the structure as Cholesta-5,22(23),24(28)-trien-1 α ,3 β ,11 α ,18-tetrol 1,18-diacetate. To the best of our knowledge, palysterol F was not isolated before from other natural sources.

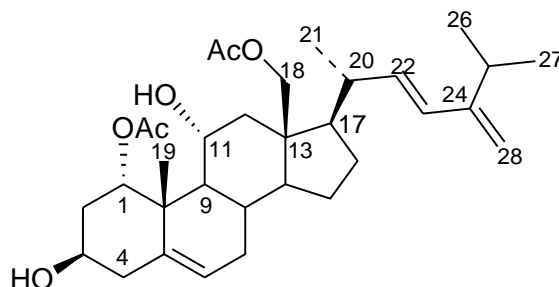


Figure 2.48: Chemical structure of palysterol F.

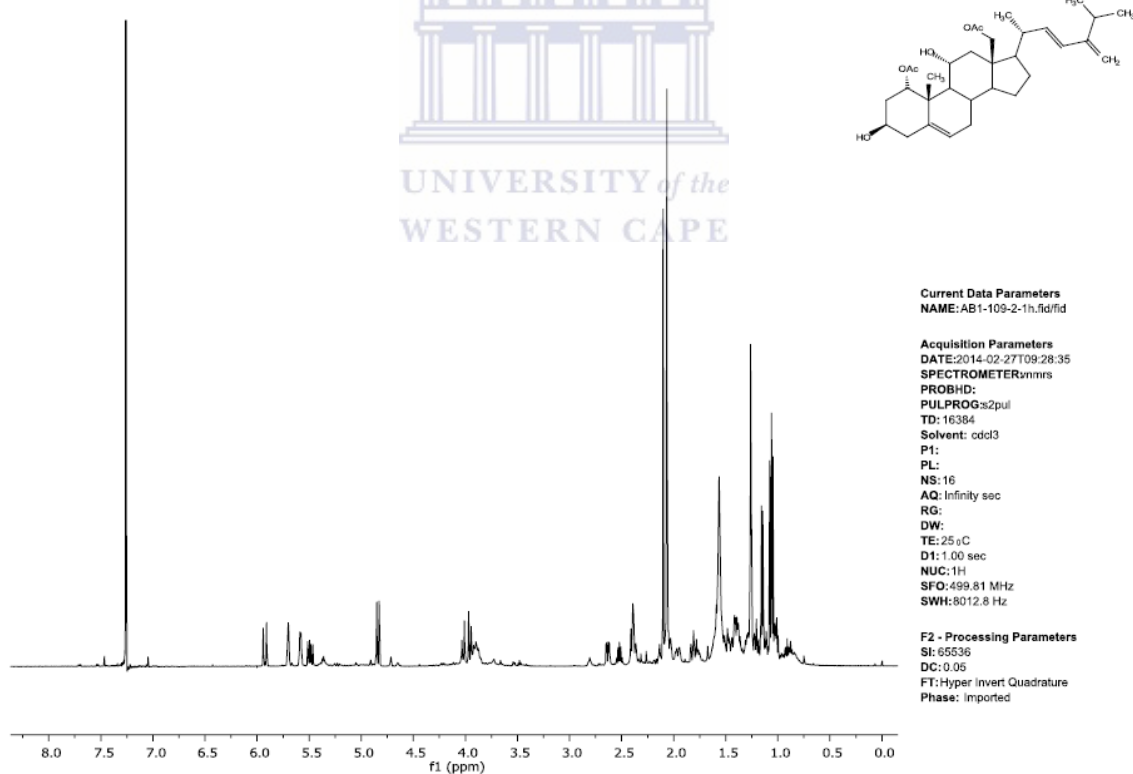


Figure 2.49: ^1H NMR (500 MHz, CDCl_3) of palysterol F.

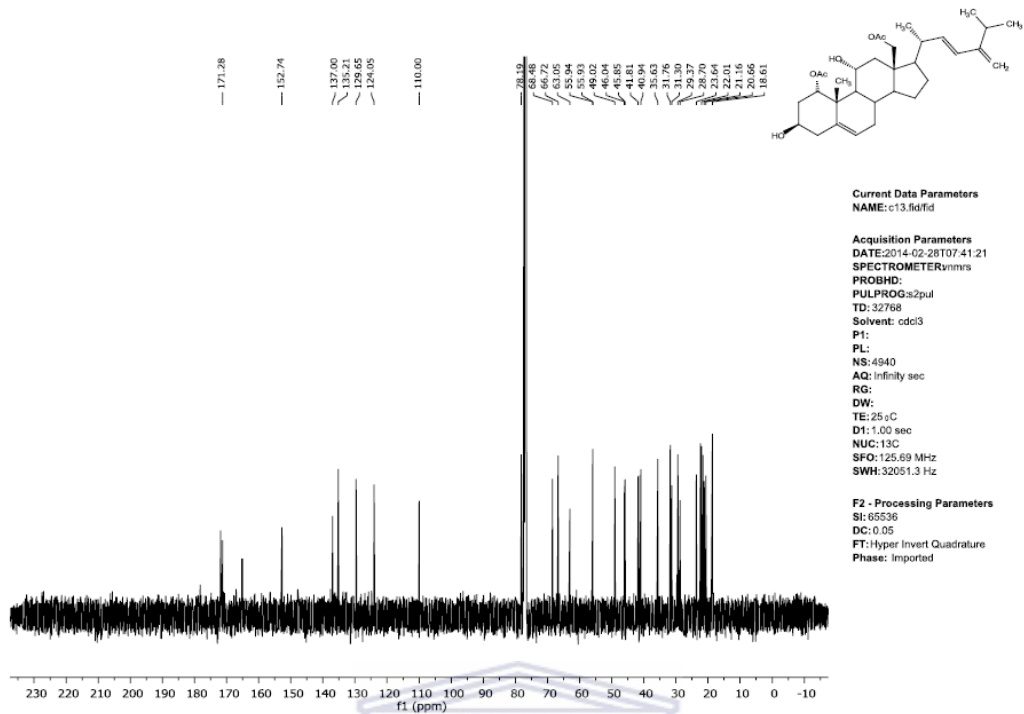


Figure 2.50: ^{13}C NMR (125 MHz, CDCl_3) of palysterol F.

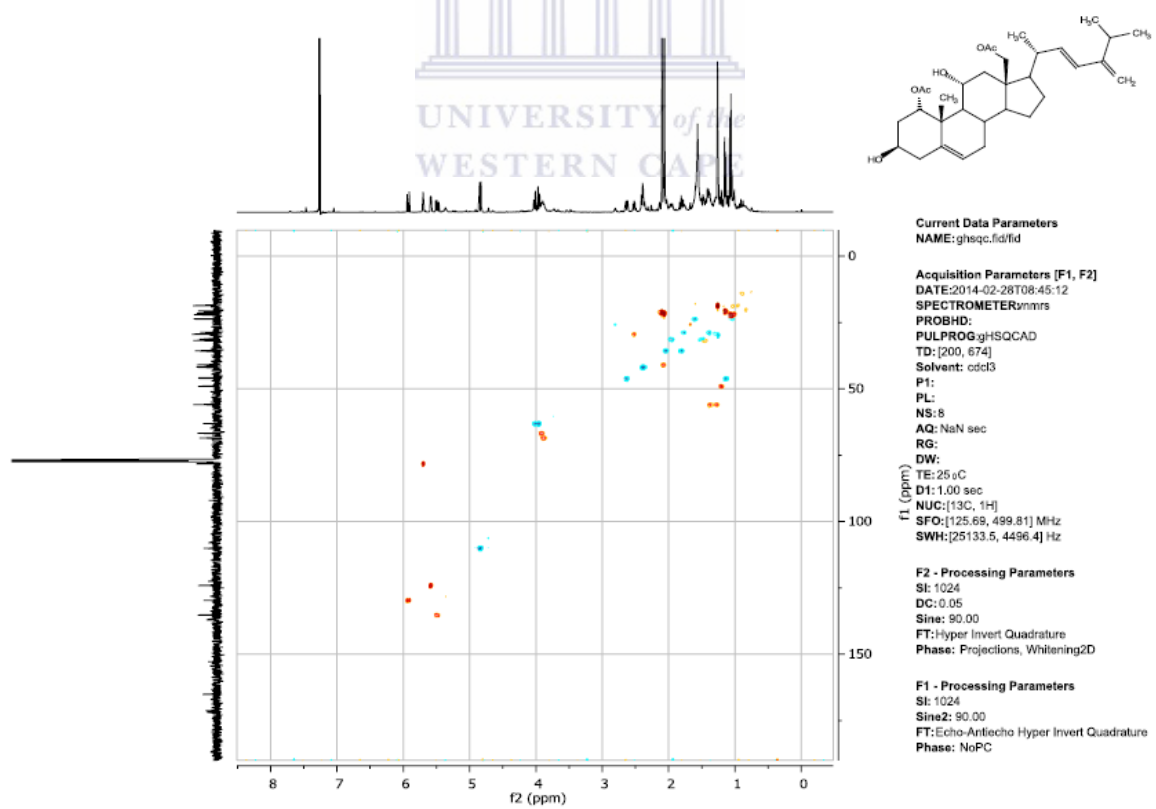


Figure 2.51: Multiplicity-edited gHSQC (methylene: blue cross peaks; methyl and methine: red cross peaks) (500 MHz, CDCl_3) of palysterol F.

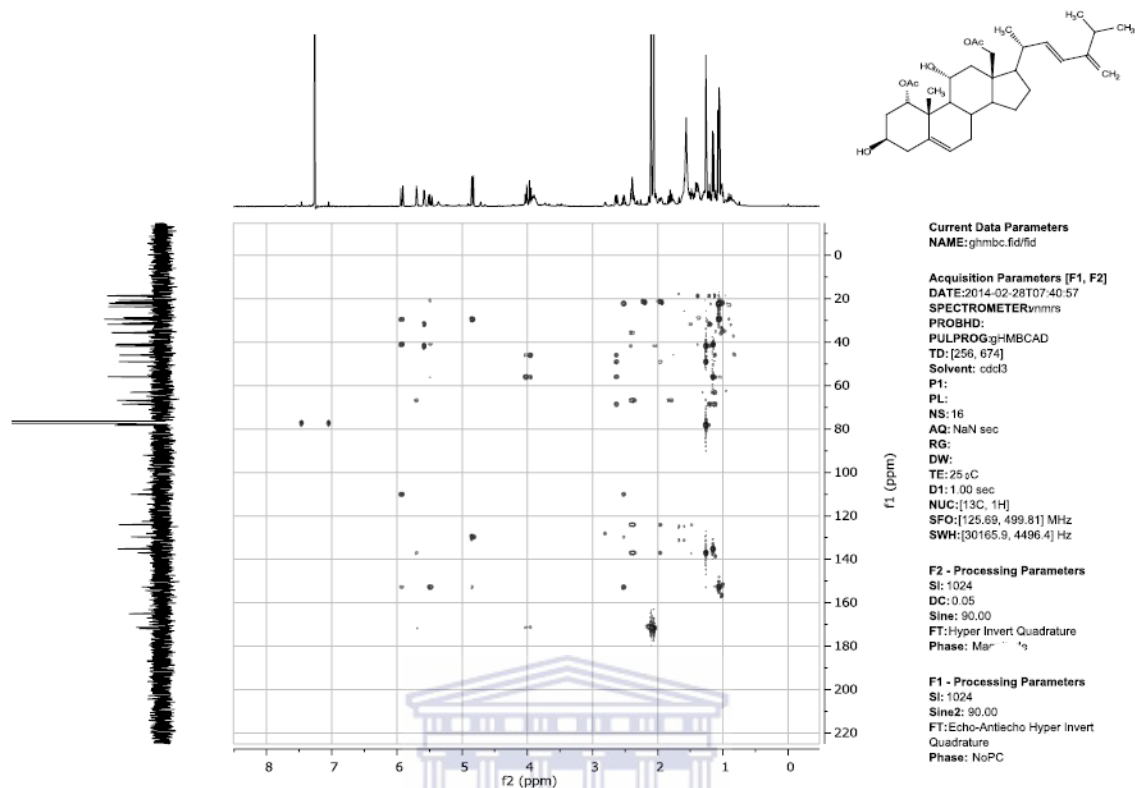


Figure 2.52: gHMBC (500 MHz, CDCl₃) of palysterol F.

2.8.7 Analysis of palysterol G

The molecular formula of palysterol G (Figure 2.53) was determined by HRMS as C₃₀H₄₄O₅. The ¹³C NMR spectroscopic data (Figure 2.55) (Table 2.3) together with analysis of its multiplicity-edited gHSQC spectrum (Figure 2.57) indicated 30 carbons, including five methyls, seven methylenes (one olefinic), thirteen methines (three oxygenated, three olefinic and one formyl carbon) and five quaternary carbons (two olefinic and one carbonyl carbons). The COSY spectrum (Figure 2.56) showed correlations between H-2/H-1 and H-3; H-11/H-12; H-6/H-7; and H-22/H-23 and H20. Additionally, the ROESY spectrum (Figure 2.59) showed correlations between Me-18/H-11, H-20 and H-8. The ¹H and ¹³C NMR (Figures 2.54 and 2.55) spectra of palysterol G are consistent with those of palysterol C (Table 2.3). The only significant difference was

the presence of extra double bond C-22/C-23 at 5.49 dd (δ_C 133.6) and 5.92 d (δ_C 130.87). The presence of a formyl group (δ_H 9.77 s, 2H; δ_C 206.45 d), combined with the same gHMBC and ROESY correlations that those for palysterol C, confirmed the structure as Cholesta-5,22(23),24(28)-trien-1 α ,3 β ,11 α ,trihydroxy-18-al 1-acetate. To the best of our knowledge, palysterol G was not isolated before from other natural sources.

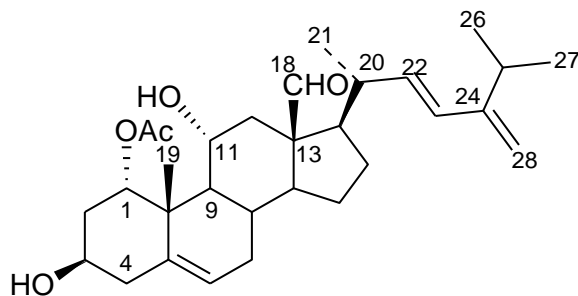


Figure 2.53: Chemical structure of palysterol G.

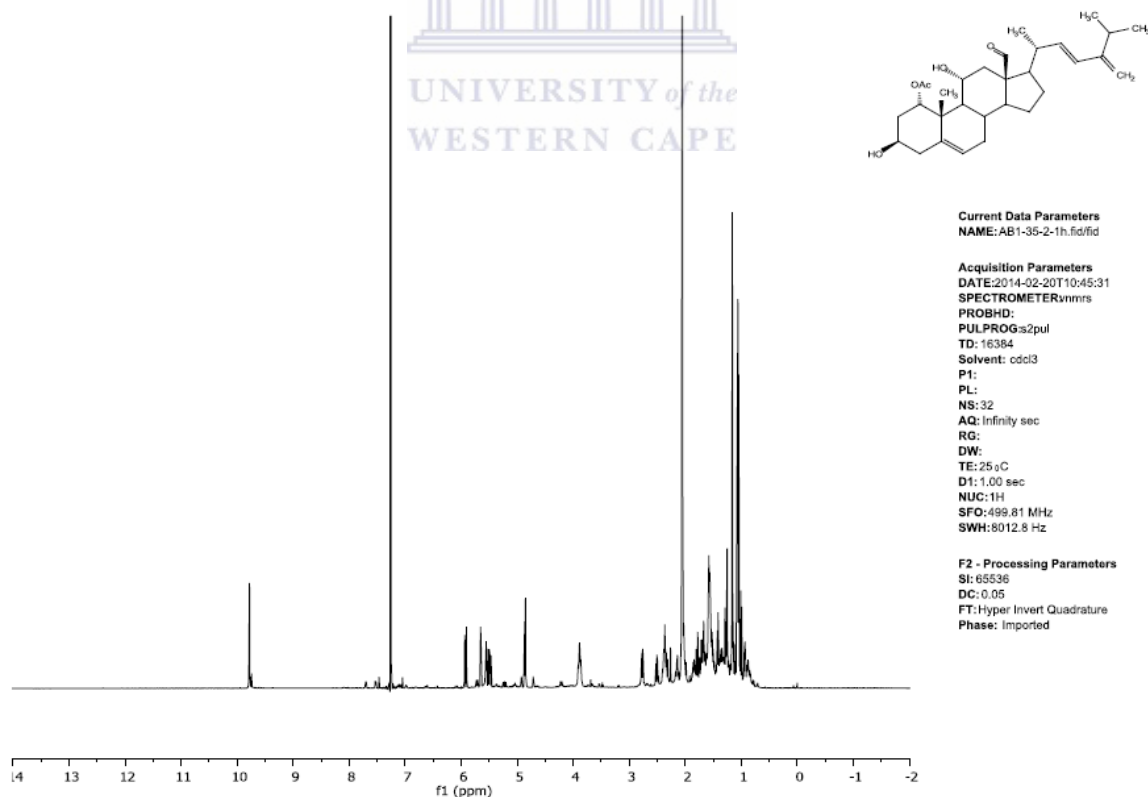


Figure 2.54: ¹H NMR (500 MHz, CDCl₃) of palysterol G.

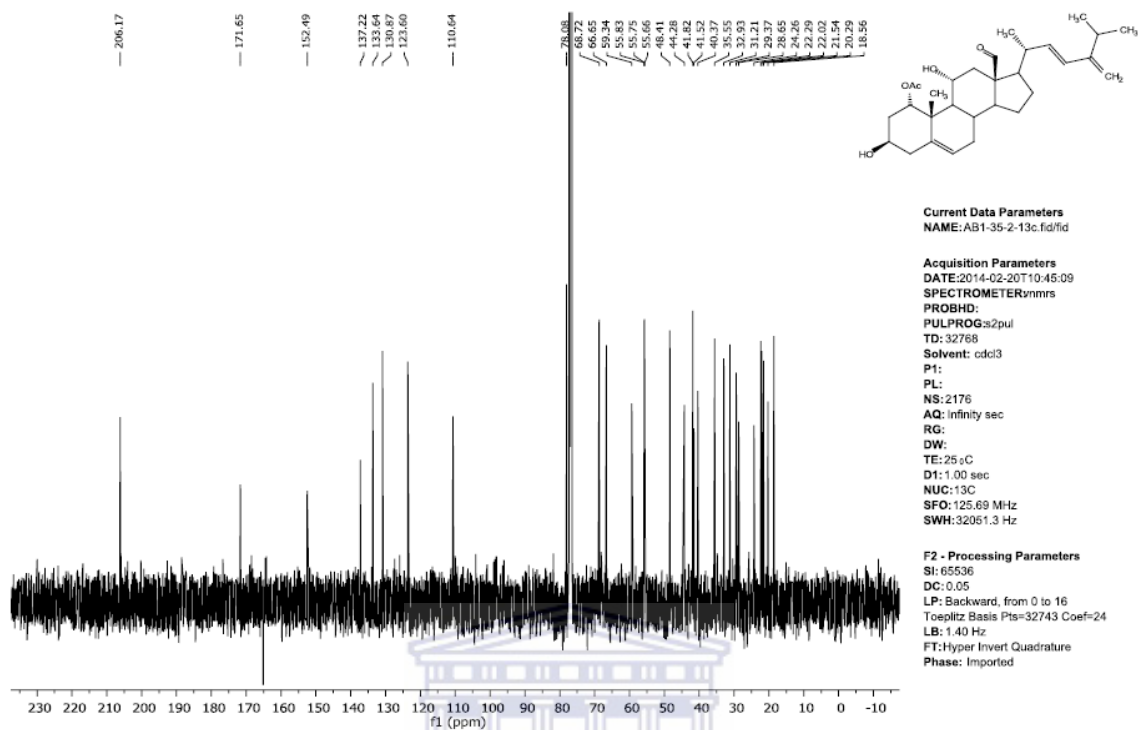


Figure 2.55: ^{13}C NMR (125 MHz, CDCl_3) of palysterol G.

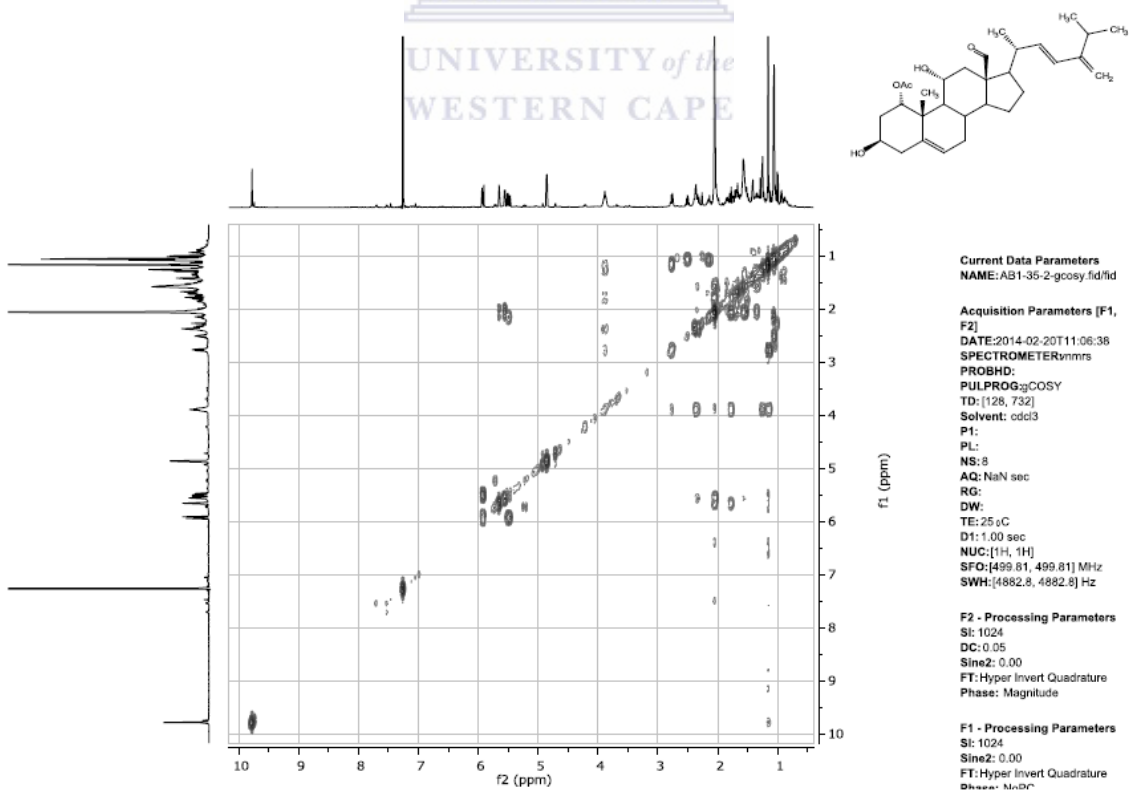


Figure 2.56: gCOSY (500 MHz, CDCl_3) of palysterol G.

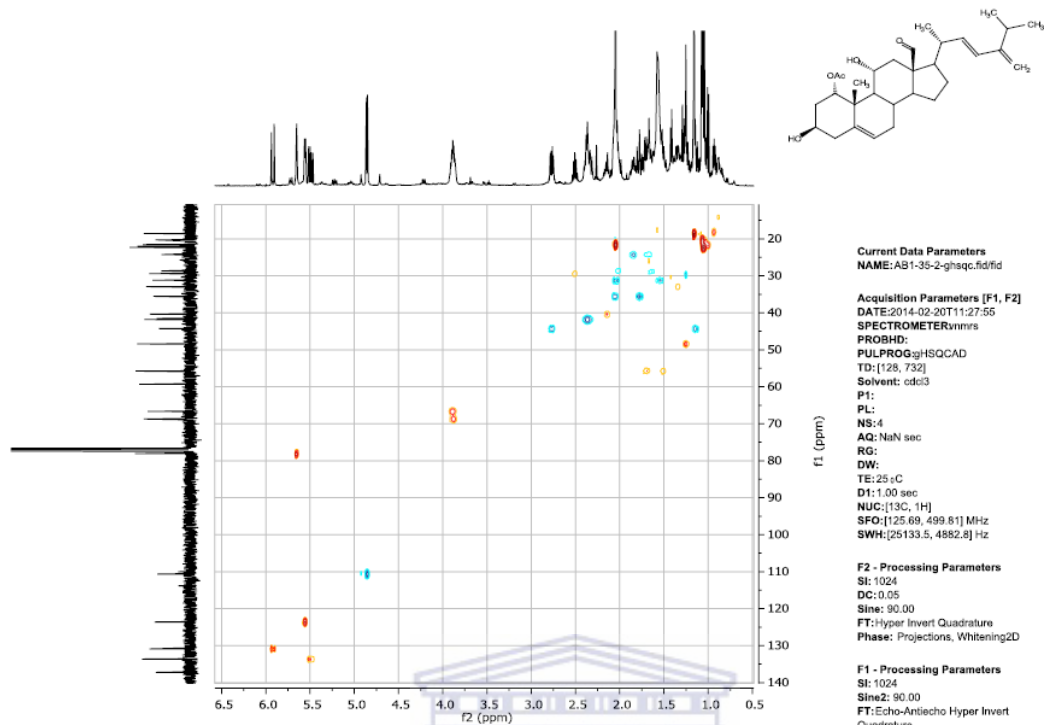


Figure 2.57: Multiplicity-edited gHSQC (methylene: blue cross peaks; methyl and methine: red cross peaks) (500 MHz, CDCl₃) of palysterol G.

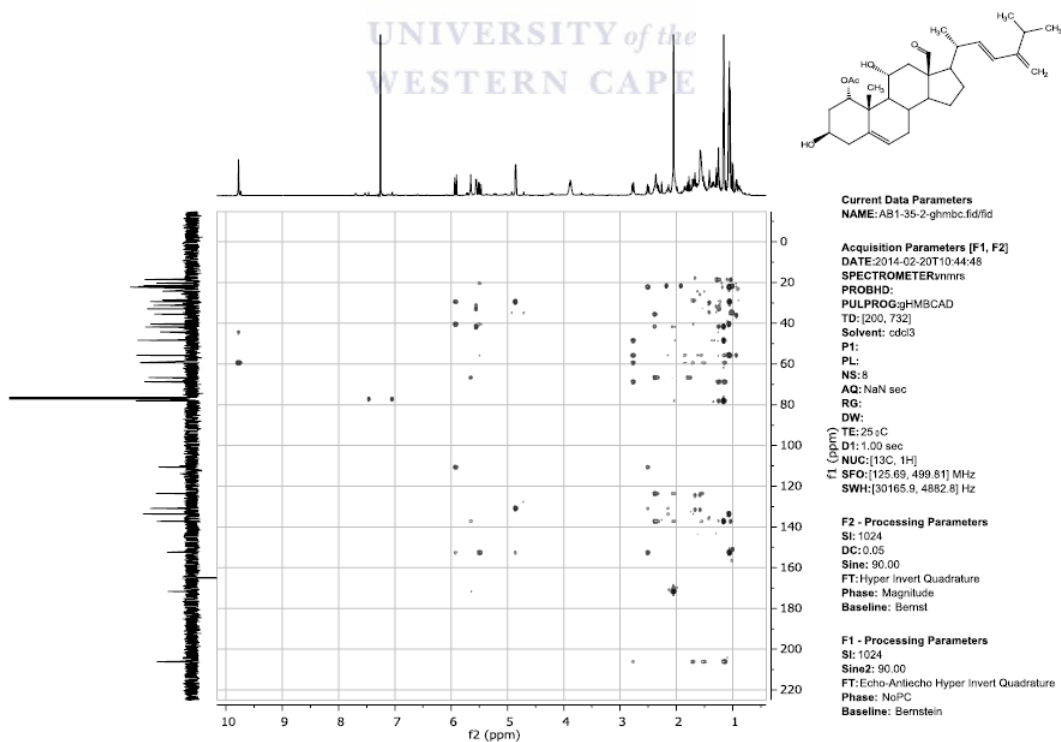


Figure 2.58: gHMBC (500 MHz, CDCl₃) of palysterol G.

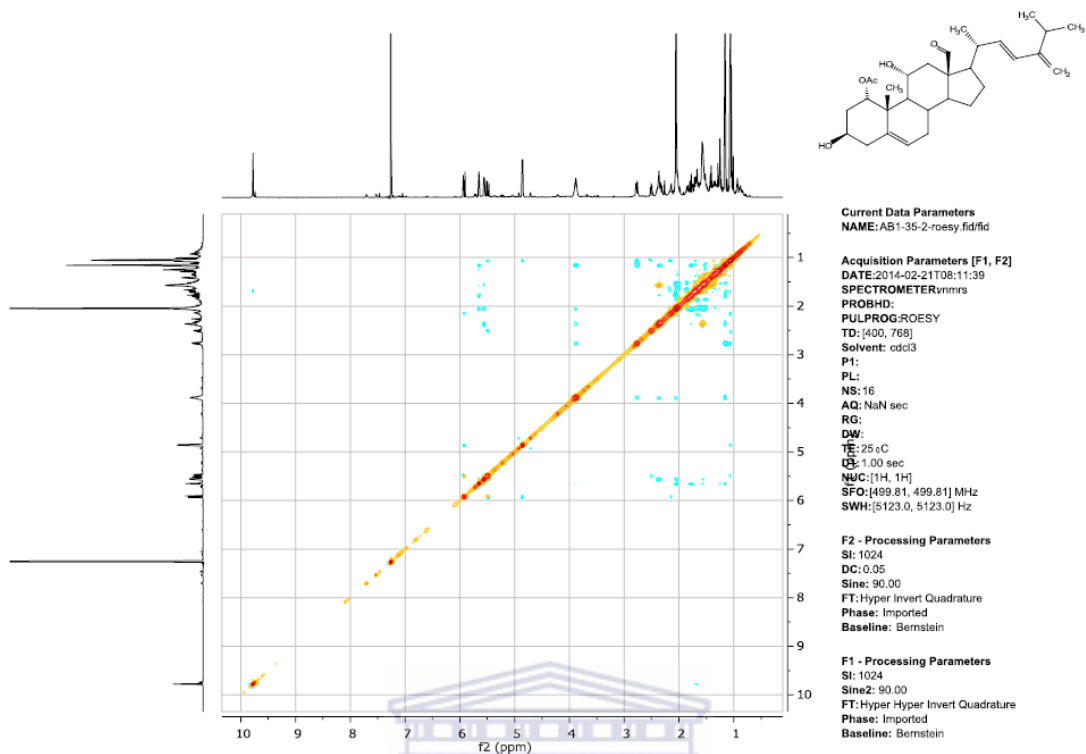


Figure 2.59: ROESY (500 MHz, CDCl_3) of palysterol G.

According to the literature, all the isolated compounds are new structures, except palysterol A, which was reported by Jagodzinska *et al.* (1985). However, those assignments were determined by comparison with other sterols with similar structure and configuration.

Table 2.3: ^1H (500 MHz) and ^{13}C (125 MHz) NMR spectral data of palysterols A-G*.

Position	A		B		C		D		E		F		G	
	^{13}C	^1H	^{13}C	^1H	^{13}C	^1H	^{13}C	^1H	^{13}C	^1H	^{13}C	^1H	^{13}C	^1H
1	74.49	4.21 t (3.3)	78.13	5.70 dd (3.9, 2.2)	78.10	5.60	74.49	4.21	78.14	5.70	78.20	5.70	78.08	5.65 dd (4.0, 2.3)
2	38.31	2.11, 1.76 ddd (-13.0, 11.6, 3.0)	35.57	2.06, 1.79 ddd (-13.9, 11.6, 2.3)	35.36	2.03, 1.75	38.30	2.11, 1.76	35.63	2.05, 1.80	35.64	2.04, 1.81	35.55	2.05, 1.78 ddd (-13.9, 11.5, 2.3)
3	66.39	3.97 tt (11.6, 4.7)	66.75	3.90	66.53	3.86	66.38	3.97	66.78	3.91	66.73	3.91	66.65	3.89
4	42.16	2.39 ddd (-12.3, 5.0, 2.6), 2.26	41.58	2.39, 2.34	41.67	2.34- 2.31	42.15	2.40, 2.26	41.86	2.38- 2.37	41.82	2.39, 2.34	41.82	2.37- 2.34
5	138.63		137.15		137.21		138.61	--	136.97	--	137.01	--	137.22	
6	124.68	5.56	124.22	5.59	123.55	5.54	124.67	5.56	124.45	5.60	124.06	5.58	123.60	5.56
7	32.46	1.99 dtt (-15.8, 5.3, 2.7), 1.68	31.51	1.96, 1.51	30.55	2.03, 1.53	32.44	1.99, 1.67	31.20	1.95, 1.53	31.32	1.96, 1.51	31.21	2.05, 1.55
8	31.75	1.51	31.79	1.45	32.96	1.27	31.76	1.51	31.50	1.38	31.77	1.45	32.93	1.35
9	48.23	1.66	48.78	1.25	48.16	1.25	48.27	1.67	49.04	1.26	49.03	1.20	48.41	1.25
10	43.00		41.83		41.42		42.95		43.08	--	41.62	--	41.52	
11	68.10	4.07 td (10.3, 5.6)	68.68	3.99 td (11.0, 4.2)	68.68	3.89	68.08	4.08	68.89	3.93	68.49	3.89	68.72	3.87
12	50.72	2.33 dd (11.9, 5.6), 1.26	46.12	2.66 dd (-12.3, 4.3), 1.07	44.50	2.75 dd (-12.4, 4.7), 1.11	50.58	2.31, 1.28	51.01	2.26, 1.18	46.05	2.64, 1.14	44.28	2.77 dd (-12.3, 4.6), 1.16
13	42.82		47.52		59.48		42.84	--	41.56	--	45.86	--	59.34	
14	55.52	1.17	55.78	1.23	55.73*	1.50*	55.56	1.17	56.40*	1.08*	55.94	1.27	55.75*	1.50*
15	24.27	1.62, 1.06	23.78	1.61, 1.01	24.32	1.85, 1.67	24.24	1.59, 1.04	23.93	1.55, 1.06	23.65	1.61, 1.03	24.26	1.85, 1.67
16	28.35	1.91, 1.30	28.19	1.93, 1.43	29.14	2.18, 1.61	28.64	1.74, 1.30	28.59	1.70, 1.29	28.72	1.78, 1.39	28.65	2.03, 1.65
17	55.63	1.20	56.12	1.27	55.64*	1.60*	55.61	1.28	55.70*	1.26*	55.94	1.38	55.66*	1.70*
18	12.53	0.67 s	61.46	3.59	206.45	9.77	12.78	0.71 (s)	13.30	0.74	63.06	4.02, 3.96	206.45	9.77
19	19.24	1.13 s	18.63	1.26 s	18.54	1.12 s	19.24	1.14 (s)	18.64	1.26 (s)	18.62	1.26 (s)	18.56	1.12 s
20	35.61	1.40	35.98	1.60	36.34	1.36	40.26	2.11	40.28	2.10	40.95	2.08	40.37	2.14
21	18.67	0.96 d (6.6)	19.25	1.07 d (6.4)	18.16	0.92 d (6.5)	20.49	1.07 (d)	20.37	1.06 (d)	20.68	1.15 (d)	20.29	1.07 d (6.7)
22	34.57	1.54, 1.15	34.66	1.52, 1.16	34.52	1.53, 1.13	35.42	5.56	35.58	5.54 (dd)	35.22	5.49	33.64	5.49 dd (15.7, 8.7)
23	30.87	2.09, 1.87	30.59	2.08, 1.88	31.20	2.02, 1.83	32.50	5.94	32.39	5.93 (d)	32.66	5.93	30.87	5.92 d (15.8)
24	156.65		156.77		156.09		152.89		152.92	--	152.75	--	152.49	
25	33.79	2.22	33.88	2.22	33.75	2.17	29.36	2.54	29.38	2.54	29.39	2.53	29.37	2.51 sept (6.8)
26	21.85	1.03	21.86	1.02	21.77	0.97	22.03	1.06	22.38	1.06	22.03	1.07	22.09	1.06
27	21.99	1.02	21.97	1.01	21.89	0.99	22.39	1.06	22.04	1.06	22.36	1.05	22.02	1.06
28	106.04	4.71, 4.65	105.95	4.71, 4.65	106.24	4.71, 4.62	109.86	4.85, 4.83	109.75	4.84, 4.82	110.02	4.85, 4.83	110.64	4.86, 4.85
OAc-1			21.55, 171.64	2.05	21.53, 171.74	2.02			21.56, 171.71	2.06		21.58, 171.87	2.06	21.53, 171.74
OAc-18											21.17, 171.29	2.10		

* Measured in CDCl₃ at 25°C. Chemical shifts in ppm and coupling constants in Hz.

Outline of Chapter Three: Anticancer evaluation of *Palythoa tuberculosa*

3.1 Introduction

3.2 Material

3.2.1 General reagents

3.2.2 Commercial kits

3.2.3 Instruments

3.3 Cell culture

3.3.1 Trypsinization of cells

3.3.2 Storage of cells

3.3.3 Counting of cells

3.4 Preparation of stock solutions of the compounds

3.5 Evaluation of the effects of treatments on the morphology of cells

3.6 Cell proliferation assay (WST-1) method

3.7 Annexin V apoptosis assay

3.8 Statistical analysis

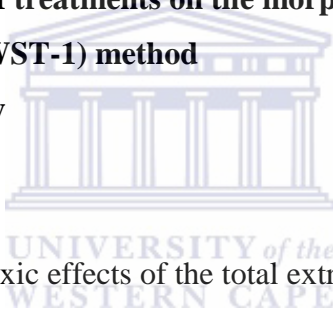
3.9 Results

3.9.1 Evaluating the cytotoxic effects of the total extract of *P. tuberculosa*

3.9.2 Evaluating the cytotoxic effects of the isolated compounds

3.9.3 Evaluating the apoptotic activity of the isolated compounds

3.10 Discussion



CHAPTER THREE

ANTICANCER EVALUATION OF *Palythoa tuberculosa*

3.1 Introduction

The literature indicates that *P. tuberculosa* possesses several highly toxic compounds to both animals (Wiles *et al.*, 1974) and humans (Uemura, 1991), with marked cytotoxic effects (Quinn *et al.*, 1974). Based on this, the study aims to evaluate the anticancer activity of this zoanthoid on several human cell lines which can be later exploited in treatment of cancer. This chapter entails evaluating the cytotoxic effects of three of the isolated novel compounds; palysterols B, C and G, and the known compound palysterol A isolated from *P. tuberculosa*. The anticancer evaluation was done on three cancer cell lines namely; MCF-7 (human breast adenocarcinoma), HeLa (human cervical carcinoma), HT-29 (human colon adenocarcinoma) and one non-cancerous human cell line KMST-6 (fibroblast) *via* colorimetric *in vitro* assay. Although several compounds were isolated from *P. tuberculosa* in this study, yet the anticancer evaluation was limited to those compounds isolated in significant amounts. The continuous understanding of the apoptotic pathways, and its relation with the progression of cancer in the body generated the drive to identify therapeutic agents that specifically induce cell death *via* apoptosis. Pro-apoptotic agents are expected to act specifically on tumour cells with minimal toxicity on normal cells (Nagle *et al.*, 2004), and consequently induce less side effects. Thus, this chapter also discusses preliminary work towards understanding the mode of action of the cytotoxic agents, by evaluating the potential of the compounds to induce apoptosis in cultured human cancer cells.

3.2 Materials

3.2.1 General reagents

Chemical	Supplier
C2-Ceramide.....	Calbiochem
Dulbecco's modified Eagle's medium (DMEM).....	Lonza
Dimethyl sulfoxide (DMSO).....	Sigma
Foetal bovine serum (FBS).....	Thermo Scientific
Penicillin-streptomycin.....	Lonza
Phosphate buffered saline (PBS).....	Lonza
Trypan blue stain 0.4%.....	Invitrogen
Trypsin.....	Gibco



3.2.2 Commercial kits

Apoptosis Kit – Annexin V Alexa Fluor [®] 488.....	Molecular probes
Cell proliferation reagent (WST-1).....	Roche

3.2.3 Instruments

12 well multiwell culture plates.....	Nest biotechnology
24 well multiwell culture plates.....	Sigma-Aldrich
96 well multiwell culture plates.....	Sigma-Aldrich
Cell Culture flasks 25 cm ²	SPL Life Sciences
Centrifuge 5417R.....	Eppendorf AG

CO ₂ Incubator.....	Shellab
Countess™ automated cell counter.....	Invitrogen
Countess™ cell counting chamber slide.....	Invitrogen
POLARstar Omega microplate reader.....	BMG Labtech
Sorvall TC-6 centrifuge.....	Sorvall
Tali® cellular analysis slides.....	Invitrogen
Tali® Image-Based Cytometer.....	Invitrogen

3.3 Cell culture

All cells (Table 3.1) were cultured in DMEM medium containing foetal bovine serum (10% v/v) and antibiotic (1% v/v).



Table 3.1: Cell lines used in this study.

Cell Line	Cell type	Species Origin	Growth Medium
Hela	Cervical adenocarcinoma	Human	DMEM
HT-29	Colon adenocarcinoma	Human	DMEM
KMST-6	Fibroblast	Human	DMEM
MCF-7	Breast adenocarcinoma	Human	DMEM

Cryogenic vials containing the cells were taken from the -150°C fridge and slowly thawed to 37°C. The cells were plated into 25 cm² flasks and cultured in humidified CO₂ incubator (5% CO₂) at 37°C until confluency was reached. The culture medium was replaced every 48 hr.

3.3.1 Trypsinization of cells

After reaching 90% of confluency, the culture medium was discarded and cells were washed with 5 mL PBS and 2 mL of pre-warmed trypsin was added for the purpose of trypsinization. The flasks were incubated at 37°C until cells detached from the bottom of flasks. Two volumes of growth medium were then added to deactivate the action of trypsin and the mixtures were transferred into sterile 15 mL centrifuge tubes. The tubes were then centrifuged at 2500 rpm for three minutes using Sorvall TC6 centrifuge at room temperature and the cell pellets were recovered after discarding the supernatant. The cell pellets were either re-suspended in growth medium or growth medium containing 10% DMSO depending on whether the cells were going to be seeded into new flasks or whether the cells are going to be stored at -150°C.

3.3.2 Storage of cells

After attaining the cells pellets after trypsinization as mentioned in section 3.3.1, the cells pellets are re-suspended in growth medium containing 10% DMSO. The suspension was then transferred to labelled cryogenic vials and stored at -150°C.

3.3.3 Counting of cells

Cell counts were performed as per the manufacturer's instructions using Countess™ automated cell counter (Invitrogen).

3.4 Preparation of stock solutions of the compounds

The compounds were weighed and dissolved in DMSO. Then the compounds were diluted in complete growth medium to reach concentration of 1000 µg/mL of each

compound in growth medium. The final concentration of DMSO after dilution was 1% in 100 μ L.

3.5 Evaluation of the effects of treatments on the morphology of cells

All cells (listed in Table 3.1) were monitored for their confluence using Nikon inverted light microscope. In order to document the morphological characteristics of treated and untreated cells, cells were cultured in 24 well multiwell culture plates to 90% confluence. The cells were treated with palysterols B and G at a concentration equivalent to their IC₅₀ values. The negative control cells were left untreated. The plate was incubated at 37 °C in a humidified CO₂ incubator. After 24 hours, the cells were photographed at 20X magnification using Leica EC3 digital camera.

3.6 Cell proliferation assay (WST-1) method

The growth inhibitory effects of the methanolic extract of *P. tuberculosa* and some of the isolated compounds were evaluated using the tetrazolium salt WST-1 colorimetric assay, as recommended by the manufacturer (Roche Diagnostics GmbH, Mannheim, Germany) (Liu *et al.*, 1995). The cells were cultured to 90% confluence and trypsinized as described in sections 3.3 and 3.3.1. The cells were seeded in a 96-well multiwell culture plates at a density of 2.0×10^4 cells/100 μ L per well. The plates were incubated at 37 °C in a humidified CO₂ incubator for 24 hours, then the culture medium was removed and the cells were treated with increasing concentrations (12.5, 25, 50, 75 and 100 μ g/mL) (The micro molar concentrations for the isolated compounds could not be calculated, since the molecular weights of the compounds were not yet known at the time of anticancer evaluation) of the total extract or the isolated compounds. As a positive control, the cells

were treated with 200 μ M C2-Ceramide, a known inducer of apoptotic cell death (Obeid *et al.*, 1993). Since DMSO is known to be toxic to cells (Da Violante *et al.*, 2002), an additional control was set up to evaluate its toxicity. The cells were therefore also treated with 1% DMSO. Untreated cells were used as a negative control. All treatments were done in triplicate. After 24 hours, WST-1 reagent was added (10 μ L) to the wells, and the plates were incubated at 37 $^{\circ}$ C for another four hours. The optical density/absorbance of the wells was determined using a BMG Labtech POLARstar Omega microplate reader, the plates were read at 430 nm, and 630 nm was used as a reference wavelength. The percentage of cell viability was calculated by comparing the absorbance of the test samples with the absorbance of the control (untreated) samples using the following calculation:


$$\% \text{ Cell Viability} = \frac{\text{sample absorbance} - \text{cell free sample blank}}{\text{control absorbance}} \times 100$$

The selectivity index (SI) of the compounds was calculated according to the following:

$$\text{SI} = \frac{\text{The half maximal inhibitory concentration of KMST-6}}{\text{The half maximal inhibitory concentration of any cell line}}$$

3.7 Annexin V apoptosis assay

This assay was done as described by the manufacturer (Invitrogen). In brief, the cells were seeded in 24-well multiwell culture plate at concentration of 2.0×10^5 cells/500 μ L per well, then the plate was incubated at 37 °C in a humidified CO₂ incubator for 24 hours. After removing the media from the wells, the cells were then treated with a concentration equivalent to the IC₅₀ values for the selected compounds for 24 hours. The cells were also treated with 100 μ M C2-ceramide as positive control, while negative control cells were left untreated. Following the 24 hours treatment, the cells were recovered by gentle trypsinization as described in section 3.3.1. The cell pellet was re-suspended in 100 μ L 1X Annexin binding buffer (ABB) and transferred to 1.5 mL Eppendorf tubes, then 5 μ L of Annexin V was added to each sample and mixed well. The cell suspensions were incubated in the dark. After 20 minutes, the samples were centrifuged at 3500 rpm for 3 min using Centrifuge 5417R, the cell pellets were re-suspended in 100 μ L of 1X Annexin binding buffer. Propidium iodide (1 μ L) was added to each sample and mixed. The cells were incubated for 5 min and 25 μ L of each sample was transferred to Tali[®] cellular analysis slides. Fluorescence resulting from either Annexin V or PI uptake was analyzed by Tali[®] Image-Based Cytometer using apoptosis settings.

3.8 Statistical analysis

The data presented are means \pm SD obtained from at least three independent experiments. Differences between the means were considered to be significant if $p < 0.05$ according to Prism's two-way ANOVA. All calculations were performed using MS Excel 2007.

3.9 Results

3.9.1 Evaluating the cytotoxic effects of the total extract of *P. tuberculosis*

Four human cell lines (KMST-6, MCF-7, HeLa and HT-29) were treated for 24 hours with the total methanolic extract of *P. Tuberculosis* as described in section 3.6. The cell viability following treatment was determined using WST-1 assay. The results (Figure 3.1) show a dose dependent decrease in the viability of the cells. The viability of all cell lines was unaffected at 12.5 µg/mL, while no viability was observed at the highest dose of 100 µg/mL. KMST-6 cells showed more resistance to the effect of the lipophilic extract as its viability was only affected at the highest concentration (100 µg/mL). Evidently, at concentration of 75 µg/mL the KMST-6 cells showed significant ($p < 0.001$) viability compared to other cancerous cell lines. At concentrations of 25 and 50 µg/mL, HeLa and MCF-7 cells appeared to be more susceptible to the effect of the lipophilic extract. HeLa was most affected ($p < 0.001$) compared to other cell lines at concentration 25 µg/mL, while MCF-7 was most susceptible ($p < 0.001$) at 50 µg/mL compared to KMST-6 and HT-29.

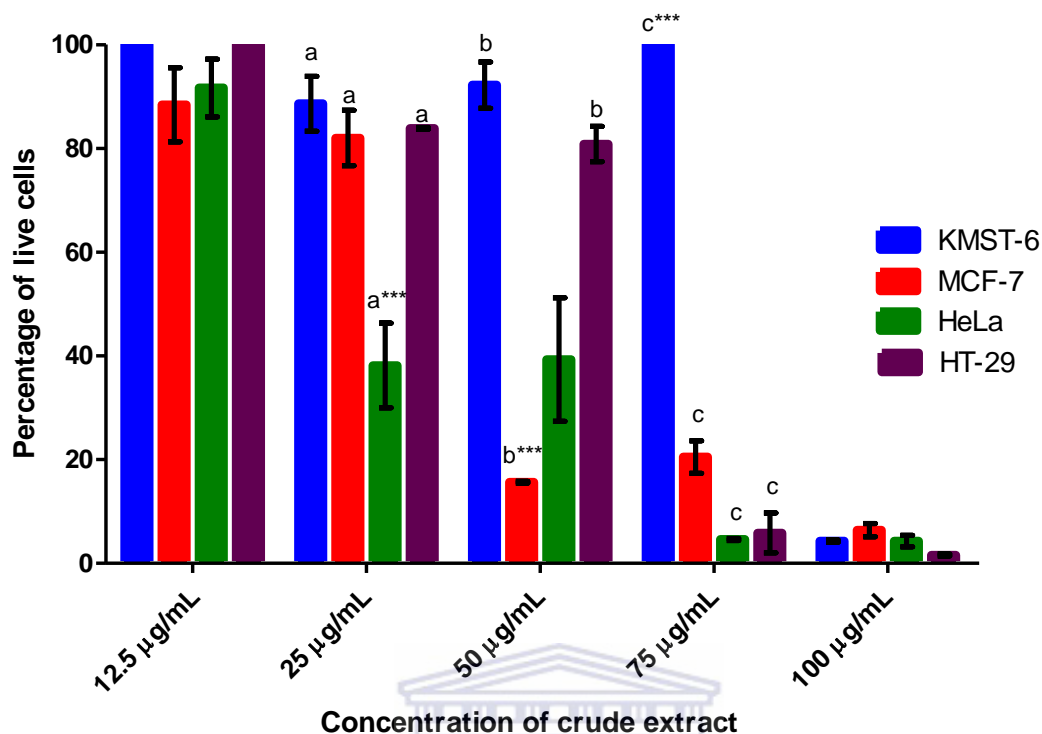


Figure 3.1: The effect of the total methanolic extract of *P. Tuberculosis* on the cell viability of HeLa, HT-29, MCF-7 and KMST-6 as determined by the WST-1 assay.

*** Statistical significance of ($p < 0.001$) compared to data labelled with the same letter.

UNIVERSITY of the
WESTERN CAPE

3.9.2 Evaluating the cytotoxic effects of the isolated compounds

Although several compounds were isolated from *P. Tuberculosis* in this study only four palysterols A, B, C and G were selected to assess if these compounds have any cytotoxic effects on KMST-6, MCF-7, HeLa and HT-29 cells. The cells were treated for 24 hours with the four compounds as described in section 3.6 and cell viability was assessed using the WST-1 assay. The IC_{50} and SI values for these compounds were determined (Table 3.2). Palysterols A and C did not demonstrate any cytotoxicity effects in the four cell lines used in this study. Palysterol G, however, was the most toxic compound with 40, 59, 61, and 62 $\mu\text{g/mL}$ ($= 82, 122, 126$ and $128 \mu\text{M}$) for MCF-7, HT-29, HeLa and KMST-6 cells, respectively. Palysterol B demonstrated selective toxicity towards HT-29 and MCF-

7 cells with IC₅₀ values of 83 and 87 µg/mL (170 and 178 µM), respectively. This compound was not toxic towards HeLa and KMST-6 cells and therefore the SI for palysterol B in MCF-7 and HT-29 could not be accurately determined.

Table 3.2: IC₅₀ (µg/mL) and SI values for palysterols A, B, C and G as determined by WST-1 assay.

Compounds	Cell Lines							
	MCF-7		HeLa		HT-29		KMST-6	
	IC ₅₀	SI	IC ₅₀	SI	IC ₅₀	SI	IC ₅₀	
Palysterol A	> 100	----	> 100	----	> 100	----	> 100	
Palysterol B	87	>1.1	> 100	----	83	>1.2	> 100	
Palysterol C	> 100	----	> 100	----	> 100	----	> 100	
Palysterol G	40	1.6	61	1.0	59	1.1	62	

UNIVERSITY of the

3.9.3 Evaluating the apoptotic activity of the isolated compounds

Only palysterols B and G were selected for this assay as they showed higher cytotoxic activity compared to palysterols A and C. The lowest IC₅₀ concentrations as determined by the WST-1 assay of both compounds were used i.e. 82 µM for palysterol G and 170 µM for palysterol B. These concentrations were used to determine if both compounds can induce apoptosis in cancer cells. The four cell lines were treated with the two compounds and the level of apoptosis was assessed using the Annexin V apoptosis assay as described in section 3.7. The result showed that only palysterol G was able to induce significant levels of apoptosis (Figure 3.2). The compound significantly (p<0.001) induced apoptosis in MCF-7 cells compared to the other cell lines used. Palysterol G induced apoptosis in about 75% of MCF-7 cells. Also, palysterol G exhibited low cytotoxic activity on

KMST-6 cells ($p < 0.05$) when compared to the negative control. Apoptosis induction was also observed under the microscope for both compounds. Notably, palysterol G was showing high count of apoptotic cells in MCF-7 cells (Figure 3.3).

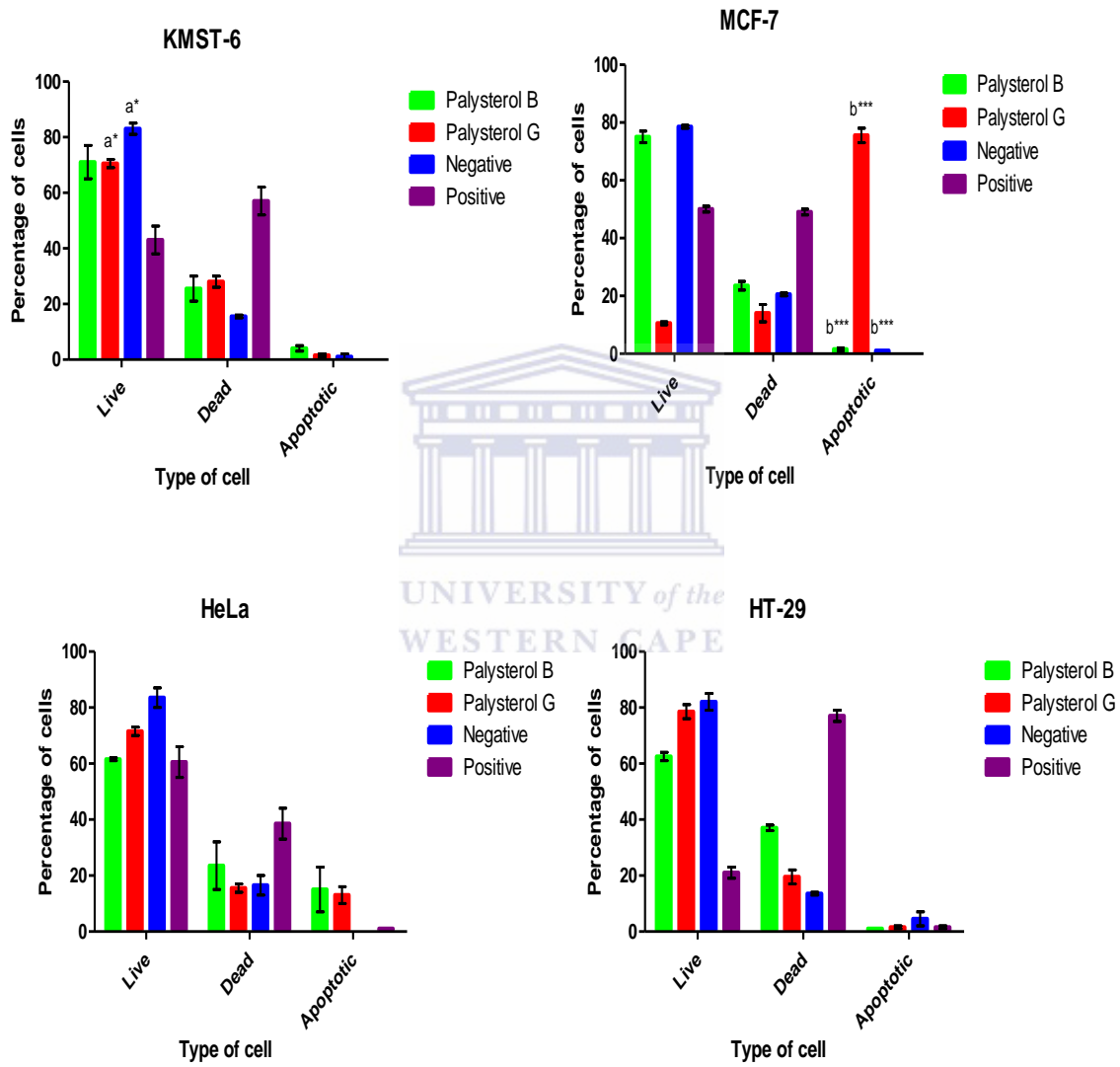


Figure 3.2: Percentage of live, dead and apoptotic cells induced by palysterols B and G on KMST-6, MCF-7, HeLa and HT-29 cell lines.

a*: statistical significance ($p < 0.05$) of palysterol G compared to negative control in KMST-6.

b***: statistical significance ($p < 0.001$) for palysterol G compared to palysterol B, negative and positive controls.

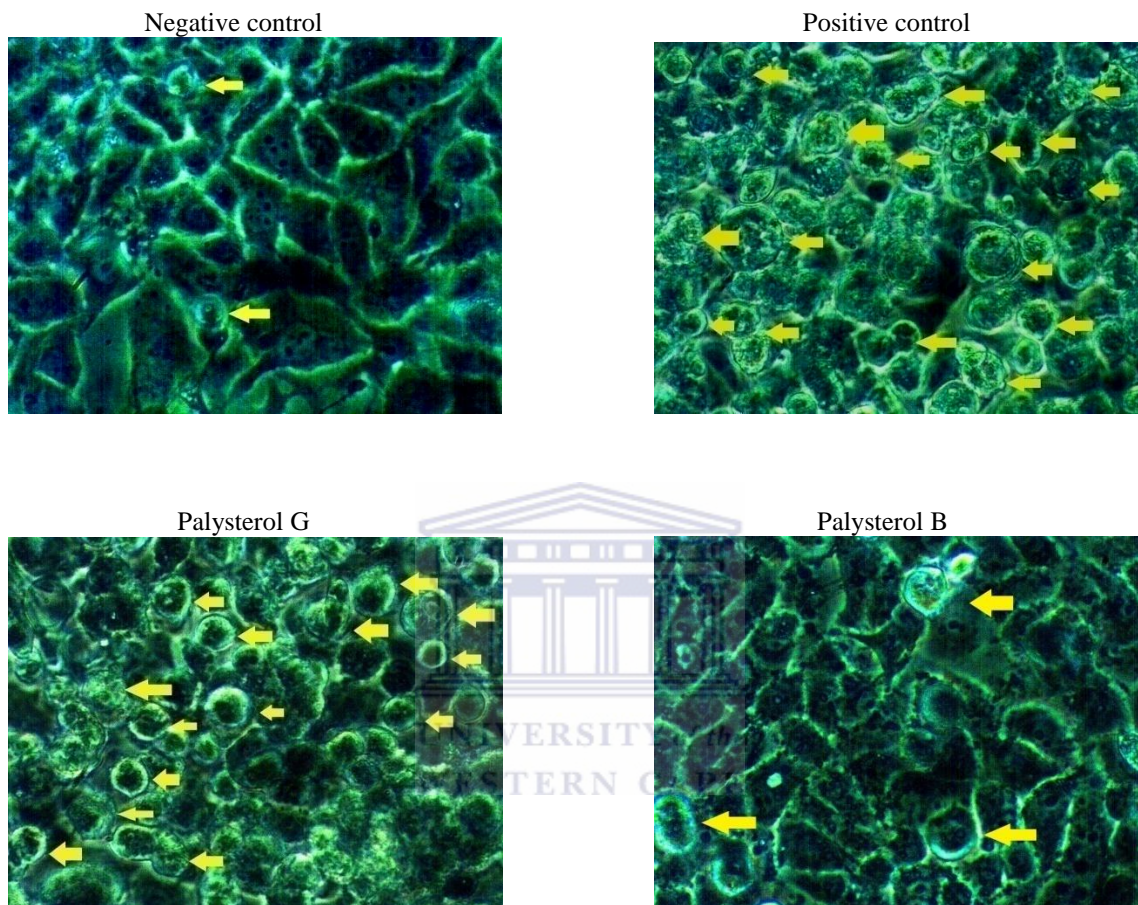
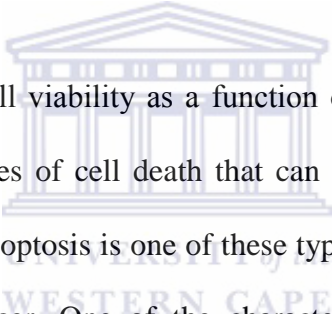


Figure 3.3: Photographss showing the apoptotic effect of the two compounds, palysterols B and G on MCF-7 cells showing apoptotic cells (yellow arrows). Notably, apoptotic cells covering the field of MCF-7 when treated with palysterol G. The morphological appearance of the labelled cells depicts the description of apoptotic cells by Lawen (2003), who stated that cells during early apoptosis become rounded up, shrink and lose contact with their neighbouring cells (Lawen, 2003) .

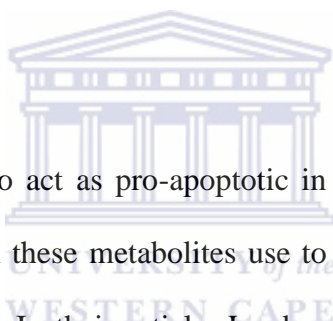
3.10 Discussion

Polyhydroxysterols or oxysterols are suggested to be potent cell replication inhibitors, and may have a role in regulation of cell proliferation, thus, are considered to have the potential to treat cancer (Sarma *et al.*, 2009). In this study, palysterols B and G were found to be the more cytotoxic amongst the compounds tested. Palysterol G showed high activity against breast adenocarcinoma cells (MCF-7) with an IC_{50} value of 82 μ M, while palysterol B demonstrated highest cell death on colon adenocarcinoma cell line (HT-29) with $IC_{50} = 170 \mu$ M. Palysterol G exhibited some degree of selectivity against cancerous cell lines, showed by results obtained by both WST-1 and Annexin V apoptosis assays.



The WST-1 assay measures cell viability as a function of the cell's metabolic activity. There are several different types of cell death that can lead to loss of cell viability as discussed in section 1.1.3.7. Apoptosis is one of these types of cell death and plays a key role in the prevention of cancer. One of the characteristics of cancer cells is their resistance to apoptosis (Hanahan and Weinberg, 2000). The targeted activation of apoptosis in cancer cells is therefore a feasible therapeutic strategy to treat cancer. It is for that reason that we also investigated if the cytotoxicity of these compounds was due to the activation of apoptosis. We found that palysterol B did not induce significant apoptosis levels in any of the cell lines tested in this study, while palysterol G induced significant ($P < 0.001$) levels of apoptosis in MCF-7 cells, but not in any of the other cell lines.

There are many assumptions with regards to structural activity relationship of oxysterols. The nature side chain is suggested to play a key role in determining the activity of the oxysterols (Liu *et al.*, 2013). This comes in agreement with our findings, as the unsaturation at Δ^{22} which is present only in palysterol G may greatly contribute to its activity, in fact, it is the only structural difference between palysterol G and the inactive palysterol C. Besides the side chain effect, the nature of substituent in C18 may also has an effect on the cytotoxicity [CHO in palysterol G > CH₂OH (palysterol B) > CH₃ (palysterol A)]. In addition, the acetylation of 1-OH may also play role in the cytotoxicity [OAc (palysterol G) and (palysterol B) > OH (palysterol A)], which was also suggested by Liu and co-workers (2013).



Many oxysterols were found to act as pro-apoptotic in various *in vitro* systems, yet a universal mechanism by which these metabolites use to induce apoptosis remains to be clarified (Lordan *et al.*, 2009). In their article, Lordan and co-workers, stated that the apoptotic studies of the polyhydroxylated sterols revealed that apoptosis was mainly triggered using intrinsic pathways, though little proof of activation of the death receptor pathway was established (Lordan *et al.*, 2009). Morrissey and Kiely (2006) suggested that pro-apoptotic action of oxysterols might be due to an increase in intracellular levels of reactive oxygen species (ROS), altering several signalling pathways and gene expression or by the induction of cell proteins modification. Furthermore, Olkkonen and Hynynen (2009) stated that common oxysterols are mostly known to interfere with cell membrane structure and cellular receptors. From the above, it is recommended that more mechanistic assays, such as Intracellular ROS, caspase 3/7 and 9 measurements and

topoisomerase inhibition determination, should be done in order to determine which apoptotic pathway is activated by palysterol G.



REFERENCES

Ahmad, I., Mehmood, Z. and Mohammad, F. (1998). Screening of some Indian medicinal plants for their antimicrobial properties. *Journal of Ethnopharmacology*, 62(2), pp.183–193.

Aicher, T., Buszek, K., Fang, F., Forsyth, C., Jung, S., Kishi, Y., Matelich, M., Scola, P., Spero, D. and Yoon, S. (1992). Total synthesis of halichondrin B and norhalichondrin B. *Journal of the American Chemical Society*, 114(8), pp.3162–3164.

Ali, A. and Hamed, M. (2006). Impact of water quality deterioration on coral reef community structure in the Northern Red Sea, Egypt. *Egyptian Journal of Aquatic Biology and Fisheries*, 10(2), pp.117–146.

Alison, M. (2001). Cancer. In: eLS. John Wiley & Sons Ltd, Chichester.

Amaravadi, R., Lippincott-Schwartz, J., Yin, X., Weiss, W., Takebe, N., Timmer, W., DiPaola, R., Lotze, M. and White, E. (2011). Principles and current strategies for targeting autophagy for cancer treatment. *Clinical Cancer Research*, 17(4), pp.654–666.

Ameisen, J. (2002). On the origin, evolution, and nature of programmed cell death: a timeline of four billion years. *Cell death and differentiation*, 9(4), pp.367–393.

Artigas, P. and Gadsby, D. (2003). Na⁺/K⁺-pump ligands modulate gating of palytoxin-induced ion channels. *Proceedings of the National Academy of Sciences*, 100(2), pp.501–505.

Badley, A., Dockrell, D. and Paya, C. (1997). Apoptosis in AIDS. *Advances in Pharmacology*, 41, pp.271–294.

Bai, R., Paull, K., Herald, C., Malspeis, L., Pettit, G. and Hamel, E. (1991). Halichondrin B and homohalichondrin B, marine natural products binding in the vinca domain of tubulin. Discovery of tubulin-based mechanism of action by analysis of differential cytotoxicity data. *Journal of Biological Chemistry*, 266(24), pp.15882–15889.

Bergmann, W., Feeney, R. and Swift, A. (1951). Contributions to the Study of Marine Products. XXXI. Palysterol and other Lipid Components of sea Anemones. *The Journal of Organic Chemistry*, 16(9), pp.1337–1344.

Blunt, J., Copp, B., Hu, W., Munro, M., Northcote, P. and Prinsep, M. (2008). Marine natural products. *Natural Product Reports*, 25(1), pp.35–94.

Brown, J. and Attardi, L. (2005). The role of apoptosis in cancer development and treatment response. *Nature Reviews Cancer*, 5(3), pp.231–237.

Burnett, W., Benzie, J., Beardmore, J. and Ryland, J. (1997). Zoanthids (Anthozoa, Hexacorallia) from the Great Barrier Reef and Torres Strait, Australia: systematics, evolution and a key to species. *Coral Reefs*, 16(1), pp.55–68.

Capon, R. (2010). Marine Natural Products Chemistry: Past, Present, and Future. *Australian Journal of Chemistry*, 63(6), p.851.

Carballeira, N. and Reyes, M. (1995). Identification of a new 6-bromo-5, 9-eicosadienoic acid from the anemone *Condylactis gigantea* and the zoanthid *Palythoa caribaeorum*. *Journal of Natural Products*, 58(11), pp.1689–1694.

Cha, J., Christ, W., Finan, J., Fujioka, H., Kishi, Y., Klein, L., Ko, S., Leder, J., McWhorter, W., Pfaff, K. and others, (1982). Stereochemistry of palytoxin. Part 4. Complete structure. *Journal of the American Chemical Society*, 104(25), pp.7369–7371.

Ciminiello, P., Dell'Aversano, C., Dello Iacovo, E., Fattorusso, E., Forino, M., Grauso, L., Tartaglione, L., Guerrini, F., Pezzolesi, L., Pistocchi, R. and Vanucci, S. (2012). Isolation and structure elucidation of ovatoxin-a, the major toxin produced by *Ostreopsis ovata*. *Journal of the American Chemical Society*, 134(3), pp.1869–1875.

Ciminiello, P., Dell'Aversano, C., Dello Iacovo, E., Fattorusso, E., Forino, M., Grauso, L., Tartaglione, L., Florio, C., Lorenzon, P., De Bortoli, M. and others, (2009). Stereostructure and biological activity of 42-hydroxy-palytoxin: a new palytoxin analogue from Hawaiian *Palythoa* subspecies. *Chemical Research in Toxicology*, 22(11), pp.1851–1859.

Clarke, P. (1990). Developmental cell death: morphological diversity and multiple mechanisms. *Anatomy and Embryology*, 181(3), pp.195–213.

Cohen, S. (1976). The lethality of arnucleotides. *Medical Biology*, 54(5), pp.299–326.

Cragg, G., Newman, D. (2005). Biodiversity: A continuing source of novel drug leads. *Pure and Applied Chemistry*, 77(1), pp.7–24.

Cuevas, C., Pérez, M., Martín, M., Chicharro, J., Fernández-Rivas, C., Flores, M., Francesch, A., Gallego, P., Zarzuelo, M., de la Calle, F. and others, (2000). Synthesis of ecteinascidin ET-743 and phthalascidin Pt-650 from cyanosafracin B. *Organic Letters*, 2(16), pp.2545–2548.

Da Violante, G., Zerrouk, N., Richard, I., Provot, G., Chaumeil, J. and Arnaud, P. (2002). Evaluation of the cytotoxicity effect of dimethyl sulfoxide (DMSO) on Caco2/TC7 colon tumour cell cultures. *Biological and Pharmaceutical Bulletin*, 25(12), pp.1600–1603.

Degterev, A., Huang, Z., Boyce, M., Li, Y., Jagtap, P., Mizushima, N., Cuny, G., Mitchison, T., Moskowitz, M. and Yuan, J. (2005). Chemical inhibitor of nonapoptotic cell death with therapeutic potential for ischemic brain injury. *Nature Chemical Biology*, 1(2), pp.112–119.

Demant, P. (2005). The genetic factors in cancer development and their implications for cancer prevention and detection. *Radiation Research*, 164(4), pp.462–466.

Dunlap, W. and Chalker, B. (1986). Identification and quantitation of near-UV absorbing compounds (S-320) in a hermatypic scleractinian. *Coral Reefs*, 5(3), pp.155–159.

Dunlap, W. and Yamamoto, Y. (1995). Small-molecule antioxidants in marine organisms: antioxidant activity of mycosporine-glycine. *Comparative Biochemistry and Physiology Part B: Biochemistry and Molecular Biology*, 112(1), pp.105–114.

Elmore, S. (2007). Apoptosis: a review of programmed cell death. *Toxicologic Pathology*, 35(4), pp.495–516.

Fabricius, K. and Metzner, J. (2004). Scleractinian walls of mouths: predation on coral larvae by corals. *Coral Reefs*, 23(2), pp.245–248.

Fairecloth, G.T., Smith, B., Grant, W., (2001). Selective antitumor activity of Kahalaide F, a marine-derived cyclic depsipeptide. *Proceedings of the American Association for Cancer Research*, 42, pp.1140.

Fenical, W., Jensen, P., Palladino, M., Lam, K., Lloyd, G. and Potts, B. (2009). Discovery and development of the anticancer agent salinosporamide A (NPI-0052). *Bioorganic & Medicinal Chemistry*, 17(6), pp.2175–2180.

Fidler, I. J. (2003). The pathogenesis of cancer metastasis: the “seed and soil” hypothesis revisited. *Nature Reviews Cancer*, 3 (6), pp. 453–458.

Fujioka, H., Christ, W., Cha, J., Leder, J., Kishi, Y., Uemura, D. and Hirata, Y. (1982). Stereochemistry of palytoxin. Part 3. C7-C51 segment. *Journal of the American Chemical Society*, 104(25), pp.7367–7369.

Garcia-Rocha, M., Bonay, P. and Avila, J. (1996). The antitumoral compound Kahalalide F acts on cell lysosomes. *Cancer Letters*, 99(1), pp.43–50.

Gupta, K. and Scheuer, P. (1969). Zoanthid sterols. *Steroids*, 13(3), pp.343–356.

Hamann, M., Otto, C., Scheuer, P. and Dunbar, D. (1996). Kahalalides: bioactive peptides from a marine mollusk *Elysia rufescens* and Its Algal Diet *Bryopsis* sp. 1. *The Journal of Organic Chemistry*, 61(19), pp.6594–6600.

Hanahan, D. and Weinberg, R. (2000). The hallmarks of cancer. *cell*, 100(1), pp.57–70.

Hart, J., Lill, R., Hickford, S., Blunt, J. and Munro, M. (2000) The halichondrins: Chemistry, biology, supply and delivery. In: **Fusetani, N.** (ed), *Drugs from the Sea*. Karger publishers, Basel, pp 134–153.

Haywick, D. and Mueller, E. (1997). Sediment retention in encrusting *Palythoa* spp.--a biological twist to a geological process. *Coral Reefs*, 16(1), pp.39–46.

Hejmadi, M. (2010). Introduction to Cancer Biology. (1st ed.). Frederiksberg, Denmark: BoonBooks.

Hibino, Y., Todd, P., Ashworth, C., Obuchi, M. and Reimer, J. (2013). Monitoring colony colour and zooxanthellae (*Symbiodinium* spp.) condition in the reef zoanthid *Palythoa tuberculosa* in Okinawa, Japan. *Marine Biology Research*, 9(8), pp.794–801.

Hildebrand, M., Waggoner, L., Liu, H., Sudek, S., Allen, S., Anderson, C., Sherman, D. and Haygood, M. (2004). bryA: An unusual modular polyketide synthase gene from the uncultivated bacterial symbiont of the marine bryozoan *Bugula neritina*. *Chemistry & Biology*, 11(11), pp.1543–1552.

Hirata, Y. and Uemura, D. (1986). Halichondrins-antitumor polyether macrolides from a marine sponge. *Pure and Applied Chemistry*, 58(5), pp.701–710.

Honig, L. and Rosenberg, R. (2000). Apoptosis and neurologic disease. *The American Journal of Medicine*, 108(4), pp.317–330.

Hung, D., Jamison, T. and Schreiber, S. (1996). Understanding and controlling the cell cycle with natural products. *Chemistry & Biology*, 3(8), pp.623–639.

Irei, Y., Nozawa, Y. and Reimer, J. (2011). Distribution patterns of five zoanthid species in Okinawa Island, Japan. *Zoological Studies*, 50, pp.426–433.

Ito, S. and Hirata, Y. (1977) Isolation and structure of a mycosporine from the zoanthid *Palythoa tuberculosa*, *Tetrahedron Letters*, 18(29), pp. 2429–2430.

Jacobson, M., Weil, M. and Raff, M. (1997). Programmed cell death in animal development. *Cell*, 88(3), pp.347–354.

Jagodzinska, B., Trimmer, J., Fenical, W. and Djerassi, C. (1985). Sterols in marine invertebrates. 49. Isolation and structure elucidation of eight new polyhydroxylated sterols from the soft coral *Sinularia dissecta*. *The Journal of Organic Chemistry*, 50(9), pp.1435–1439.

Jemal, A., Bray, F., Center, M., Ferlay, J., Ward, E. and Forman, D. (2011). Global

cancer statistics. *CA: A Cancer Journal for Clinicians*, 61(2), pp.69–90.

Ji, H., Li, X. and Zhang, H. (2009). Natural products and drug discovery. Can thousands of years of ancient medical knowledge lead us to new and powerful drug combinations in the fight against cancer and dementia?. *EMBO Reports*, 10(3), pp.194–200.

Jiménez C. (2001). Bleaching and mortality of reef organisms during a warming event in 1995 on the Caribbean coast of Costa Rica. *Revista De Biología Tropical* 49:233–238.

Jimeno, J., Faircloth, G., Sousa-Faro, J., Scheuer, P. and Rinehart, K. (2004). New Marine Derived Anticancer Therapeutics— A Journey from the Sea to Clinical Trials. *Marine Drugs*, 2(1), pp.14–29.

Jou, G., González, I., Albericio, F., Lloyd-Williams, P. and Giralt, E. (1997). Total synthesis of dehydrodidemnin B. Use of uronium and phosphonium salt coupling reagents in peptide synthesis in solution. *The Journal of Organic Chemistry*, 62(2), pp.354–366.

Kanzaki, A., Takebayashi, Y., Ren, X., Miyashita, H., Mori, S., Akiyama, S. and Pommier, Y. (2002). Overcoming multidrug drug resistance in P-glycoprotein/MDR1-overexpressing cell lines by ecteinascidin 743. *Molecular Cancer Therapeutics*, 1(14), pp.1327–1334.

Kepp, O., Galluzzi, L., Lipinski, M., Yuan, J. and Kroemer, G. (2011). Cell death assays for drug discovery. *Nature Reviews Drug Discovery*, 10(3), pp.221–237.

Kerr, J., Wyllie, A. and Currie, A. (1972). Apoptosis: a basic biological phenomenon with wide-ranging implications in tissue kinetics. *British Journal of Cancer*, 26(4), pp.239–257.

Kimura, S. and Hashimoto, Y. (1973) Purification of the toxin in a zoanthid *Palythoa tuberculosa*. *Publications of the Seto Marine Biological Laboratory*. 20, pp.713–718.

Klein, L., McWhorter, W., Ko, S., Pfaff, K., Kishi, Y., Uemura, D. and Hirata, Y. (1982). Stereochemistry of palytoxin. Part 1. C85-C115 segment. *Journal of the American Chemical Society*, 104(25), pp.7362–7364.

Ko, S., Finan, J., Yonaga, M., Kishi, Y., Uemura, D. and Hirata, Y. (1982). Stereochemistry of palytoxin. Part 2. C1-C6, C47-C74, and C77-C83 segments. *Journal of the American Chemical Society*, 104(25), pp.7364–7367.

Kopelovich, L. (1982). Hereditary adenomatosis of the colon and rectum: relevance to cancer promotion and cancer control in humans. *Cancer Genetics and Cytogenetics*, 5 (4), pp. 333–351.

Kumar, V. and Robbins, S. (2007). Robbins Basic Pathology, (1st ed.). Philadelphia, PA: Saunders/Elsevier.

Lawen, A. (2003). Apoptosis—an introduction. *Bioassays*, 25(9), pp.888–896.

Liu, S., Saijo, K., Todoroki, T. and Ohno, T. (1995). Induction of human autologous cytotoxic T lymphocytes on formalin-fixed and paraffin-embedded tumour sections. *Nature Medicine*, 1(3), pp.267–271.

Liu, T., Lu, X., Tang, H., Zhang, M., Wang, P., Sun, P., Liu, Z., Wang, Z., Li, L., Rui, Y. and others, (2013). 3 β ,5 α ,6 β -Oxygenated sterols from the South China Sea gorgonian *Muriceopsis flavida* and their tumour cell growth inhibitory activity and apoptosis-inducing function. *Steroids*, 78(1), pp.108–114.

Lopez Martin, J.A., Nieto, A., Demetri, G., Misset, J.L., Ray-Coquard, I., Guzman, C., Sancho, M.A., Parra, M.C., Ibarra, I., Millan, S., Martin, C., Ruiz, A., De Alvaro, J., Lopez-Lazaro, L., Gomez, J., Jimeno, J. (2002) Safety profile of ecteinascidin 743 (ET-743) in phase II clinical trials (CT) in adult patients with solid tumours. *Proceedings of the American Society Clinical Oncology*, 21: 96a.

López-Maciá, A., Jiménez, J.C., Royo, M., Giralt, E., Albericio, F. (2001) Synthesis and structure determination of Kahalalide F. *Journal of the American Chemical Society*, 123, 11398–11401.

Lordan, S., Mackrill, J. and O'Brien, N. (2009). Oxysterols and mechanisms of apoptotic signaling: implications in the pathology of degenerative diseases. *The Journal of Nutritional Biochemistry*, 20(5), pp.321–336.

Löwenberg, B. (2013). Sense and nonsense of high-dose cytarabine for acute myeloid leukemia. *Blood*, 121(1), pp.26–28.

Macfarlane, R. D., Uemura, D., Ueda, K. and Hirata, Y. (1980). ²⁵²Cf plasma desorption mass spectrometry of palytoxin. *Journal of the American Chemical Society*, 102, 875–876.

McClintock, J. and Baker, B. (2001). Marine Chemical Ecology, (1st ed.). Boca Raton, Fla.: CRC Press.

Mendola, D. (2000). Aquacultural production of bryostatin 1 and ecteinascidin 743. In: **Fusetani, N.** (ed) *Drugs from the Sea*. Karger publishers, Basel, pp 120–133.

Menna, M. (2009). Antitumor potential of natural products from Mediterranean ascidians. *Phytochemistry Reviews*, 8(2), pp.461–472.

Minuzzo, M., Marchini, S., Brogini, M., Faircloth, G., D'Incalci, M. and Mantovani, R. (2000). Interference of transcriptional activation by the antineoplastic

drug ecteinascidin-743. *Proceedings of the National Academy of Sciences*, 97(12), pp.6780–6784.

Molinski, T., Dalisay, D., Lievens, S. and Saludes, J. (2009). Drug development from marine natural products. *Nature Reviews Drug discovery*, 8(1), pp.69–85.

Montaser, R. and Luesch, H. (2011). Marine natural products: a new wave of drugs?. *Future Medicinal Chemistry*, 3(12), pp.1475–1489.

Moore, R. and Bartolini, G. (1981). Structure of palytoxin. *Journal of the American Chemical Society*, 103(9), pp.2491–2494.

Moore, R. and Scheuer, P. (1971). Palytoxin: a new marine toxin from a coelenterate. *Science*, 172(3982), pp.495–498.

Moore, R. E., Dietrich, R. F., Hatton, B., Higa, T., Scheuer, P. J. (1975). Nature of the λ 263 chromophore in the palytoxins. *Journal of Organic Chemistry*, 40, 540–542

Morrissey, P. and Kiely, M. (2006). Oxysterols: formation and biological function. In: *Advanced Dairy Chemistry Volume 2 Lipids*, Springer US, pp.641–674.

Munro, M., Blunt, J., Dumdei, E., Hickford, S., Lill, R., Li, S., Battershill, C. and Duckworth, A. (1999). The discovery and development of marine compounds with pharmaceutical potential. *Journal of Biotechnology*, 70(1), pp.15–25.

Muramatsu, I., Nishio, M., Kigoshi, S. and Uemura, D. (1988). Single ionic channels induced by palytoxin in guinea-pig ventricular myocytes. *British journal of pharmacology*, 93(4), pp.811–816.

Muramatsu, I., Uemura, D., Fujiwara, M. and Narahashi, T. (1984). Characteristics of palytoxin-induced depolarization in squid axons. *Journal of Pharmacology and Experimental Therapeutics*, 231(3), pp.488–494.

Nagle, D., Zhou, Y., Mora, F., Mohammed, K. and Kim, Y. (2004). Mechanism targeted discovery of antitumor marine natural products. *Current medicinal chemistry*, 11(13), pp.1725-1756.

Newman, D. and Cragg, G. (2004). Marine natural products and related compounds in clinical and advanced preclinical trials. *Journal of Natural Products*, 67(8), pp.1216–1238.

Newman, D. and Cragg, G. (2012). Natural products as sources of new drugs over the 30 years from 1981 to 2010. *Journal of Natural Products*, 75(3), pp.311–335.

Newman, D. and Cragg, G. (2014). Marine-sourced anti-cancer and cancer pain control agents in clinical and late preclinical development. *Marine Drugs*, 12(1), pp.255–278.

Nkunya, M., Weenan, H. and Brat, D. (1990). Chemical evaluation of Tanzanian medicinal plants for the active constituents as a basis for the medicinal usefulness of the plants, *Proceedings of an International Conference of Experts from Developing Countries on Traditional Medicinal Plants*. Dar es Salaam, Tanzania, pp. 101–111.

Nuijen, B., Bouma, M., Manada, C., Jimeno, J., Schellens, J., Bult, A. and Beijnen, J. (2000). Pharmaceutical development of anticancer agents derived from marine sources. *Anti-cancer Drugs*, 11(10), pp.793–811.

Obeid, L., Linardic, C., Karolak, L. and Hannun, Y. (1993). Programmed cell death induced by ceramide. *Science*, 259(5102), pp.1769–1771.

Olkkonen, V. and Hynynen, R. (2009). Interactions of oxysterols with membranes and proteins. *Molecular Aspects of Medicine*, 30(3), pp.123–133.

Orth, M., Lauber, K., Niyazi, M., Friedl, A., Li, M., Maihöfer, C., Schüttrumpf, L., Ernst, A., Niemöller, O. and Belka, C. (2014). Current concepts in clinical radiation oncology. *Radiation and Environmental Biophysics*, 53(1), pp.1–29.

Penaloza, C., Lin, L., Lockshin, R. and Zakeri, Z. (2006). Cell death in development: shaping the embryo. *Histochemistry and Cell Biology*, 126(2), pp.149–158.

Pettit, G. and Fujii, Y. (1982). Antineoplastic Agents. 81. The Glycerol Ethers of *Palythoa liscia*. *Journal of Natural Products*, 45(5), pp.640–643.

Pettit, G., Fujii, Y., Hasler, J., Schmidt, J. and Michel, C. (1982a). Antineoplastic Agents 78. Isolation of Palystatins 1-3 From the Indian Ocean *Palythoa liscia*. *Journal of Natural Products*, 45(3), pp.263–269.

Pettit, G., Fujii, Y., Hasler, J. and Schmidt, J. (1982b). Isolation and characterization of palystatins A-D. *Journal of natural products*, 45(3), pp.272–276.

Quinn, R., Kashiwagi, M., Moore, R. and Norton, T. (1974). Anticancer activity of zoanthids and the associated toxin, palytoxin, against ehrlich ascites tumour and P-388 lymphocytic leukemia in mice. *Journal of Pharmaceutical Sciences*, 63(2), pp.257–260.

Reed, J. (2000). Mechanisms of apoptosis. *The American Journal of Pathology*, 157(5), pp.1415–1430.

Reed, J. and Pellicchia, M. (2005). Apoptosis-based therapies for hematologic malignancies. *Blood*, 106(2), pp.408–418.

Reimer, A. (1971a). Feeding behavior in the Hawaiian zoanthids *Palythoa* and *Zoanthus*. *Pacific Science*, 25, pp.512–520.

Reimer, A. (1971b). Observations on the relationships between several species of tropical zoanthids (Zoanthidea, Coelenterata) and their zooxanthellae. *Journal of Experimental Marine Biology and Ecology*, 7(2), pp.207–214.

Reimer, J. (2014). *Palythoa Lamouroux*, 1816. Accessed through: World Register of Marine Species at <http://www.marinespecies.org/aphia.php?p=taxdetails&id=205785> on 2014-08-27.

Reimer, J., Ono, S., Fujiwara, Y., Takishita, K. and Tsukahara, J. (2004). Reconsidering *Zoanthus* spp. diversity: molecular evidence of conspecificity within four previously presumed species. *Zoological Science*, 21(5), pp.517–525.

Reimer, J., Ono, S., Takishita, K., Tsukahara, J. and Maruyama, T. (2006). Molecular evidence suggesting species in the zoanthid genera *Palythoa* and *Protopalythoa* (Anthozoa: Hexacorallia) are congeneric. *Zoological Science*, 23(1), pp.87–94.

Rinehart, K., Gloer, J., Cook, J., Mizsak, S. and Scahill, T. (1981). Structures of the didemmins, antiviral and cytotoxic depsipeptides from a Caribbean tunicate. *Journal of the American Chemical Society*, 103(7), pp.1857–1859.

Rinehart, K., Holt, T., Fregeau, N., Stroh, J., Keifer, P., Sun, F., Li, L. and Martin, D. (1990). Ecteinascidins 729, 743, 745, 759A, 759B, and 770: potent antitumor agents from the Caribbean tunicate *Ecteinascidia turbinata*. *Journal of Organic Chemistry*, 55(15), pp.4512–4515.

Ruggieri, G. (1976). Drugs from the sea. *Science*, 194(4264), pp.491–497.

Sarma, N., Krishna, M., Pasha, S., Rao, T., Venkateswarlu, Y. and Parameswaran, P. (2009). Marine Metabolites: The Sterols of Soft Coral. *Chemical Reviews*, 109(6), pp.2803–2828.

Sebens, K. (1982). Intertidal distribution of zoanthids on the Caribbean coast of Panama: effects of predation and desiccation. *Bulletin of Marine Science*, 32(1), pp.316–335.

Sertürner F. W. A. (1806). Darstellung der reinen Mohnsäure (Opiumsäure) nebst einer Chemischen Untersuchung des Opiums mit vorzüglicher Hinsicht auf ein darin neu entdeckten Stoff und die dahin gehörigen Bemerkungen. *Journal der Pharmacie fuer Aerzte und Apotheker*, 14, pp.47–93.

Shigemori, H., Sato, Y., Kagata, T. and Kobayashi, J. (1999). Palythoalones A and B, new ecdysteroids from the marine zoanthid *Palythoa australiae*. *Journal of Natural Products*, 62(2), pp.372–374.

Solecki, R.S. (1975). Shanidar IV, a neanderthal flower burial in northern Iraq. *Science*, 190(28), pp.880–881.

Stonik, V. (2009). Marine natural products: a way to new drugs. *Acta Naturae*, 1(2), p.15-25.

Story, M. and Kodym, R. (1998). Signal transduction during apoptosis; implications for cancer therapy. *Frontier in Bioscience*, 3, pp.365–375.

Suchanek, T. and Green, D. (1981). Interspecific competition between *Palythoa caribaeorum* and other sessile invertebrates on St. Croix reefs, U.S. Virgin Islands. *Proceedings of the Fourth International Coral Reef Symposium*, Manila, Philippines. 2, pp.679–684.

Sudek, S., Lopanik, N., Waggoner, L., Hildebrand, M., Anderson, C., Liu, H., Patel, A., Sherman, D. and Haygood, M. (2007). Identification of the putative bryostatin polyketide synthase gene cluster from “Candidatus Endobugula sertula”, the uncultivated microbial symbiont of the marine bryozoan *Bugula neritina*. *Journal of Natural Products*, 70(1), pp.67–74.

Swain, T. (2010). Evolutionary transitions in symbioses: dramatic reductions in bathymetric and geographic ranges of Zoanthidea coincide with loss of symbioses with invertebrates. *Molecular Ecology*, 19(12), pp.2587–2598.

Takano, S., Uemura, D. and Hirata, Y. (1978 a). Isolation and structure of a new amino acid, palythine, from the zoanthid *Palythoa tuberculosa*. *Tetrahedron Letters*, 26, pp.2299–2300.

Takano, S., Uemura, D. and Hirata, Y. (1978 b). Isolation and structure of two new amino acids, palythinol and palythene, from the zoanthid *Palythoa tuberculosa*. *Tetrahedron Letters*, 49, 4909–4912.

Trosko, J. (2001). Commentary: is the concept of “tumor promotion” a useful paradigm?. *Molecular Carcinogenesis*, 30(3), pp.131–137.

Uemura, D. (1991). Bioactive polyethers. In: *Bioorganic Marine Chemistry*, Springer Berlin Heidelberg, 4, pp.1–31.

Uemura, D. (2006). Bioorganic studies on marine natural products—diverse chemical structures and bioactivities. *The Chemical Record*, 6(5), pp.235–248.

Uemura, D. (2010). Exploratory research on bioactive natural products with a focus on biological phenomena. *Proceedings of the Japan Academy. Series B, Physical and biological sciences*, 86(3), pp.190-201.

Uemura, D., Hirata, Y., Iwashita, T. and Naoki, H. (1985). Studies on palytoxins. *Tetrahedron*, 41(6), pp.1007–1017.

Uemura, D., Takahashi, K., Yamamoto, T., Katayama, C., Tanaka, J., Okumura, Y. and Hirata, Y. (1985). Norhalichondrin A: an antitumor polyether macrolide from a marine sponge. *Journal of the American Chemical Society*, 107(16), pp.4796–4798.

Uemura, D., Toya, Y., Watanabe, I. and Hirata, Y. (1979). Isolation and structures of two new pyrazines, palythazine and isopalythazine from *Palythoa tuberculosa*. *Chemistry Letters*, 8(12), pp.1481–1482.

Uemura, D., Ueda, K., Hirata, Y., Naoki, H. and Iwashita, T. (1981a). Further studies on palytoxin. I. *Tetrahedron Letters*, 22, 1909–1912.

Uemura, D., Ueda, K., Hirata, Y., Naoki, H. and Iwashita, T. (1981b). Further studies on palytoxin. II. Structure of palytoxin. *Tetrahedron Letters*, 22, 2781–2784

Ukena, T., Satake, M., Usami, M., Oshima, Y., Naoki, H., Fujita, T., Kan, Y. and Yasumoto, T. (2001). Structure elucidation of ostreocin D, a palytoxin analog isolated from the dinoflagellate *Ostreopsis siamensis*. *Bioscience, biotechnology, and biochemistry*, 65(11), pp.2585–2588.

Vanneman, M. and Dranoff, G. (2012). Combining immunotherapy and targeted therapies in cancer treatment. *Nature Reviews Cancer*, 12(4), pp.237–251.

Venugopal, V. (2009). *Marine Products for Healthcare*, (1st ed.). Boca Raton: CRC Press/Taylor & Francis.

Vermeulen, K., Van Bockstaele, D. and Berneman, Z. (2003). The cell cycle: a review of regulation, deregulation and therapeutic targets in cancer. *Cell Proliferation*, 36(3), pp.131–149.

Wagner, H., Blatt, S. and Zgainski, E. (1984). *Plant Drug Analysis: A Thin Layer Chromatography Atlas*, (1st ed.). Berlin: Springer-Verlag.

Walsh, G. and Bowers, R. (1971). A review of Hawaiian zoanthids with descriptions of three new species. *Zoological Journal of the Linnean Society*, 50(2), pp.161–180.

Wiles, J., Vick, J. and Christensen, M. (1974). Toxicological evaluation of palytoxin in several animal species. *Toxicon*, 12(4), pp.427–433.

Withrow, S. J. and Vail, D. M. (2007). *Withrow & MacEwen's Small Animal Clinical Oncology*, (4th ed.). St. Louis, Mo.: Saunders Elsevier.

Wright, A., Forleo, D., Gunawardana, G., Gunasekera, S., Koehn, F. and McConnell, O. (1990). Antitumor tetrahydroisoquinoline alkaloids from the colonial ascidian *Ecteinascidia turbinata*. *The Journal of Organic Chemistry*, 55(15), pp.4508–4512.